UNIVERSITY OF PAVIA

Department of Molecular Medicine

PhD Program in Translational Medicine

XXXV Cycle

Functional Characterization of Antiapoptotic and Metabolic Activities of PINK1 in Cellular Models of Aging and Neurodegeneration

Supervisor

Prof. Enza Maria Valente

PhD Candidate

Francesco Brunelli, MD

Academic Year 2021/2022

Table of Contents

1. Abstract

Parkinson's Disease (PD) is a common neurodegenerative disease with growing incidence and prevalence. Its etiology is multifactorial, determined by a complex interaction of genetic and environmental factors. A subset of patients, however, presents with rare inheritable monogenic forms of PD.

PINK1 is a causative gene for early-onset PD with autosomal recessive inheritance. It encodes a kinase known to play a central role in mitochondrial homeostasis as a regulator of mitophagy, which is the degradation of dysfunctional mitochondria through autophagy. The protein PINK1, however, exerts neuroprotective and cytoprotective functions beyond mitophagy, favoring cell cycle progression, promoting macroautophagy, and inhibiting apoptosis. Its activity has been proven to be effective against neurodegeneration even outside the context of PD, raising interest in this protein and in the pathways it regulates as potential therapeutical targets.

The aim of this doctoral dissertation is providing further insights into novel and unconventional functions of PINK1 in cellular models relevant to neurodegeneration and aging.

The results of my work are organized as follows:

I) I generated and characterized iPSC-based cellular models from fibroblasts of PD patients carrying pathogenic variants of *PINK1*;

II) based on previous research findings from our group showing that PINK1 protects SH-SY5Y cells against apoptosis induced by staurosporine through preventing the proapoptotic cleavage of Beclin1, I analyzed the transcriptional regulation of *PINK1* after staurosporine treatment and investigated whether iPSC-derived neurons recapitulate the effects observed in SH-SY5Y cells;

III) I explored a novel phenotype of fibroblasts, SH-SY5Y cells and iPSC-derived neurons lacking a functional PINK1, i.e., the dysregulation of serine metabolism, highlighting a downregulation of serine biosynthetic genes after *PINK1* silencing and defects in neurogenesis in conditions of serine deprivation.

These findings shed light on different, lesser-known functions of the protein PINK1 and, most importantly, underline the value of iPSC-based systems to create models that better recapitulate the features of neurons *in vivo*, prompting the study of biological mechanisms in a disease-relevant context and in a comprehensive translational approach.

§

Il morbo di Parkinson è una comune malattia neurodegenerativa con incidenza e prevalenza in forte aumento. La sua eziologia è multifattoriale, determinata da una complessa interazione tra fattori genetici e ambientali. Un sottogruppo di pazienti, tuttavia, presenta rare forme ereditarie monogeniche di malattia di Parkinson.

PINK1 è un gene causativo di malattia di Parkinson ad esordio precoce con ereditarietà autosomica recessiva. Codifica una chinasi che riveste un ruolo centrale nell'omeostasi mitocondriale in quanto regolatrice della mitofagia, che è il processo di degradazione dei mitocondri disfunzionali attraverso l'autofagia. La proteina PINK1, tuttavia, esercita anche funzioni neuroprotettive e citoprotettive indipendenti dalla mitofagia, ad esempio favorendo la progressione del ciclo cellulare, promuovendo la macroautofagia, e inibendo l'apoptosi. La sua attività si è dimostrata efficace nel prevenire la neurodegenerazione anche al di fuori del contesto della malattia di Parkinson, alimentando interesse verso questa proteina e i pathways da essa regolati come potenziali obiettivi terapeutici.

Lo scopo di questa tesi dottorale è approfondire la conoscenza di funzioni nuove o alternative di PINK1 in modelli cellulari collegati alla neurodegenerazione e all'invecchiamento.

I risultati sono organizzati come segue:

I) ho generato e caratterizzato modelli cellulari basati su cellule staminali pluripotenti indotte da fibroblasti di pazienti parkinsoniani portatori di varianti patogenetiche di *PINK1*;

II) sulla base di pregressi risultati di ricerca del nostro gruppo, che mostrano che PINK1 protegge le cellule SH-SY5Y dall'apoptosi indotta dalla staurosporina attraverso

l'inibizione del clivaggio proapoptotico di Beclin1, ho analizzato la regolazione trascrizionale di *PINK1* dopo trattamento con staurosporina e ho investigato se i neuroni derivati da cellule staminali pluripotenti indotte ricapitolano gli effetti osservati in cellule SH-SY5Y;

III) ho esplorato un nuovo fenotipo di vari modelli cellulari (fibroblasti, cellule SH-SY5Y, e neuroni derivati da cellule staminali) privi di una forma funzionale di *PINK1*, ovvero la disregolazione del metabolismo della serina, rilevando una downregolazione dei geni biosintetici della serina in seguito a silenziamento di *PINK1* e difetti nella neurogenesi in condizioni di deprivazione di serina.

Questi risultati fanno luce su funzioni differenti e meno conosciute della proteina PINK1 e, soprattutto, evidenziano l'importanza di usare sistemi basati su cellule staminali per creare modelli che ricapitolino in maniera più fedele le caratteristiche dei neuroni *in vivo*, accelerando lo studio dei meccanismi biologici in un contesto coerente con la malattia e con un approccio traslazionale di larghe vedute.

2. General Introduction

2.1. Parkinson's Disease

Parkinson's Disease (PD) is a common and heterogeneous neurodegenerative disorder pathologically defined by distinctive intracellular protein aggregates and the loss of dopaminergic neurons in the *substantia nigra*. Neuronal degeneration and the consequent dopamine deficit in the basal nuclei result in the classic motor symptoms, which were first described as a recognizable clinical syndrome by James Parkinson in his 1817 *Essay on the Shaking Palsy*. After three decades, the neurologist Jean-Martin Charcot provided a detailed and systematic pathognomonic account of the disease, mentioning tremor, rigidity, slowness of movement, and postural instability as key signs and symptoms (Goetz, 2011).

Interestingly, references to the syndromic picture of PD are present since ancient times in Indian medicine, with a first full recapitulation of the symptoms provided by Charaka around 300 BCE (Ovallath & Deepa, 2013). The remedy prescribed by Sanskrit physicians against this affliction consisted of the leguminous fruits of *Mucuna pruriens*, from which levodopa was isolated in 1937 (Damodaran & Ramaswamy, 1937).

PD is the second most common neurodegenerative disorder after Alzheimer's disease and affects approximately 1-2% of the population over the age of 60 (Ascherio & Schwarzschild, 2016; Epidemiology of Parkinson's Disease, 2017; Willis et al., 2022). Its incidence increases exponentially with age, which is considered the strongest risk factor, peaking around 80 years (Kalia & Lang, 2015). Males are at higher risk than females, but epidemiological data show great heterogeneity in this regard, and several recent studies rather focused on differences in clinical manifestations and access to treatment between sexes (Bloem et al., 2021).

The number of people affected by PD globally has been growing more rapidly than any other neurological disease due to population aging, increasing industrialization, and other

unknown factors. This increase has led several authors to use the expression “Parkinson pandemic”, highlighting the societal burden of the disease, which is projected to surge in the next decades (Deuschl et al., 2020; E. R. Dorsey et al., 2018; Feigin et al., 2019).

2.1.1. Clinical Presentation and Diagnosis

The semiology of PD generally follows a classification in motor and nonmotor symptoms. Motor symptoms consist of low frequency resting tremor, muscular rigidity, bradykinesia, and postural instability. These are classically referred to as *cardinal symptoms* of PD (Váradi, 2020). Nonmotor symptoms are various and include sleep disorders, autonomic dysfunction, psychiatric disturbances, and cognitive impairment. Some nonmotor manifestations can precede the full presentation as a movement disorder; in this case, they can be referred to as *prodromal symptoms* (Bloem et al., 2021; Tolosa et al., 2021).
A systematic identification of early signs of PD is useful to prevent diagnostic delays, especially in the optic of potential disease-modifying treatments reaching the clinical setting (Armstrong & Okun, 2020; Simon et al., 2020). In fact, despite consistent advances in the definition of radiologic (Burciu et al., 2017) as well as serum/CSF biomarkers (Hall et al., 2016; Lin et al., 2019; Marques et al., 2019; Oosterveld et al., 2020), the diagnosis today remains, in clinical practice, entirely based on physical examination and history taking.
Univocal and internationally accepted criteria for the diagnosis of PD are not available, but several sets of guidelines have been proposed and often revised along the years, including United Kingdom Parkinson’s Disease Society Brain Bank (UKPDSBB), Gelb, and the most recent International Parkinson and Movement Disorder Society (MDS) PD criteria. Originally designed for use in research, the MDS-PD criteria have proven useful in the clinical setting, although their use is still limited in daily practice (Bloem et al., 2021; Marsili et al., 2018; Poston et al., 2022).
Most sets of criteria — including MDS-PD — start from the presence of Parkinsonism, defined as bradykinesia combined with either tremor or rigidity, or both. The recent MDS-PD criteria further included nonmotor symptoms in the diagnostic process, and clearly

described prodromal PD as a self-standing entity (Postuma et al., 2015). The proposed diagnostic process is based on a weighing system in which supporting criteria are compared to so-called *red flags*, i.e., signs and symptoms providing an argument against the diagnosis of PD (Bloem et al., 2021; Postuma et al., 2015).

Typical parkinsonian tremor is low in frequency (4-6 Hz), often presenting unilaterally in one extremity in the early disease stages and reduced or suppressed during movement. The term *resting tremor*, however, can be misleading, as complete relaxation often eliminates it. It is frequently the symptom bringing patients to seek medical attention, but it is neither sensitive nor specific for PD (Hayes, 2019; Váradi, 2020).

Bradykinesia and *akinesia* are synonyms for slowness of movement and deficit of spontaneous motor activity. They are in a strict relationship with several pathognomonic signs of PD, such as hypomimia (or *masked facies*, loss of facial expressivity), freezing of movement and gait, micrographia (writing becoming small and cramped), slowness and monotony of speech, difficulty in swallowing and sialorrhea (Hayes, 2019; Váradi, 2020).

Muscle rigidity or *rigor*, due to increased tonus, is sometimes shown as a light flexion of elbows, core, and neck, and becomes evident during physical examination as a higher resistance to passive movement, often resulting in a jerky motion referred to as cogwheel phenomenon (Hess & Hallett, 2017).

Postural instability and gait disturbances often appear later than other motor symptoms and result from decomposition of movements, disappearance of arm swinging, forward or backward leaning, reduced stride length, and a general deficit of reflexes ensuring postural stability (Hayes, 2019; Váradi, 2020).

Motor symptoms are almost invariably accompanied by a constellation of nonmotor symptoms, which vary from patient to patient and can precede or follow classic parkinsonism in onset. Anosmia or hyposmia (the loss or reduction of the sense of smell), constipation, and REM sleep behavior disorder (RBD) are very frequent sensory, autonomic, and sleep-related conditions that can accompany or precede motor symptoms (Haehner et al., 2009; Váradi, 2020). Other PD manifestations affecting the vegetative nervous system include circulatory disturbances (e.g., orthostatic

hypotension, related to cardiac autonomic denervation), urinary complaints, sexual dysfunction, and deficits in thermoregulation (Lamotte & Benarroch, 2021; Post et al., 2008; Rafanelli et al., 2019).

Psychiatric, cognitive, and mood disorders are also part of the clinical picture, and include depression, apathy, anxiety, psychosis and hallucination (which may also be related to pharmacologic stimulation of the dopaminergic system), and dementia. Cognitive impairment may affect up to 30-40% of PD patients, frequently in the later phases of the disease, and is thought to originate from a spread of the neurodegenerative process to cortical brain regions. Executive functions are particularly affected in PD-dementia, with a general slowing of thought processes and difficulty in planning and executing tasks, in contrast with other forms of dementia such as Alzheimer's, in which memory and language are most affected (Hanagasi et al., 2017; Petrelli et al., 2015; Sezgin et al., 2019).

2.1.2. Etiology and Pathophysiology

PD is described as a genetic and sporadic neurodegenerative disease. Apart from the notable exception of purely monogenic forms of the disease, accounting for ~5% of the cases, its cause is a complex interaction between genetic and environmental aspects (Bloem et al., 2021; Reed et al., 2019). Several environmental or behavioral factors have been identified as either positively or negatively correlated with the risk of developing PD in distinct epidemiological studies. Risk factors include pesticides (R. Dorsey et al., 2020), head injury (Camacho-Soto et al., 2017; Mackay et al., 2019), rural living and agricultural occupation, chronic β-blocker treatment (Noyce et al., 2012). Factors with a supposedly protective role include tobacco smoke, coffee consumption, anti-inflammatory drugs, increased uremia, and physical activity (Fang et al., 2018; Noyce et al., 2012; Rossi et al., 2018). In these studies, however, statistical associations are often not complemented by an explanation of the causal relationship, and their clinical utility is limited by the intrinsic difficulty of analyzing a patient's ever-changing exposure to environmental factors (Bloem et al., 2021).

The identification of genetic causal and predisposing variants is useful not only to offer a definite diagnosis and etiological explanation to a subset of patients, but also to provide precious insight on the molecular pathways responsible for the disease. An account of the most relevant genes involved in PD pathogenesis is in section 2.1.3.

The central neuropathological finding in PD is the progressive degeneration of dopaminergic neurons in the *substantia nigra pars compacta* (SNpc), leading to dopamine depletion in the basal nuclei, in particular in the areas of the striatum that receive dopaminergic endings, responsible for motor functions. Motor symptoms, however, do not become apparent until after the loss of 70-80% of nigrostriatal connections; during the early stages of the disease, in fact, compensatory mechanisms such as a switch towards more anterior corticostriatal circuits and recruitment of alternative cortical regions, are activated (Bernheimer et al., 1973; Michely et al., 2015). The neurodegenerative process is not limited to the SNpc, but also involves other regions of the central nervous system (CNS), resulting in nonmotor symptoms that are hardly responsive to dopaminergic therapy (Exner et al., 2012).
A second pathological hallmark of PD is the intracellular accumulation of misfolded proteins, lipids, and organelle parts, forming definite histological features known as Lewy Bodies and Lewy neurites. These aggregations are composed of α-synuclein, ubiquitin, neurofilament protein, mitochondria, lysosomes, and membrane lipids among others. Lewy pathology is not exclusive to neurons, but rather widespread also in tissues outside the CNS such as the skin or salivary glands, providing an opportunity for novel histopathological diagnostic means (Chahine et al., 2020; Shahmoradian et al., 2019; Spillantini et al., 1997). A great uncertainty remains concerning the pathogenic role of Lewy Bodies, which may be a marker, rather than a cause, of the disease (Espay & Okun, 2023).

2.1.3. Genetics

Variants in numerous genes have been linked to PD as probable or definite causal factors. Several authors highlighted that an inverse relationship subsists between the frequency and the penetrance of genetic variants, defining a spectrum in which more than 90 variants that are common in the population may constitute a weak risk factor for the development of PD, uncommon variants such as those in the GBA gene are a strong risk factor, and very rare variants show complete penetrance, defining fully monogenic forms of PD with either autosomal dominant or autosomal recessive patterns of inheritance (Cherian & Divya, 2020; Day & Mullin, 2021).

Gene	**Inheritance**	**PD Phenotype**	**Penetrance**
GBA	AD	Typical	Variable
LRRK2	AD	Typical	Variable/high
SNCA	AD	Early-onset	High
VPS35	AD	Typical	High
EIF4G1	AD	Typical	?
CHCHD2	AD	Typical	?
TMEM230	AD	?	?
LRP10	AD	PD, PDD, DLB	?
NUS1	AD	Early-onset	?
PRKN	AR	Early-onset	High
PINK1	AR	Early-onset	High
PARK7 (DJ-1)	AR	Early-onset	High
DNAJC6	AR	Early-onset	High
ARSA	AR	?	?

Table 1. List of PD genes. AD: autosomal dominant; AR: autosomal recessive; PDD: PD dementia; DLB: dementia with Lewy bodies.

The gene *GBA*, encoding glucocerebrosidase (a lysosomal enzyme catalyzing the degradation of glucocerebroside/glucolylceramide), is described either as the strongest genetic risk factor for PD, with an odds ratio of 5, or as a causative gene with very low penetrance and AD inheritance. Heterozygous variants in *GBA* are found in ~10% of PD patients (Klein & Westenberger, 2012; Sidransky et al., 2009; Sidransky & Lopez, 2012; Skrahina et al., 2021). Biallelic loss-of-function mutations in GBA cause Gaucher Disease, a lysosomal storage disorder.

LRRK2 encodes Leucine-rich kinase 2, a large multidomain protein with GTPase and serine/threonine kinase activity. Most reported mutations are harbored in these catalytic domains and are characterized by a gain-of-function mechanism. This gene accounts for most genetic cases of PD, being mutated in 3-41% of familial cases in different populations and ethnic groups (Cherian & Divya, 2020; Day & Mullin, 2021). Being such a complex multidomain protein, LRRK2 is involved in several biological processes, including synaptic plasticity, membrane trafficking, autophagy, and protein synthesis (Cookson, 2012; S. Lee et al., 2012; Martin et al., 2014; Sanna et al., 2012).

Variants in *SNCA* were the first identified genetic causal factor of PD, but they are very rare. The gene encodes α-synuclein, a protein which was then found to be the main component of Lewy Bodies (Spillantini et al., 1997). Mutations responsible for PD are gene multiplications, variations in the promoter region leading to increased expression of the wild-type protein, as well as missense mutations favoring aggregation (Book et al., 2018). α-synuclein is abundantly expressed in neurons and involved in trafficking of vesicles and release of neurotransmitters at presynaptic terminals; it has an *intrinsically disordered* structure which causes a high propensity to aggregate (Diao et al., 2013; Fakhree et al., 2018).

VPS35 encodes Vacuolar protein sorting 35, which is part of the Retromer complex, involved in trafficking of endosomal vesicles and tubules in neuronal dendrites (Choy et

al., 2014). Pathogenic variants result in accumulation of α-synuclein and in mitochondrial dysfunction in neurons (Hanss et al., 2021).

Mutations in *EIF4G1*, *CHCHD2, TMEM230*, *LRP10*, and *NUS1* have been reported in few families where PD is inherited with autosomal dominant pattern, but evidence in support of a causative role for these genes is considered insufficient (Bandres-Ciga et al., 2020; Chartier-Harlin et al., 2011; Funayama et al., 2015; Kalia & Lang, 2015).

PRKN, *PINK1*, and *PARK7* are the genes unequivocally linked to AR familial forms of PD, ordered from the most frequent to the least frequent causal factor. The clinicopathological picture is similar in patients with biallelic loss-of-function variants in either of these genes, showing early onset disease (EOPD) with a rather typical slow progression and good response to levodopa, with loss of dopaminergic neurons and gliosis in the SNpc, but not always showing Lewy Bodies (Klein & Westenberger, 2012).
PRKN encodes Parkin, a E3 ubiquitin ligase involved in mitophagy, the autophagic degradation of depolarized mitochondria, as well as in maintenance of mtDNA integrity and mitochondrial structure, and in the proteasomal degradation system (Rothfuss et al., 2009; Zhang et al., 2000). PINK1 acts upstream of Parkin in the mitophagy pathway, phosphorylating ubiquitin, Parkin, and other substrates to promote degradation of dysfunctional organelles; it is then involved in antiapoptotic, immune and inflammatory functions (Day & Mullin, 2021).

The genes *ATP13A2*, *FBXO7*, and *PLA2G6* are associated to atypical parkinsonism-related syndromes, while different variants in the gene *ARSA* have been proposed to be causative of autosomal-recessive PD or protective (Bandres-Ciga et al., 2020).

Further understanding of PD genetics came, in the last decade, from several large genome-wide association studies (GWAS) that identified over 90 independent risk loci associated with sporadic PD, partially overlapping with regions containing causal genes of familial/monogenic PD. Numerous GWAS strengthened the so-called *common*

disease-common variant hypothesis, explaining the genetic component in PD as the combined effect of numerous common low-risk alleles (Bandres-Ciga et al., 2020).

2.2. PINK1

2.2.1. Gene, Expression, Protein Synthesis, Structure, and Subcellular Localization

The gene *PINK1* was identified in 2001 as a transactivated target of *PTEN* in ovarian cancer (Unoki & Nakamura, 2001) and associated to autosomal recessive EOPD in 2004 (Valente et al., 2004).

The transcript of the *PINK1* gene is expressed in various tissues, with particularly high levels in skeletal and cardiac muscle, testis, adrenal gland, and all brain areas (Kawaji et al., 2017; Noguchi et al., 2017). The protein PINK1 similarly shows a widespread tissue distribution, although at low levels in physiological conditions (Uhlén et al., 2015).

Human *PINK1* encodes a 581-amino acid, ~63 kDa protein characterized by a N-terminal mitochondrial targeting sequence (MTS, residues 1-77), a short transmembrane peptide (TM, residues 94-110), a serine/threonine protein kinase domain (residues 156-511) with three unique insertions, and a C-terminal extension (CTE, residues 511-581).

Figure 1. Schematic structure of human PINK1.

The structure of human or mammalian PINK1 has not yet been resolved by X-ray diffraction or nuclear magnetic resonance, but the orthologues from two insect species, *Tribolium castaneum* and *Pediculus humanus corporis*, have been heavily used for this kind of studies since 2017 (Kumar et al., 2017; Schubert et al., 2017). *In silico* models of the human protein exist since 2017 (Puschmann et al., 2017). The greatest limits in tridimensional determination are the N-terminal region (MTS and TM), which seem to be

rather unstructured, and the three insertions within the kinase domain, which show high inter-species variability.

PINK1, in most cells, co-localizes with mitochondrial markers. However, functional studies demonstrated a relevant role also for a cytoplasmic post-translationally produced isoform (Thul et al., 2017).

2.2.2. Functions of PINK1 in Health and Disease: Mitophagy

The nuclear-encoded protein is synthesized in the cytosolic compartment and immediately directed to mitochondria through the MTS. Here, it presumptively crosses both the outer and inner mitochondrial membranes via the TOM/TIM complex (Lazarou et al., 2012). The N-terminus is processed by matrix and inner membrane proteases including MPP, m-AAA, ClpX, and PARL; finally, the cleaved isoform is released in the cytosol and degraded by the proteasome (Eldeeb & Ragheb, 2020; Guardia-Laguarta et al., 2019; Yamano & Youle, 2013). This mechanism maintains the physiological concentration of full-length PINK1 at low levels in conditions of conserved mitochondrial membrane potential.

Conversely, in the event of mitochondrial membrane depolarization, the processes of PINK1 import and cleavage come to a halt, resulting in a sizeable accumulation of the protein on the outer membrane. Different studies suggest that this effect may be either due to transport arrest and entrapment in the TOM complex (Lazarou et al., 2012), or to the inactivation of intramitochondrial proteases after the loss of membrane potential (Deas et al., 2011; Greene et al., 2012; Jin et al., 2010; Meissner et al., 2011). In this position, PINK1 dimerization and autophosphorylation occur, leading to kinase activation (Okatsu et al., 2013; Puschmann et al., 2017). Two recent structural studies showed that, within the dimer, a N-terminal helix, located between the TM and kinase domain, interacts with the CTE and with the TOM complex, allowing protein docking and autophosphorylation in *trans* configuration, eventually causing a conformational change that switches on ubiquitin kinase activity (Gan et al., 2021; Rasool et al., 2022).

PINK1 phosphorylates ubiquitin at residue Ser65 and the ubiquitin-like domain of Parkin, causing its activation and the downstream ubiquitination of several mitochondrial proteins (Kane et al., 2014; Kazlauskaite et al., 2014; Koyano et al., 2014; Schubert et al., 2017).

Among the targets of Parkin are the GTPases Mitofusin 1 and 2, responsible for mitochondrial fusion, which are primed for degradation through the ubiquitin-proteasome system (UPS), preventing fusion of depolarized mitochondria with healthy organelles (Tanaka et al., 2010). The ubiquitination of RHOT1, instead, results in the arrest of mitochondrial movement (Wang et al., 2011). This process is amplified by a positive feedback mechanism, with recruitment of more Parkin units and formation of K63-linked ubiquitin chains (Wade Harper et al., 2018). These are recognized by p62/SQSTM1 and other proteins of the autophagy receptor family, which in turn bind LC3 and GABARAP on the autophagosome surface resulting in the engulfment and degradation of the depolarized organelle via the autophagy-lysosomal pathway (Heo et al., 2015; Lazarou et al., 2015; Richter et al., 2016). This process is altogether known as *mitophagy*.

Although the molecular steps of PINK1-Parkin mitophagy have been elucidated in detail, most experiments on this subject took place in immortalized cancer cell lines or simple animal models such as *Drosophila melanogaster*, often using overexpressed recombinant proteins and high concentrations of depolarizing agents such as carbonyl cyanide m-chlorphenyl hydrazine (CCCP) or valinomycin. Evidence in support of PINK1-dependent mitophagy *in vivo* is lacking, and whether defects in this pathway may contribute to neurodegeneration in the human brain remains an open question (Brunelli et al., 2020; Chen, Wang, et al., 2022).

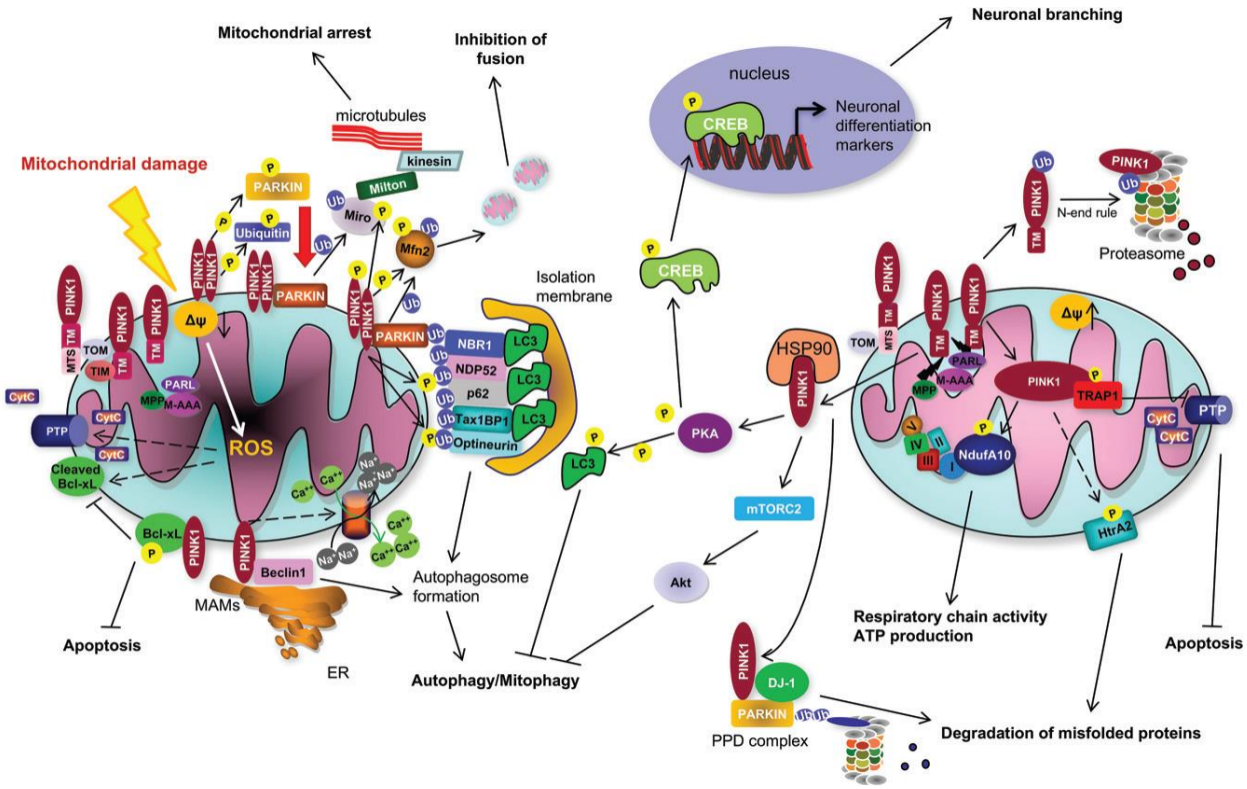

Figure 2. Functions of PINK1 in human pathology. Adapted from PINK1 in the limelight: multiple functions of an eclectic protein in human health and disease *(Arena & Valente, 2017).*

2.2.3. PINK1 and Mitochondria-Associated ER Membranes

Besides mitophagy, PINK1 is associated to several cellular processes taking place in mitochondria-associated ER membranes (MAMs), the contact sites between ER and mitochondria (Yoboue & Valente, 2020). These structures, for example, give origin to the omegasome, the membranous construct which evolves to become the autophagosome (Hamasaki et al., 2013). In response to mitophagic or proautophagic stimuli Beclin1, a master regulator of autophagy, binds with PINK1 in the MAMs; this protein-protein interaction concurs to the regulation of early autophagosome formation (Gelmetti et al., 2017; Michiorri et al., 2010).

Another key cellular function taking place in this subcellular compartment is calcium homeostasis. This divalent cation, in fact, is stored in high concentration within the ER and exchanged with other organelles and the cytoplasm through specialized channels

located in the MAMs; a dysregulation of this mechanism was observed in models of neurodegeneration (K. S. Lee et al., 2018; Patergnani et al., 2011). Several studies highlighted a dysregulation of calcium exchange in PINK1-deficient cellular and animal models, proposing different mechanisms to explain the observed effect (Gandhi et al., 2009; Kostic et al., 2015; Marongiu et al., 2009; Soman et al., 2017).

2.2.4. Antiapoptotic and Pro-Survival Functions of PINK1

Mitophagy can account for an antiapoptotic effect by removing depolarized mitochondria before they activate the intrinsic pathway of apoptosis (Arena & Valente, 2017). However, other mechanisms through which PINK1 may hinder cell death have been described. Following proapoptotic stimuli the mitochondrial kinase phosphorylates a Bcl-2 superfamily member named Bcl-xL, preventing its cleavage and release of a fragment which is a known strong inducer of apoptosis (Arena et al., 2013).

2.2.5. PINK1 and Immunity

A recent, intriguing line of research linked PINK1 with molecular pathways of immunity. Through the regulation of mitochondria-derived vesicles (MDVs), PINK1 and Parkin participate in a process of adaptive immunity named mitochondrial antigen presentation (Matheoud et al., 2016). PINK1 KO mice, generally asymptomatic, develop pathological neurodegeneration and PD-like symptoms in response to intestinal infection due to the activation of an autoimmune mechanism mediated by mitochondrial antigen presentation (Matheoud et al., 2019).

In addition, PINK1 and Parkin have been reported to interact with the cGAS-STING pathway. Their loss of function, in fact, caused an increase in inflammatory cytokines leading to neurodegeneration in mouse models (Sliter et al., 2018). This result is seemingly in contrast with another study showing that PINK1 knockdown causes a decrease in cytokine production in response to viral infection via the RLR pathway (Zhou

et al., 2019). An involvement of PINK1 in antiviral response finds further support from the work of other research groups (Kim, Khan, et al., 2013; Kim, Syed, et al., 2013).

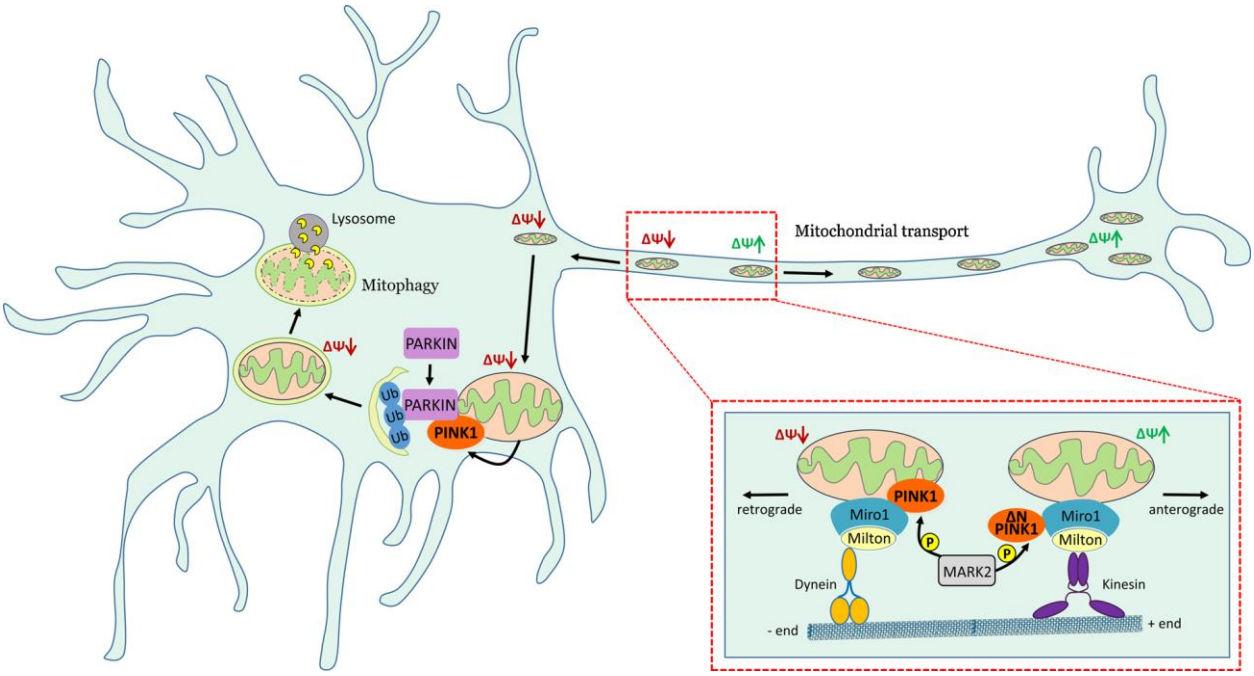

Figure 3. Overview of the neuroprotective functions exerted by PINK1 in neurons, adapted from Mechanisms of neurodegeneration in Parkinson's Disease: keep neurons in the PINK1 *(Brunelli et al., 2020).*

3. Aims and Objectives

Despite being a rare cause of PD, the loss of function of PINK1 has been widely studied as a reliable disease model, in the hope of discovering or developing neuroprotective approaches that could benefit not only patients with pathogenic variants, but a large group of subjects affected by PD or by other neurodegenerative diseases. This protein has been proven to play an important role in several molecular pathways relevant for cell survival and homeostasis, including, among others, the modulation of mitochondrial dynamic properties and function, the regulation of cell cycle progression, protection from apoptotic stimuli, and the participation in immune mechanisms.

PINK1/Parkin-dependent mitophagy, the process through which damaged mitochondria are removed by means of autophagy, has been investigated with particular biochemical detail. However, most studies concerning the role of PINK1 in the mitophagic pathway have been performed in immortalized cell lines and/or with recombinantly overexpressed proteins. Whether all the molecular steps of mitophagy take place *in vivo* in the human brain and, most importantly, whether a deficit in the mitophagic machinery is the central cause of neurodegeneration in PD remain open questions.

In parallel, smaller attention has been dedicated to studying non-mitophagic functions of PINK1 within and without mitochondria. In this regard, the research group led by Prof. Enza Maria Valente demonstrated in 2010 that PINK1 binds the pro-autophagic protein Beclin1, inducing the activation of the autophagic machinery both in basal conditions and during starvation (Michiorri et al., 2010). This protein-protein interaction was later shown by the same authors to regulate autophagosome formation in the mitochondria-associated ER membranes (MAMs), the contact sites between ER and mitochondria (Gelmetti et al., 2017). Another binding partner of PINK1 was identified within the interactome of Beclin1, namely Bcl-xL, a member of the Bcl-2 superfamily involved in the regulation of autophagy and apoptosis (Arena et al., 2013). Preliminary results from our group suggested that PINK1 could protect cells from staurosporine-induced apoptosis by impairing the proapoptotic cleavage of Beclin1.

The overarching purpose of this doctoral project was providing further insights into novel and unconventional functions of PINK1 in cellular models relevant to neurodegeneration and aging. To move towards this aim, on one hand I generated iPSC-based cellular models carrying new pathogenic variants of PINK1, on the other I performed studies concerning its non-mitophagic activities using more simple cell models such as fibroblasts and SH-SY5Y neuroblastoma cells. Such studies had the following objectives.

1) Completing the characterization of the role of PINK1 in the context of staurosporine-induced apoptosis.
2) Tackling a novel candidate function of PINK1, verifying whether this protein regulates serine metabolism in different cellular models.
3) Performing a preliminary analysis of the functional effects of PINK1 deficiency in the context of serine deprivation.

4. Material and Methods

4.1. Cell Lines

Several cell lines have been used for the experiments described in this work, including cancer cell lines (SH-SY5Y neuroblastoma cells, HEK293T cells), human primary dermal fibroblasts, iPSCs and iPSC-derived cells (smNPCs, midbrain dopaminergic neurons, astrocytes). Recipes and instructions for the preparation of cell media are described in the *Appendix*. All cells were maintained in humidified incubators (Heraeus HERAcell) at 37°C and 5% CO_2.

4.2. Culture and Maintenance of Cancer Cell Lines

Wild-type and PINK1 KO SH-SY5Y neuroblastoma cells and HEK293T cells were grown in *Complete DMEM 10%* unless otherwise specified. These cells were grown on sterile, uncoated, cell culture-tested vessels such as 6-well-plates (Sarstedt #83.3920) or T75 flasks with filter caps (Sarstedt #83.3910).

Cells were passaged when appropriate using Trypsin-EDTA (EuroClone #ECM0920D) at 37°C after a wash with DPBS without calcium and magnesium (Thermo Fisher Scientific #14190169).

SH-SY5Y cells and HEK293T cells were regularly banked in liquid nitrogen in 900 µL *Complete DMEM 10%* with 100 µL dimethyl sulfoxide (DMSO, EuroClone #APA36720250) in Nalgene® cryogenic vials (Merck #Z359033); cell freezing was performed in a Mr. Frosty™ Freezing Container (Thermo Fisher Scientific #5100-0001) placed at -80°C to achieve a rate of cooling of 1°C/min. Cell thawing was performed by placing a cryovial in a 37°C water bath for 2 minutes, followed by a centrifugation at 300g for 5 minutes to remove DMSO.

4.3. Fibroblasts

Primary dermal fibroblasts derived from skin biopsies of patients and healthy subjects were maintained in *Complete DMEM 10%*. When confluent, these cells were passaged using Trypsin-EDTA (EuroClone #ECM0920D) for 5-10 minutes at 37°C after a wash with DPBS without calcium and magnesium (Thermo Fisher Scientific #14190169). Cryopreservation and thawing of fibroblasts were performed with the same reagents and protocols described in *section 4.2.* for SH-SY5Y cells.

	Sex	**Phenotype (onset)**	**PINK1 genotype (c.)**	**Protein variant (p.)**
ITME21	F	PD patient (38)	1311G>A homozygous	W437X homozygous
ITME31	M	PD patient (39)	502G>C homozygous	A168P homozygous
ITME33	F	PD patient (30)	1311G>A homozygous	W437X homozygous
ITME66	M	PD patient (41)	1311G>A homozygous	W437X homozygous
NG6138	M	PD patient (35)	1366C>T/ 1600_1602dupCAA	Q456X/Q534dup
NG6301	M	PD patient (50)	1366C>T/1448_1449insTCAG TGCCTCCAGACTTGAG	Q456X/R483SfsX7
HDF108	M	Healthy subject	Wild-type	Wild-type
HDF109	F	Healthy subject	Wild-type	Wild-type

Table 2. Patients and healthy subjects, with indication of sex (M: male, F: female), age of disease onset (years), and characterization of PINK1 variants (c. and p.).

4.4. Reprogramming of Fibroblasts to iPSCs

Reprogramming of fibroblasts to iPSCs was performed with the CytoTune™-iPS 2.0 Sendai Reprogramming Kit (Thermo Fisher Scientific #A34546), which uses a modified, non-transmissible form of Sendai virus to deliver three vectors encoding for the Yamanaka factors Oct3/4, Klf4, Sox2, and c-Myc. With this system, reprogramming vectors do not integrate into the genome of the target cell avoiding potential disruption of important genes.

Two days before transduction, 2 x 10^5 fibroblasts passage 2-4 were plated in replicate wells of a 6-well-plate in *"CytoTune" Fibroblast Medium*. On the day of transduction, fibroblasts in one well were detached with Trypsin-EDTA and counted to determine the volume of virus mixture needed to reach the required MOI in the replicate well, according to the manufacturer's instructions. The transduction medium was changed the following day and during the following 7 days with fresh *"CytoTune" Fibroblast Medium*. On day 7 post-transduction, transduced cells were passaged and plated in culture vessels coated with Vitronectin (Thermo Fisher Scientific #A31804). On the following day, *"CytoTune" Fibroblast Medium* was replaced with *E8 Flex Medium* (Thermo Fisher Scientific #A2858501), changed the day after seeding and then every second day for 2-3 weeks. During this time, iPSC colonies with a distinct morphology emerged between transduced fibroblasts.

Visible colonies were picked with a sterile syringe needle and plated in 6-well plates coated with Vitronectin. was. The iPSCs were split at a 1:3 or 1:4 ratio using 0.5 mM EDTA (diluted from UltraPure™ 0.5M EDTA, pH 8.0, Thermo Fisher Scientific #15575038). iPSCs were cultured at 37°C, 5% CO_2 in a dedicated incubator.

iPSCs were maintained in *E8 Flex Medium* during the reprogramming process and for the first 5-6 cell passages and then switched to *Homemade E8 Medium*, requiring daily media changes.

iPSCs were cryopreserved in 900 µL *E8 Flex Medium* or *Homemade E8 Medium* with 100 µL DMSO with the same procedure used for SH-SY5Y cells and fibroblasts.

4.5. Derivation of smNPCs and Midbrain Dopaminergic Neurons from iPSCs (Reinhardt's Protocol)

The differentiation of iPSCs to midbrain dopaminergic neurons was performed in two steps, namely from iPSCs to smNPCs and from smNPCs to midbrain dopaminergic neurons, following Reinhard's Protocol or adaptations thereof (Reinhardt et al., 2013). smNPCs are neuroepithelial neuronal progenitor cells that can be expanded and maintained virtually indefinitely.

smNPCs were derived from iPSCs as described in the original protocol (Reinhardt et al., 2013). First, iPSCs were cultured for 2 days in modified *Homemade E8 Medium* without FGF2 and heparin, with addition of 10 µM SB-431542 (Merck #S4317), 1 µM dorsomorphin (Merck #P5499), 3 µM CHIR-99021 (MedChemExpress #HY-10182), 0.5 µM purmorphamine (Merck #SML0868). Then, cells were switched to *N2B27 Medium* supplemented with 10 µM SB-431542 (Merck #S4317), 1 µM dorsomorphin (Merck #P5499), 3 µM CHIR-99021 (MedChemExpress #HY-10182), 0.5 µM purmorphamine (Merck #SML0868) for 2 days, with daily feeding. Finally, from differentiation day 4, cells were grown in standard *smNPC Maintenance Medium*, which was changed every second day. During this process, the morphology of cells changes, with darker, cell-dense, tridimensional structures called neuroepithelial ridges developing on top of iPSC colonies. These structures, that sometimes detach in the form of floating cell aggregates, can be "picked" with a pipet tip approximately at day 5-6, and plated on plates coated with Geltrex (Thermo Fisher Scientific #A1413302). The obtained smNPCs should be passaged several times using Accutase® (Merck #6964) until a cell population showing consistent morphology is obtained. These cells can be passaged virtually indefinitely, can be cryopreserved and thawed multiple times, and can in case be genetically manipulated.

For neuronal differentiation, smNPCs were cultured for 8 days in *N2B27 Medium* supplemented with 1 µM purmorphamine (Merck #SML0868), 100 ng/mL FGF8b (Peprotech #100-25), and 200 µM ascorbic acid (Merck #A8960). During this time, cells proliferate quickly and need to be passaged to larger, Geltrex-coated culture vessels with Accutase® (e.g., from one well of a 6-well-plate to a T25 flask, and then from T25 to T75 flask). Afterwards, the growth medium was changed to N2B27 Medium with 0.5 µM purmorphamine (Merck #SML0868) and 200 µM ascorbic acid (Merck #A8960) for 2 days. Finally, the medium was switched to *Neuron Maturation Medium*, requiring changes every second day, and neurons were cultured until differentiation day 30, unless otherwise specified.

4.6. Differentiation of Astrocytes from smNPCs

To obtain the differentiation of smNPCs into astrocytes, $4x10^5$ smNPCs were plated in a Geltrex-coated well of a 6-well-plate in *smNPC Maintenance Medium*. After 2 days, the medium was changed to *smNPC Maintenance Medium* with addition of 20 ng/mL FGF2 (Peprotech #100-18B), in which cells were cultured for 2 days.

After this, cells were passaged into new Geltrex-coated 6-well-plates in DMEM/F-12 medium (Thermo Fisher Scientific #21331046) with 1% L-glutamine (EuroClone #ECB3000D), 1% penicillin/streptomycin (EuroClone #ECB3001D), 1% N-2 Supplement (Thermo Fisher Scientific #17502048), 0.5% B-27™ Supplement (Thermo Fisher Scientific #17504044), 40 ng/mL EGF (Peprotech #AF-100-15), 40 ng/mL FGF2 (Peprotech #100-18B), 1.5 ng/mL LIF (Peprotech #AF-300-05). Cells were maintained in this medium and passaged at least 4 times, until showing a definite neural stem cell morphology. At this point, $1x10^6$ cells were seeded in a Geltrex-coated T25 flask in the same medium. After 2 days, the medium was switched to *Astrocyte Medium*.

Astrocytes were maintained for differentiation and maturation in the same Geltrex-coated culture vessel for 40 days with changes of *Astrocyte Medium* every 2-3 days. At day 40, astrocytes were split with a ratio 1:2 into fresh Geltrex-coated T25 flasks and cultured until day 60. This protocol is an adaptation of a previously described one (Palm et al., 2015).

4.7. Differentiation of Neurons as Neurospheres from smNPCs

Neurospheres are an established culture system used to investigate neurogenesis *in vitro* (da Silva Siqueira et al., 2021). To obtain neurospheres as a model of dopaminergic neurogenesis, smNPCs were cultured in uncoated 6-well-plates with orbital agitation at 37°C, 5% CO_2 for 4 days and then plated on Geltrex-coated 6-well-plates and grown for 2 additional days.

The media used throughout the differentiation process to assess the impact of L-serine on neurogenesis were *Ser/Gly-free N2B27 Medium* supplemented with 1 ng/mL TGFβ3

(Peprotech #100-36E), 500 µM dbcAMP (Santa Cruz #sc-201567C), 20 ng/ml BDNF (Peprotech #450-02), 10 ng/ml GDNF (Peprotech #450-10), 200 µM ascorbic acid (Merck #A8960), with or without addition of 0.4 mM L-serine (Merck #S4311) and 0.4 mM Glycine (Merck #G8790).

The estimation of neurosphere diameter was performed on Fiji-ImageJ (Schindelin et al., 2012) by thresholding images, using the automated tool for measuring the surface area of projections of neurospheres, and then calculating the diameter from the area of circles. Quantifiable features of the neuritic arborization grown from neurospheres were obtained with the plugin SNT Neuroanatomy on Fiji-ImageJ (Arshadi et al., 2021).

4.8. iPSC Trilineage Differentiation

iPSC *in vitro* Trilineage Differentiation into endoderm, mesoderm, and ectoderm was performed with the StemMACS™ (Miltenyi Biotech #130-115-660) Trilineage Differentiation Kit according to the manufacturer's instructions.

4.9. DNA Extraction

DNA extraction from cultured cells has been performed with a standard salting-out technique as follows.

1. Resuspending and washing cells in TE 20:5 buffer (Tris 20 nM, EDTA 5 nM).
2. Overnight lysis of phospholipidic membrane and proteins at 37°C in 10 mg/mL proteinase K (Thermo Fisher Scientific) and 10% Sarcosyl to induce cell membrane lysis and partly remove DNA binding proteins.
3. Precipitation of genomic DNA using a combination of supersaturated NaCl and isopropanol solutions, followed by washing in 100% ethanol and complete evaporation of ethanol at room temperature for 1 hour.
4. Elution of the purified genomic DNA in TE 20:1 buffer (Tris 20 nM, EDTA 1 nM) on a spinning wheel until the loose DNA pellet completely disappears.

An alternative DNA extraction method has been used for samples needed for molecular karyotyping, namely extraction on column with NucleoSpin® Blood columns (Macherey-Nagel #740951.50) following manufacturer's instructions.
The concentration and quality of DNA samples have been assessed with a Nanodrop 1000 spectrophotometer (Thermo Fisher Scientific) at λ=260 nm. 260/280 and 260/230 ratios have been considered acceptable between 1.8 and 2.3. Purified DNA has been conserved at -20°C.

4.10. RNA Extraction

RNA isolation from cultured cells has been performed with TRIzol™ Reagent (Thermo Fisher Scientific #15596026) followed by purification on column with Direct-zol™ RNA Miniprep Plus Kit (Zymo Research #R2072) according to manufacturer's instructions, including on-column DNase treatment for 15 minutes at RT. In general, cells from one well of a 6-well-plate have been resuspended in 600 µL of TRIzol™ Reagent; hard-to-break cells, such as fibroblasts, underwent an additional step to help breaking membranes, i.e., a passage through a syringe needle. The samples were then loaded on column, equilibrated, treated with DNase, and washed following the kit's instructions. The elution buffer was added directly onto the column membrane and left for one minute of incubation at RT before elution.
RNA concentration and purity have been assessed with a Nanodrop 1000 spectrophotometer (Thermo Fisher Scientific) for each sample. 260/280 and 260/230 ratios have been considered acceptable between 1.8 and 2.3 and optimal if $2 \leq 260/280 \leq 2.2$ and $2.1 \leq 260/230 \leq 2.3$. Purified RNA has been conserved at -80°C.

4.11. Retrotranscription

Reverse transcription of RNA to cDNA has been performed with the High-Capacity RNA-to-cDNA™ Kit (Thermo Fisher Scientific #4387406) according to the manufacturer's instructions. For each sample, 1000 ng of RNA have been mixed with 10 µL of 2x RT

Buffer and 1 µL of 20x RT Enzyme, adding nuclease-free water up to a total volume of 20 µL. For each set of reactions, two different negative controls have been prepared to test for contamination from genomic DNA, i.e., a “no-template” control (NTC) without template RNA and a “no-RT” control (RT-) without RT enzyme.
The reverse transcription reaction was performed in a S1000™ thermal cycler (Bio-Rad) set with the following program:

37°C	60 minutes
95°C	5 minutes
4°C	∞

cDNA samples were stored at -20°C.

4.12. Polymerase Chain Reaction (PCR)

Polymerase chain reactions (PCRs) were performed using FIREPol® DNA Polymerase (Solis Biodyne #01-01-02000) according to the manufacturer’s instructions on T100 Thermal Cyclers (Bio-Rad).
When appropriate, reaction products were analyzed by agarose gel electrophoresis. Gels were made with Topvision Agarose Tablets (Thermo Fisher Scientific #R2802) in TBE buffer (Thermo Fisher Scientific #15581028); images were acquired with Chemidoc XRS+ (Bio-Rad).

4.13. Real-Time PCR (qPCR)

Real-Time PCR (qPCR) was performed to quantitatively evaluate gene expression in different cells or different conditions, using cDNA as template (RT-qPCR). Each reaction was set up mixing 15 µg of template cDNA diluted in nuclease-free water with 10 µL of PowerUP™ SYBR™ Green Master Mix (Thermo Fisher Scientific #A25742) and 0.6 µL of primer mix (containing 40 mM forward primer and 40 mM reverse primer).
The reaction was performed on a Real-Time PCR CFX Connect cycler (Bio-Rad) with the following program:

UDG activation	50°C	2 minutes
Denaturation	95°C	10 minutes
40 Cycles	95°C	15 seconds
	60°C	30 seconds
Melt curve	60-95°C	Variable times

ACTB, *TBP*, *PPIA*, and *GAPDH* were tested as housekeeping genes and all of them showed a stable expression across different cell types and conditions; *ACTB* was used for normalization in most experiments. Relative gene expression levels have been calculated with the formula:

$$relative\ mRNA\ expression = 2^{-(\Delta\Delta Ct)}.$$

Gene	Forward primer	Reverse primer
PINK1	CGGCCGGGCAGTCTTTCT	CCTCTCCCTGGAAGCAACCC
PHGDH	CTTACCAGTGCCTTCTCCAC	GCTTAGGCAGTTCCCAGCATTC
PSAT1	ACTTCCTGTCCAAGCCAGTGGA	CTGCACCTTGTATTCCAGGACC
PSPH	GACAGCACGGTCATCAGAGAAG	CGCTCTGTGAGAGCAGCTTTGA
SLC1A4	CATGGACGGAGCAGCCATC	GGCAGTCACTAGAATGGTGAAAA
SHMT1	GCTGGGCTACAAAATAGTCA	AAGTCCACGGGACGTCAG
SHMT2	GCTCAACCTGGCACTGACTG	CACTGATGTGGGCCATGTCT
ATF4	CAACAACAGCAAGGAGGATG	CAACGTGGTCAGAAGGTCAT
EIF2A	TCTTTCCGGGACAACATGGC	GGCAAACAAGGTCCCATCCT
IFRG15	TCGAAGGGCTCTCCTGATACT	GGGGTCAGAAAAACCTGGCA
OAS1	ACAGCTGGAAGCCTGTCAAA	GGGTTAGGTTTATAGCCGCCA
OCT4	TGTACTCCTCGGTCCCTTTC	TCCAGGTTTTCTTTCCTAGC
SOX2	GCTAGTCTCCAAGCGACGAA	GCAAGAAGCCTCTCCTTGAA
NANOG	CAGTCTGGACACTGGCTGAA	CTCGCTGATTAGGCTCCAAC
PAX6	GTCCATCTTTGCTTGGGAAA	TAGCCAGGTTGCGAAGAACT
SOX1	CACAACTCGGAGATCAGCAA	GGTACTTGTAATCCGGGTGC

ACTA2	GTCCCAGACATCAGGGAGTAA	TCGGATACTTCAGCGTCAGGA
TBXT	TGTACTCCTTCCTGCTGGACTT	AGCTTGTTGGTGAGCTTGACTT
GATA4	GGAAGCCCAAGAACCTGAAT	GTTGCTGGAGTTGCTGGAA
FOXA2	GTCCGACTGGAGCAGCTACTAT	CACGTACGACGACATGTTCA
ACTB	ACCATGGATGATATCGC	TCATTGTAGAAGGTGTGGTG

Table 3. List of primers used in RT-qPCR experiments.

4.14. Sanger Sequencing

The sequencing reaction was set up from purified PCR products using Big Dye v3.1 Cycle Sequencing Kit (Applied Biosystems #4337456).

The sequencing program was set up as follows:

	96°C	1 minute
25 cycles	96°C	20-30 seconds
	50°C	15 seconds
	60°C	1 minute
	60°C	1 minute/kb

The sequencing products were analyzed on a 3500 DX Series automated sequencer (Applied Biosystems).

The analysis and alignment of electropherograms was performed with the software SnapGene.

4.15. STR Analysis

STR amplification was performed with AmpFLSTR™ Identifiler™ Plus PCR Amplification Kit (Thermo Fisher Scientific #A26182) according to the manufacturer's instructions. The reaction products were run on a 3500 DX Series Genetic Analyzer (Applied Biosystems) and analyzed with the software GeneMapper™ 6 (Thermo Fisher Scientific).

4.16. Compound Treatments

Staurosporine (Merck #S5921) was dissolved at a concentration of 1 mM in DMSO and added to cell media in 1:1000 ratio, obtaining a final concentration of 1 µM for the indicated times. As control, cells were treated with an equal volume of DMSO.
L-serine (Merck #S4311) and Glycine (Merck #G8790) were dissolved in water at a concentration of 400 mM and sterilized through a 0.2 µm syringe filter. Unless otherwise specified, L-serine and glycine were added to cell media in 1:1000 ratio, obtaining a final concentration of 0.4 mM, equal to that of common media e.g., DMEM. An equal volume of sterile water was used as control.

4.17. Silencing via Lentiviral Transduction

PINK1 gene silencing was achieved via pMISSION validated shRNA constructs (Merck, NM_032409, TRCN0000199193), whose efficiency was shown in a previous publication (Arena et al., 2013). The MISSION pLKO.1-puro Non-Mammalian shRNA Control Plasmid DNA (SHC002, Merck), targeting no known mammalian genes, was used as negative control. Plasmids were amplified in the *TOP10 E. coli* bacterial strain and purified with the QIAGEN Plasmid Maxi Kit (Qiagen #12162). HEK293T cells were used to generate lentiviral particles with the following protocol.

1. The plasmid mix is prepared by adding 16 µg psPAX2, 8 µg pMD2G, 16 µg lentiviral construct (e.g., shPINK1), 200 µL 1M $CaCl_2$, sterile water to bring the volume to 800 µL.
2. While making bubbles in the transfection mixture with a 2ml serological pipette in the plasmid mix, add 800 µL of HBS 2x Solution (280 mM NaCl, 10 mM KCl, 1.5 mM Na_2HPO_4, 12 mM dextrose, 50 mM HEPES pH 7.05), then allow 10 minutes of incubation.
3. In the meantime, add 13 µL of 25 mM Chloroquine to each T75 flask (~1:1000); swirl very gently.

4. Add transfection mixture to each flask; swirl very gently and incubate at 37°C 5% CO_2 for 4-6 hours.
5. Remove medium and add 15 ml DMEM/10% FBS
6. Supernatant containing viral particles is collected from flasks 48 hours after transfection, can be frozen at -80°Cand used to transduce cells.

4.18. Cell Proliferation Assay

The same number of cells was seeded in each well of a 12-well plate in *Complete DMEM 10%*. After 24 hours, after cells had adhered, the medium was changed to either *Starvation MEM* without Ser/Gly, or *Starvation MEM* supplemented with Ser/Gly 0.4 mM. After 48 hours, cells were counted by three blinded operators.

4.19. Western Blot

Western Blot is a widely used molecular biology technique to detect and analyze proteins. To perform it, proteins spread on a polyacrylamide gel (NuPAGETM 4 to 12% Bis-Tris gel, Thermo Fisher Scientific #NP0322BOX) by means of SDS-PAGE were transferred on a nitrocellulose membrane (Merck #GE10600004); then, through subsequent incubations with primary and secondary antibodies, the proteins of interest were detected and visualized as a chemiluminescent signal generated by the horseradish peroxidase (HRP, Pierce™ ECL Western Blotting-Substrate, Thermo Fisher Scientific #32106) conjugated with the secondary antibodies. Images were acquired on a Chemidoc XRS+ (Bio-Rad) instrument and analyzed with the Image Lab Software (Bio-Rad).

Antibody	**Ab type**	**Producer #**	**Dilution**
PHGDH	Primary	Cell Signaling Technology #13428	1:1000 in 5% BSA
PSAT1	Primary	Sigma #SAB2108040	1:1000 in 5% BSA
PSPH	Primary	Santa Cruz #sc-365183	1:1000 in 5% BSA

SLC1A4	Primary	Cell Signaling Technology #8442	1:1000 in 5% BSA
BECN1	Primary	Novus #NB500-249	1:1000 in 5% BSA
PARP	Primary	Cell Signaling Technology #5625	1:1000 in 5% BSA
LC3-A/B	Primary	Cell Signaling Technology #4108	1:1000 in 5% BSA
ACTB	Primary	Cell Signaling Technology #3700	1:10000 in 5% BSA
Goat α-Rb	Secondary	Bethyl #A120-501P (HRP)	1:5000 in 5% BSA
Goat α-Ms	Secondary	Bethyl #A90-516P (HRP)	1:5000 in 5% BSA

Table 4. List of antibodies used in Western Blot experiments.

4.20. Immunocytofluorescence

Immunocytofluorescence is a technique used to visualize the expression and localization of target proteins in cells by means of antibody-conjugated fluorophores.

To perform this technique, cells were grown on glass microscopy coverslips and then, at the desired confluence, fixed with cold 4% paraformaldehyde (Thermo Fisher Scientific #A1131336) in DPBS for 15 minutes at 4°C. After three washes with DPBS containing calcium and magnesium (Thermo Fisher Scientific #14040117), cells were treated for 1 hour with a blocking and permeabilizing solution containing 0.1% Triton X-100 (Merck #X100) and 2% w/v BSA (EuroClone #SE1193003) in DPBS with calcium and magnesium. Afterwards, cells were incubated overnight at 4°C with primary antibodies at the appropriate dilution in blocking solution. The following day, after three washes with DPBS, cells were incubated for 1 hour at room temperature with secondary fluorophore-conjugated antibodies at the appropriate dilution in blocking solution. Finally, after three washes with DPBS, cells were treated with DPBS containing 300 nM DAPI for nuclear staining (Thermo Fisher Scientific #D1306) for 5 minutes at room temperature.

The coverslips were then mounted on microscopy slides with ProLong™ Gold Antifade Mountant (Thermo Fisher Scientific #P10144).

Antibody (Ab)	Ab type	Producer #	Dilution
Rabbit pAb to SOX2	Primary	Abcam #ab97959	1:250
Mouse mAb to TRA-1-60 (R)	Primary	Abcam #ab16288	1:500
Rabbit pAb to OCT4 - ChIP Grade	Primary	Abcam #ab19857	1:250
Mouse mAb [MC813] to SSEA4	Primary	Abcam #ab16287	1:500
Mouse mAb [TU-20] to βIIITubulin	Primary	Abcam ab7751	1:500
Rabbit pAb to Synaptophysin	Primary	Abcam #ab7837	1:500
Rabbit mAb to GFAP	Primary	Abcam #ab68428	1:250
Goat Anti-Rabbit IgG DyLight™488	Secondary	Thermo Fisher #35553	1:500
Goat Anti-Mouse IgG DyLight™488	Secondary	Thermo Fisher #35503	1:500
Goat Anti-Rabbit IgG DyLight™550	Secondary	Thermo Fisher #SA5-10033	1:500
Goat Anti-Mouse IgG DyLight™550	Secondary	Thermo Fisher #SA5-10173	1:500

Table 5. List of antibodies used in immunocytochemistry experiments.

5. Part I: Generation and Characterization of iPSC-Based Cellular Models for PINK1

5.1. Background

Most studies on the protein PINK1 and the effects of its depletion have been performed in immortalized cell lines or simple animal models, such as *Drosophila melanogaster*, frequently using recombinantly expressed proteins. Some examples include initial groundbreaking discoveries about mitophagy (Jin & Youle, 2013; Narendra et al., 2010) and the early experiments that delineated the PINK1 interactome (Michiorri et al., 2010; Moisoi et al., 2009; Plun-Favreau et al., 2007; Pridgeon et al., 2007; Vande Walle et al., 2008). Such cellular and animal models have the great advantages of simplicity, affordability, and scalability, but differ substantially from mature cells and tissues in a complex organism, and constitute reductionist systems that may overexpose some functions and hide others (Brunelli et al., 2020).

Since the discovery of the *Yamanaka factors* in 2006 (Takahashi & Yamanaka, 2006), iPSCs have emerged as a powerful tool in all fields of cellular biology, including PD and neurodegeneration research. Thanks to ever improving protocols for differentiation of midbrain dopaminergic neurons and other cells of the CNS, scientists all around the world in the last 10-15 years have been able to reprogram somatic cells from patients carrying variants in *PINK1* or other genes into iPSCs, and then differentiate them to obtain mature neurons with the same genetic background of the affected individual.

Experiments in iPSC-derived neurons sometimes failed to recapitulate the findings of studies on immortalized cells. Contrasting results either supported or disproved the role of mitophagy in iPSC-derived dopaminergic neurons (Imaizumi et al., 2012; Rakovic et al., 2013), and the question whether mitophagy is a relevant mechanism of degeneration in neurons lacking a functional PINK1 remains open.

A further argument in support of the utility of iPSC-based methods, although not the objective of this project, is their potential use as therapeutic means. In this regard, clinical

research is advancing at a fast pace and the first human trials are ongoing (Gravitz, 2021; Hiller et al., 2022). Furthering knowledge on this cell type, therefore, can certainly benefit patients in the near future.

5.2. Results and Discussion

5.2.1. Generation and Characterization of iPSC Lines from Two PD Patients with Compound Heterozygous Mutations in *PINK1*

I reprogrammed primary dermal fibroblasts obtained from two male PD patients with compound heterozygous mutations in *PINK1* (NG6138, NG6301) to iPSCs using a Sendai virus-based approach to deliver three vectors encoding the Yamanaka factors Oct3/4, Klf4, Sox2, and c-Myc. I transferred emerging iPSC colonies to vitronectin-coated plates and subsequently maintained them in E8 Flex medium, passaging cells with EDTA when needed.

After > 10 passages, I performed RT-PCR using vector-specific primers followed by electrophoresis on agarose gel, confirming that the cultured cells had lost the three viral reprogramming vectors. iPSCs were induced to differentiate into endoderm, mesoderm, ectoderm using the StemMACS Trilineage Differentiation Kit and expression of lineage-specific markers (GATA4 and SOX17 for endoderm, ACTA2 and CXCR4 for mesoderm, PAX6 and SOX1 for ectoderm) was confirmed by RT-qPCR.

RT-qPCR analysis confirmed a high expression of the stemness markers SOX2, NANOG, OCT4, returning calculated relative mRNA levels 3 or 4 orders of magnitude higher relative to fibroblasts.

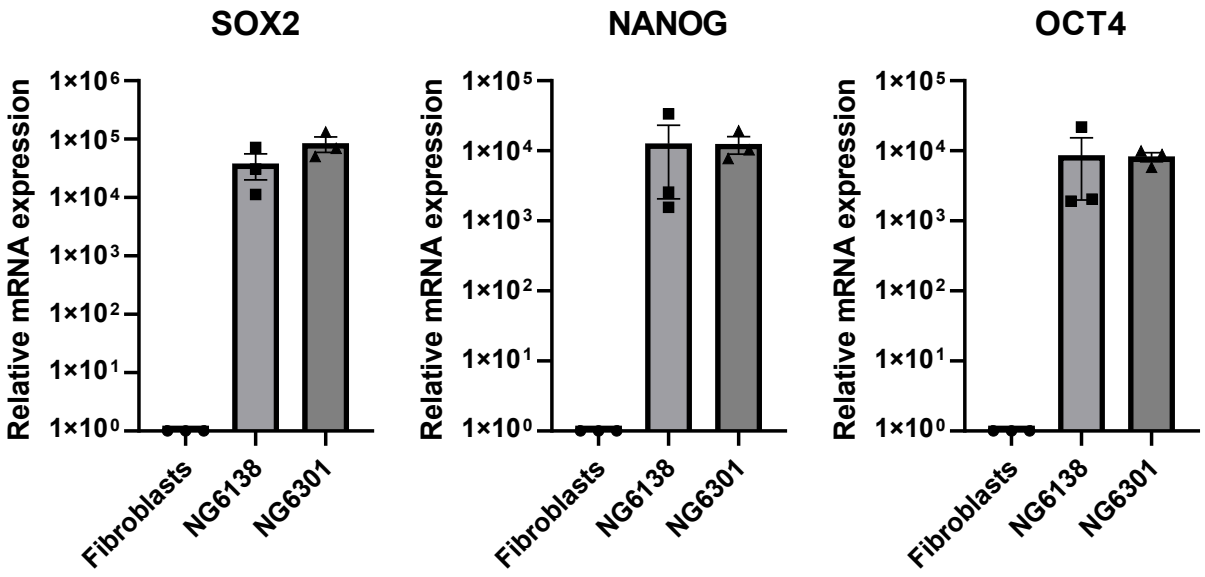

Figure 4. RT-qPCR to detect the mRNA expression of stemness markers SOX2, NANOG, and OCT4 in iPSC lines NG6138 and NG6301 relative to fibroblasts.

I also evaluated the expression of stem cell markers SOX2, TRA-1-60, OCT4, and SSEA4 by immunocytochemistry, confirming a good expression in both cell lines, as shown in figure 5.

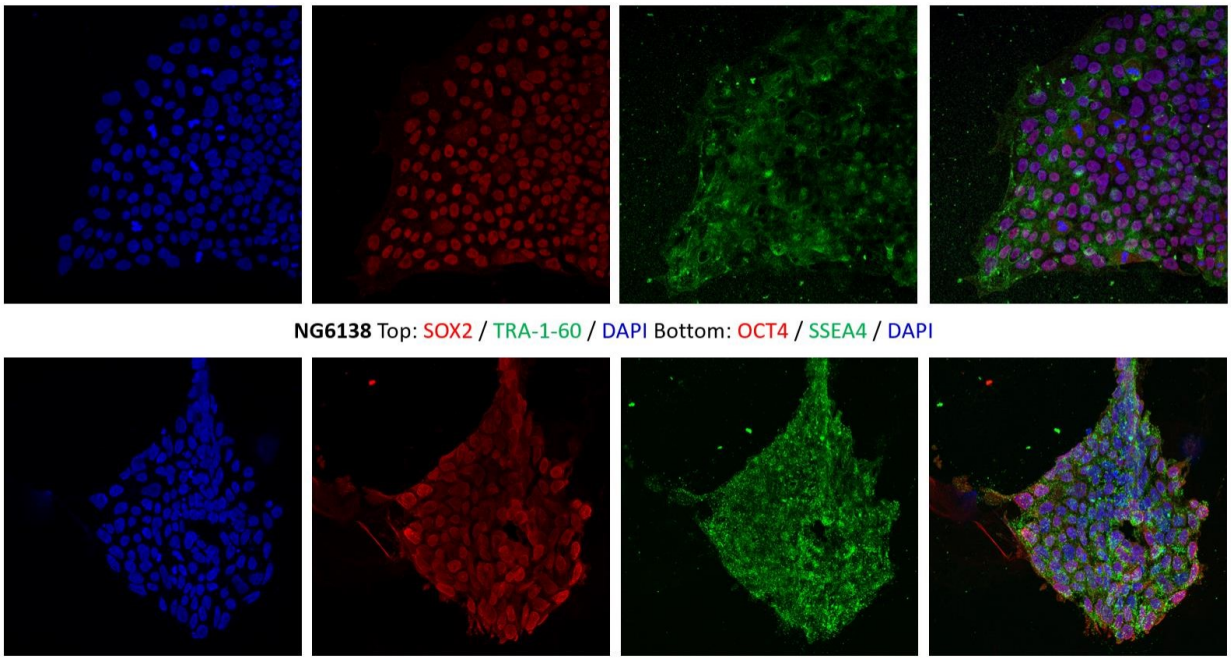

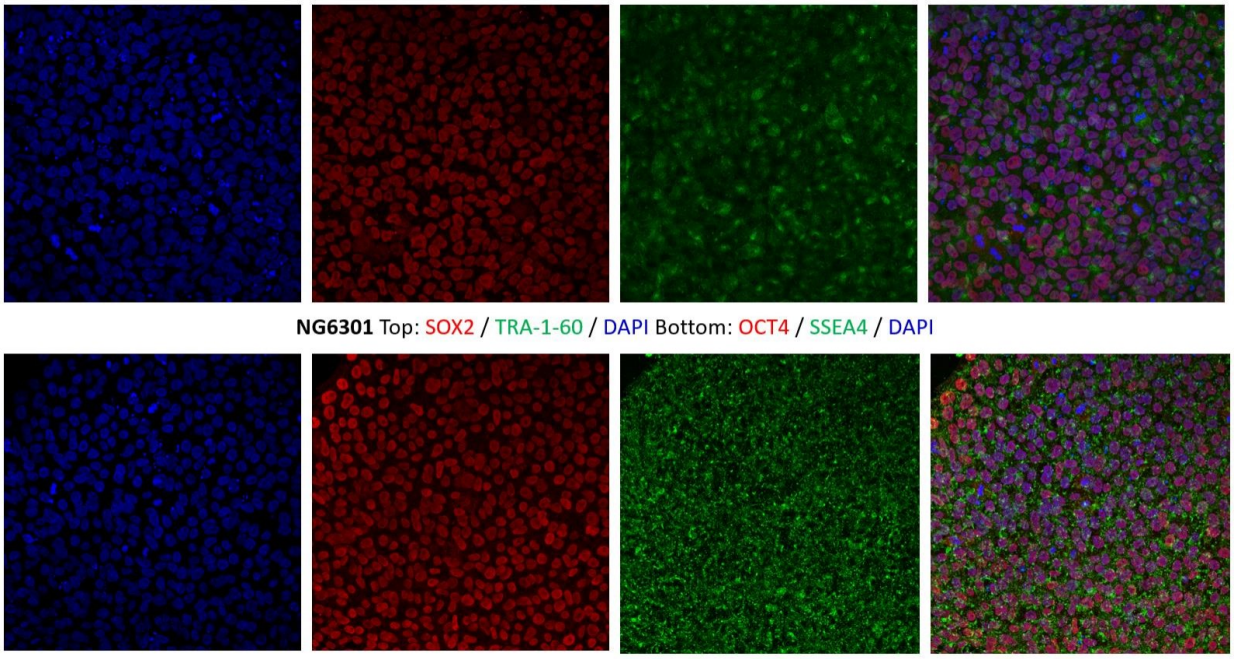

Figure 5. Immunofluorescence images showing expression of the stemness markers SOX2, TRA-1-60, OCT4, SSEA4, and DAPI in iPSCs NG6138 and NG6301.

I performed Sanger sequencing on DNA extracted from the obtained iPSCs to confirm the presence of the patients' variants and STR analysis, comparing iPSC and fibroblast DNA, for identity analysis.

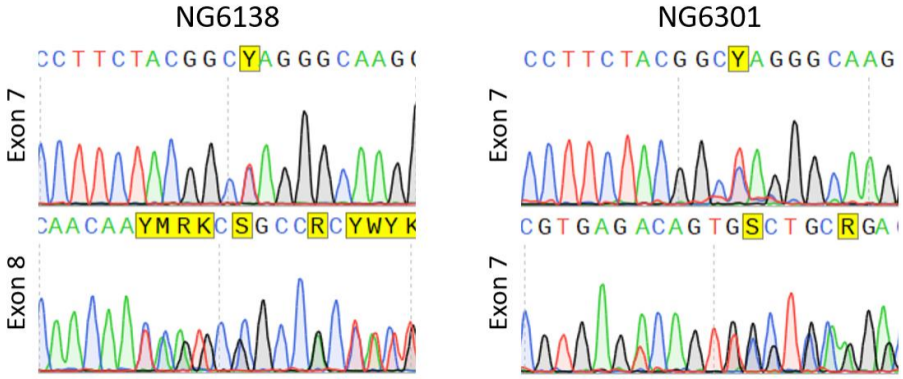

Figure 6. Electropherograms obtained by Sanger sequencing confirming the presence of the heterozygous variants c.1366C>T (p.Gln456) in exon 7 and c.1600_1602dupCAA (p.Gln534dup) in exon 8 in NG6138 and the variants c.1366C>T (p.Gln456*) and c.1448_1449insTCAGTGCCTCCAGACTTGAG (p.Arg483SerfsTer7), both in exon 7, in NG6301.*

All the 16 STR loci analyzed matched in each fibroblast-iPSC pair.

Finally, molecular karyotyping of iPSCs was performed at Life&Brain GmbH (Bonn), using an array-based method that does not detect translocations or inversions, alterations in chromosome structure, mosaicism, or polyploidy. This analysis ruled out the presence of major unbalanced chromosomal abnormalities in the two lines, including genetic defects that are recurrent in cultured cells such as the 20q11.21 amplification (Assou et al., 2018; Kanchan et al., 2020). A more in-depth analysis of the data generated by this analysis is however ongoing.

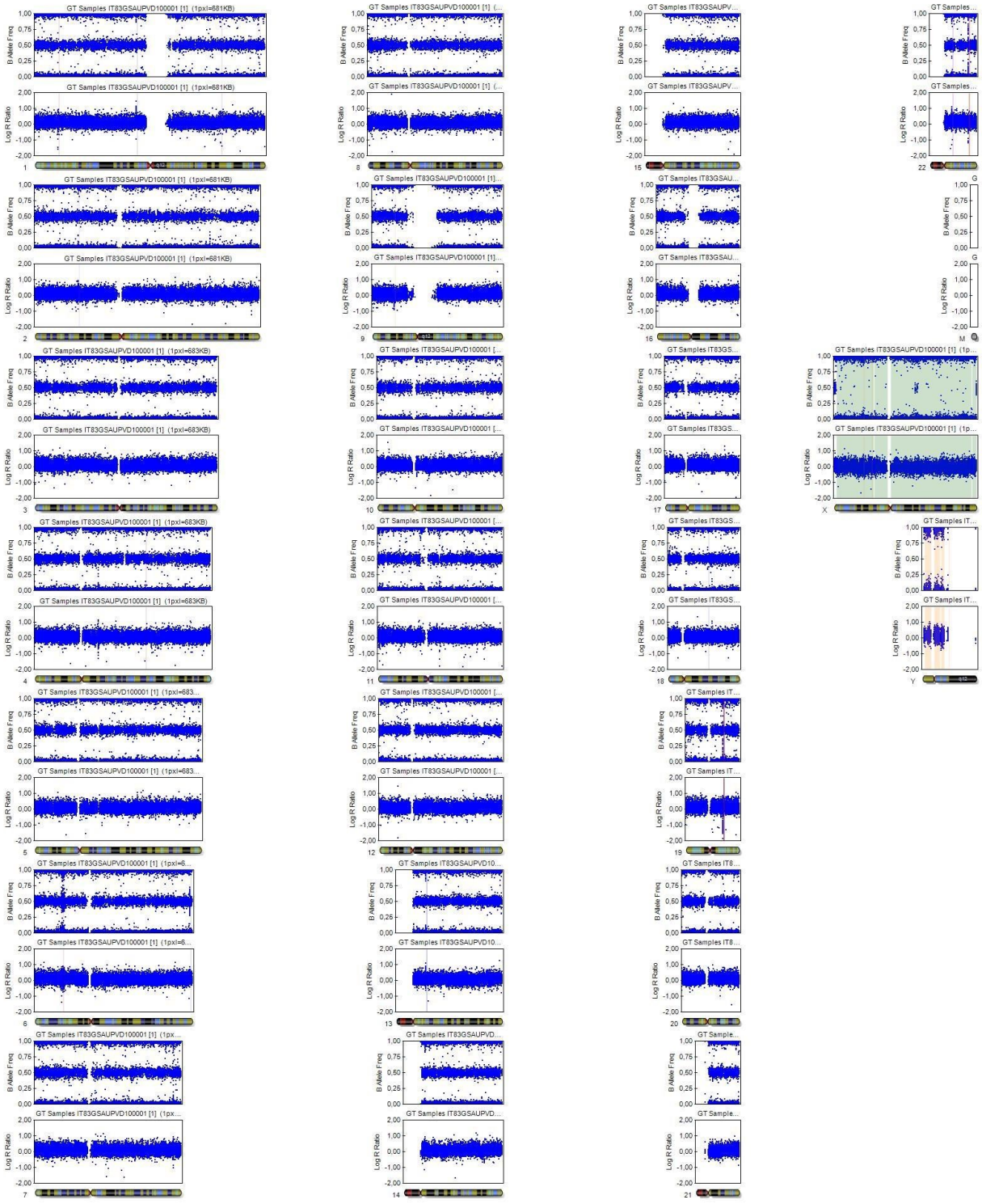

Figure 7. Molecular karyotyping of NG6138 iPSCs.

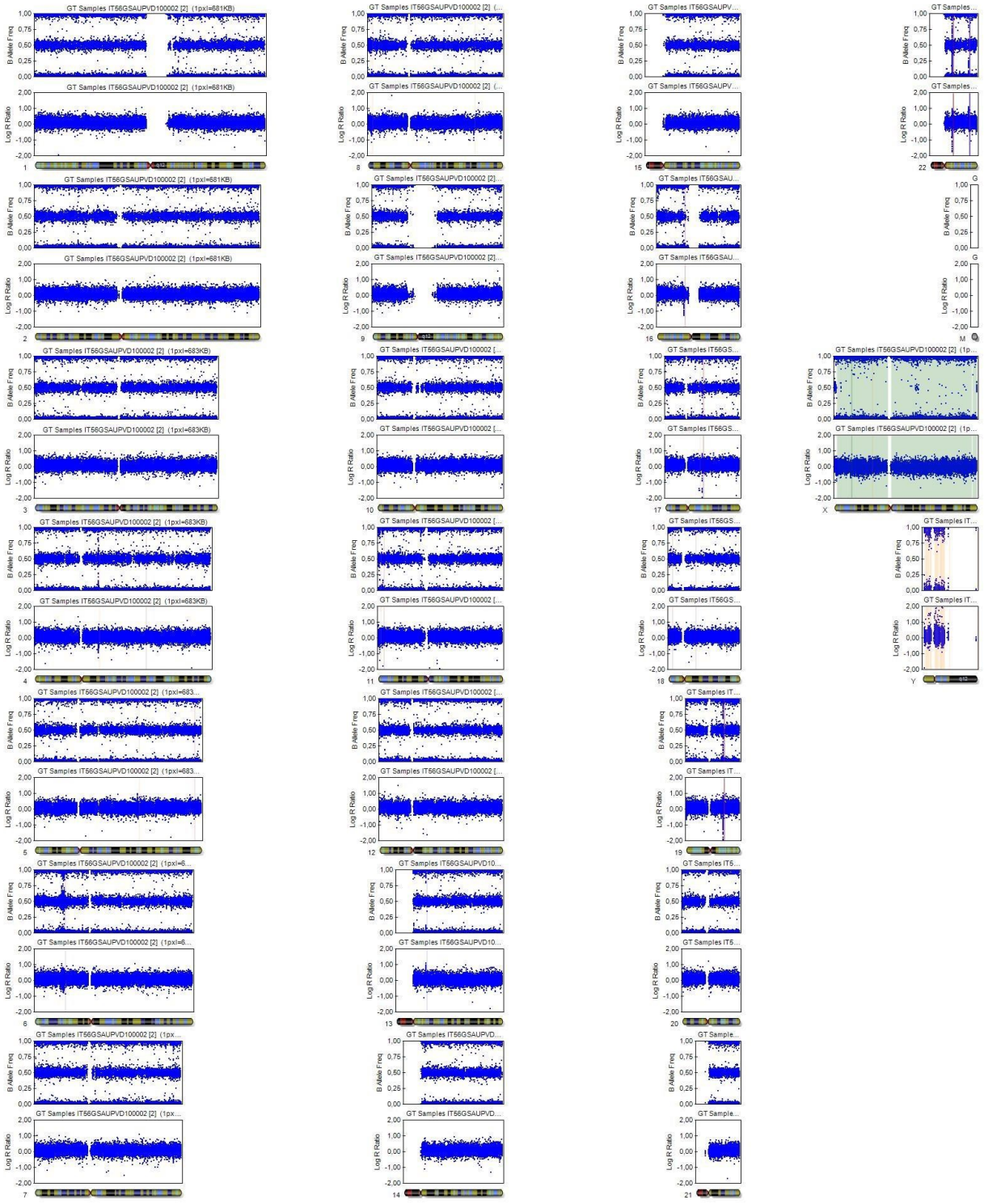

Figure 8. Molecular karyotyping of NG 6301 iPSCs.

5.2.2. Differentiation of iPSCs to Midbrain Dopaminergic Neurons

iPSCs can be used to produce mature midbrain dopaminergic neurons. In the experiments described in this dissertation, neuronal differentiation was achieved following Reinhardt's protocol or variations thereof (Reinhardt et al., 2013).

This process is divided in two steps. In the first one, iPSCs are differentiated to neuroepithelial neural precursor cells (smNPCs, *small molecule-neural precursor cells*) using a combination of simple and relatively cheap chemicals, namely SB 431542 (inducing ectodermal differentiation), dorsomorphin (a SMAD inhibitor), CHIR 99021 (acting as agonist on the WNT pathway), purmorphamine (activates Hedgehog signaling via the Smoothened receptor), and the antioxidant ascorbic acid. The obtained smNPCs are cheap, versatile, and relatively stable cell lines that can be expanded indefinitely, cryopreserved, or engineered. Within this project, for example, I used isogenic gene-corrected (GC) lines obtained with a TALEN-based gene editing approach from patient-derived smNPCs carrying the *PINK1* Q456X variant (this modification was realized by other researchers).

The second step of differentiation *à la Reinhardt* allows to obtain dopaminergic neurons or other cells of the nervous system from smNPCs. This is largely based on small-molecule and recombinant factors that direct differentiation strongly and specifically. To obtain midbrain dopaminergic neurons, I used purmorphamine and FGF8b to induce differentiation, followed by dbcAMP, BDNF, GDNF, and TGFβ3 to achieve neuron maturation, as described in the *Material and Methods*.

I performed analytical FACS runs on populations of mature (day 30) dopaminergic neurons obtained with this differentiation protocol to understand in what proportion cells expressed neuronal and dopaminergic markers. As shown in figure 9, approximately 90% of cells expressed the neuron-specific marker Tubulin β-III (TUBB3) and 20-30% of cells expressed Tyrosine Hydroxylase (TH), which identifies dopaminergic neurons. These numbers were considered satisfactory, but it is important to note that the final cellular population is heterogeneous, and the proportion of specific cell types could vary significantly between experiments.

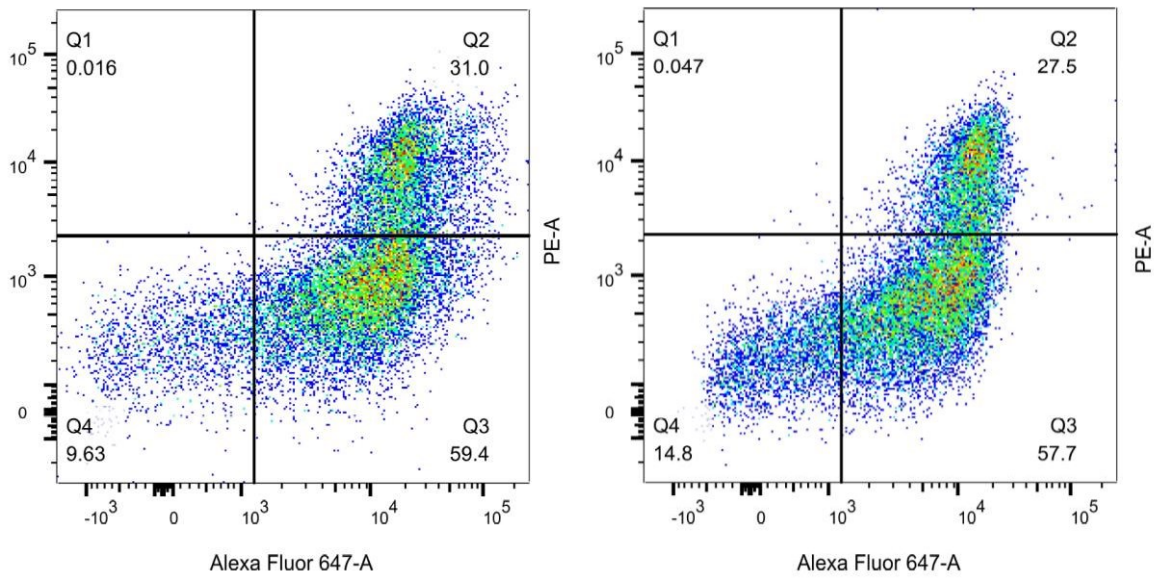

Figure 9. Representative FACS dot plots of wild-type day 30 midbrain dopaminergic neurons stained with TUBB3 antibody (Alexa 647, x axis) and TH antibody (PE-Alexa 700, y axis). Cells in Q2 express both TUBB3 and TH, cells in Q3 express TUBB3 but not TH, cells in Q4 express neither marker.

Day 30 dopaminergic neurons	
$TUBB3^-$ and TH^- (%)	9.77 ± 2.86
$TUBB3^+$ (%)	90.2 ± 2.83
$TUBB3^+$ and TH^+ (%)	24.5 ± 4.85
$TH^+/TUBB3^+$ ratio	27.45 ± 5.86

Table 6. Percentage of $TUBB3^-$ and TH^-, $TUBB3^+$ (irrespective of TH status), $TUBB3^+$ and TH^+ neurons (analyzed through FACS) and ratio $TH^+/TUBB3^+$; mean ± SEM.

6. Part II: The role of PINK1 in Staurosporine-Induced Apoptosis

6.1. Background

PINK1 has been deeply described and characterized in its vest of regulator of mitophagy and guardian of mitochondrial health, while other functions of this protein (e.g., pro-macroautophagic, pro-survival, antiapoptotic) have been subject of fewer studies.

The research group led by Prof. Enza Maria Valente initially identified a protein-protein interaction between PINK1 and Beclin1, often referred to as a *master regulator of autophagy*. This study demonstrated that the two proteins directly interact with each other, and that this interaction favors autophagy at large, even outside of the context of mitophagy (Michiorri et al., 2010).

A subsequent study by the same researchers discovered that the PINK1-Beclin1 interaction takes place in a specific subcellular location, namely the *mitochondrial-associated membrane* (MAM), that is the area of contact between mitochondria and endoplasmic reticulum (ER). In such contact sites, that are crucial for the regulation of several cellular functions including calcium homeostasis and mitochondrial dynamics, Beclin1 on the ER membrane links PINK1 on the mitochondrial outer membrane (MOM) to promote autophagosome formation in the early phase of autophagy (Gelmetti et al., 2017).

At the cellular level, mitochondrial health is directly connected to apoptosis. In fact, the mitochondrion is at the center of the *intrinsic pathway* of apoptosis, which is characterized by mitochondrial membrane permeabilization and release of Cytochrome c in response to various stimuli. Mitochondrial depolarization, the same event that causes PINK1 accumulation on the MOM, is in itself one of the stimuli leading to mitochondrial permeabilization, Cytochrome c release, and apoptosis. In this context, PINK1 acts as inhibitor of apoptosis by phosphorylating Bcl-xL, a member of the Bcl-2 family of proteins, preventing its cleavage and subsequent release of its C-terminal fragment, which is a potent inducer of cell death (Arena et al., 2013).

Staurosporine (STS) is a substance derived from the bacterium *Streptomyces staurosporeus* in 1977, commonly used in cellular biology as inducer of apoptosis (Omura et al., 1977).

Previous work done in our research group showed that, in SH-SY5Y cells, treatment with 1 µM STS causes first a robust activation of autophagy, detected as an increase in the marker LC3-II and reaching a maximum approximately 90 minutes after starting the treatment, and then initiation of apoptosis, highlighted by an accumulation of cleaved PARP and the appearance of pyknotic nuclei at later timepoints. This phenomenon is paralleled by a gradual, continuous decrease in protein levels of PINK1, thought to be due to enhanced degradation via the ubiquitin-proteasome system (Yoo & Chung, 2018). In the early phase, PINK1 interacts with Beclin1, preventing its cleavage and therefore favoring autophagy. In the later phase, dropping PINK1 levels allow the accumulation of proapoptotic cleaved Beclin1, resulting in a switch from autophagy to apoptosis (Brunelli et al., 2022).

6.2. Results and Discussion

6.2.1. *PINK1* mRNA Levels Do Not Change Significantly after Treatment with Staurosporine

To test whether the decrease in PINK1 protein levels observed after treatment of SH-SY5Y cells with 1 µM STS may be explained by a regulatory mechanism at the transcriptional level, I performed RT-qPCR on cells treated with DMSO or STS for 1, 2, or 3 hours.

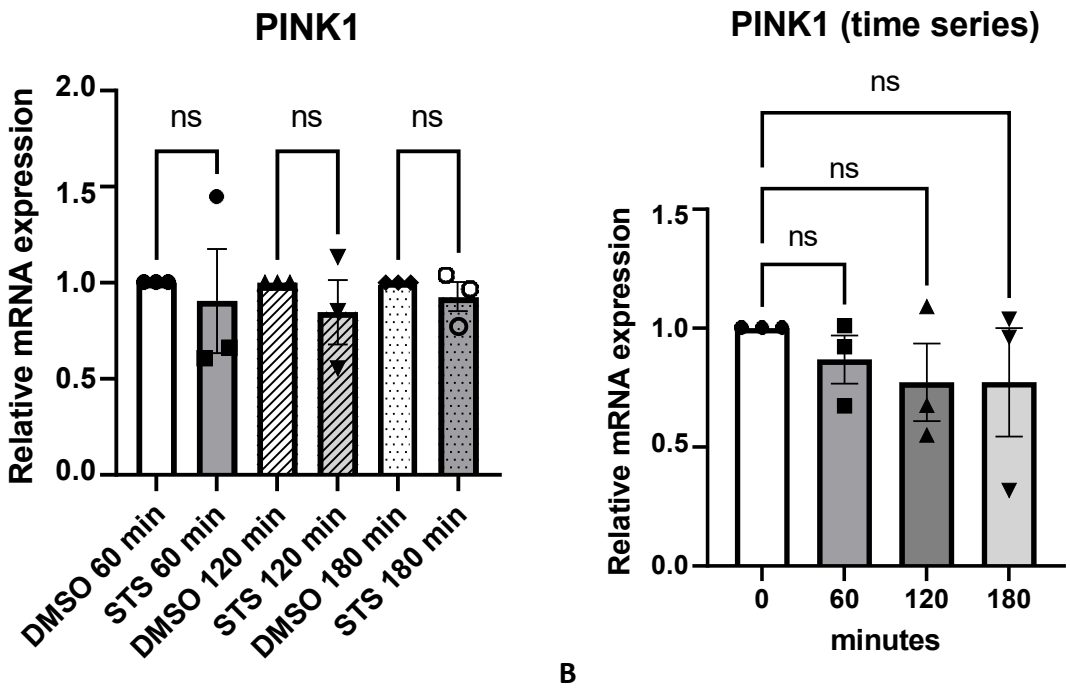

Figure 10. A. RT-qPCR data showing relative mRNA levels of PINK1 in SH-SY5Y cells treated with STS or vehicle (DMSO) for the indicated times; normalized to ACTB, mean ± SEM. B. RT-qPCR time series showing the variation of relative PINK1 mRNA levels over time after STS treatment; normalized to ACTB, mean ± SEM.

Relative mRNA levels of endogenous *PINK1* did not change significantly in comparison with the control at the examined timepoints, suggesting that the regulation is post-translational and supporting the hypothesis of enhanced protein degradation through the ubiquitin-proteasome system (figure 10A). The time-course analysis showed a slight trend towards a reduction of *PINK1* mRNA, reaching after 3 hours ~80% of the initial level, but this reduction is statistically nonsignificant, not present in every individual experiment, and much smaller than the substantial decrease observed at the protein level (figure 10B). Altogether, these results provided evidence against a transcriptional regulation of *PINK1* after STS treatment.

6.2.2. The Role of PINK1 in Staurosporine-Induced Apoptosis in iPSC-Derived Dopaminergic Neurons

I attempted to replicate the results obtained in SH-SY5Y neuroblastoma cells in iPSC-derived midbrain dopaminergic neurons. Neurons on differentiation day 29 were treated with 1 µM STS overnight and then harvested for Western Blot.

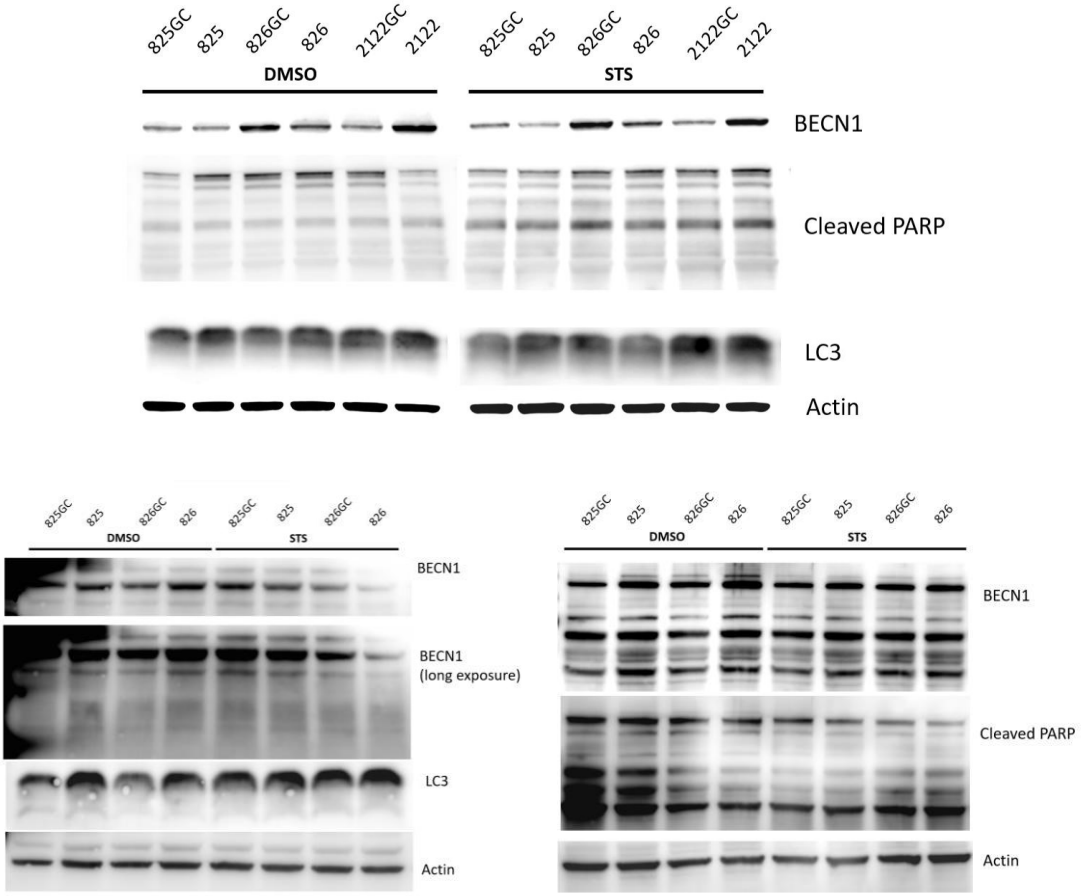

Figure 11. Western Blots showing the proteins Beclin1 (BECN1), cleaved PARP, and LC3 in cell lysates of iPSC-derived neurons at differentiation day 30. Three patient-derived lines carrying the PINK1 Q456X variant (825, 826, 2122) are shown, in parallel with respective isogenic gene-corrected lines (825-GC, 826-GC, 2122-GC).

Unfortunately, neurons did not show any consistent activation of autophagy or apoptosis in the tested conditions. The autophagic marker LC3B was undetectable in untreated and

treated samples of all cell lines, and levels of cleaved PARP did not increase in treated neurons compared to untreated cells. The cleaved form of Beclin1 was difficult to identify even with longer exposures, with multiple nonspecific bands appearing on the membranes below the molecular weight of full-length BECN1. Anyways, no band in the molecular weight range expected for cleaved-Beclin1 (~35 kDa) showed significant changes in concentration or was influenced by the presence or absence of a functional PINK1 protein.

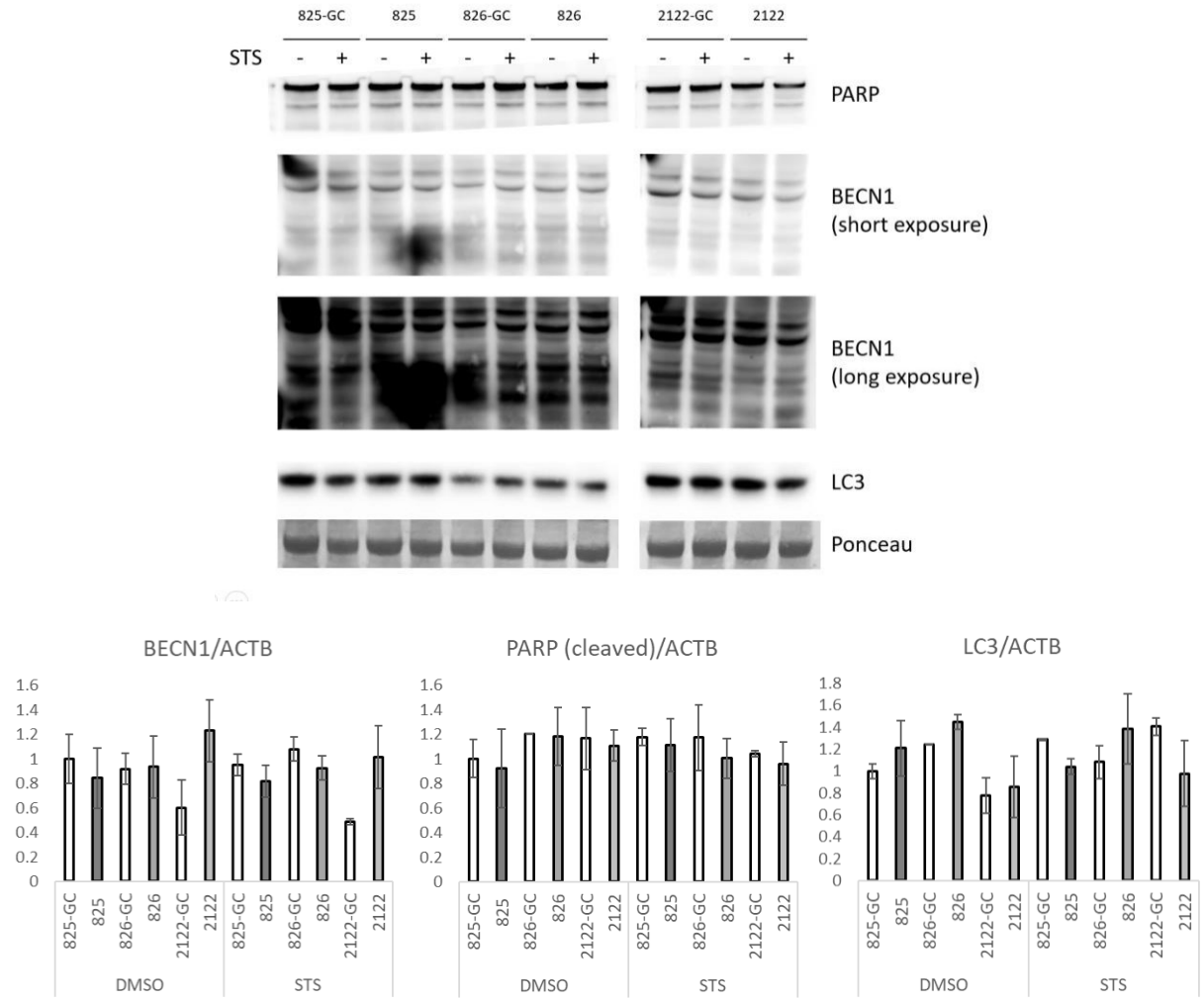

Figure 12. Western Blot showing the proteins Beclin1, cleaved PARP, and LC3 in cell lysates of iPSC-derived neurons at differentiation day 30. Three patient-derived lines carrying the PINK1 Q456X variant (825, 826, 2122) are shown, in parallel with respective isogenic gene-corrected lines (825-GC, 826-GC, 2122-GC); densitometric analysis of figure 11 and figure 12; mean ± SEM.

This cellular model appeared to be resistant to STS-induced apoptosis and did not show a significant activation of autophagy after treatment with 1 μM STS overnight. Differences in the response to STS between neurons and other cell types have been noted by other authors and most studies concerning STS-induced neuronal apoptosis have so far been performed in primary cultures from animal models rather than iPSC-derived neurons (Jantas et al., 2009; Koh et al., 1995). In particular, dopaminergic neurons have been previously described as resistant to STS-induced apoptosis, although these studies used lower STS concentrations (Ha et al., 2014; Wakita et al., 2014). Such effect – or rather absence thereof – could be explained by intrinsic characteristics of dopaminergic neurons (e.g., their postmitotic nature, prolonged high oxidative burden, enhanced mitochondrial activity) or by the high amount of trophic and antiapoptotic factors included in the media used during differentiation and maturation. Mature dopaminergic neurons produced with Reinhardt's protocol are known to be robust (Reinhardt et al., 2013) and could mask some susceptibility phenotypes. Higher concentrations of STS, longer treatments, or substantial changes to the composition of media could be necessary to observe STS-induced activation of autophagy and apoptosis in this cellular model.

7. Part III: Serine-Glycine Dysmetabolism in PINK1-Deficient Neuronal Models of Parkinson's Disease

7.1. Background

Serine is a non-essential amino acid synthesized inside cells from the glycolytic intermediate 3-Phosphoglyceric acid (3PG). The pathway of serine biosynthesis, also known as *phosphorylated pathway*, is a series of three reactions taking place in the cytosol. In the first reaction, catalyzed by the enzyme phosphoglycerate dehydrogenase (encoded by *PHGDH*), 3PG is converted to 3-phosphohydroxypyruvate (3PHP) with concomitant reduction of one molecule of NAD^+ to NADH and H^+. The second step, catalyzed by the enzyme phosphoserine aminotransferase (encoded by *PSAT1*), is a pyridoxal-phosphate-dependent transamination reaction in which one amino group is transferred from glutamate to 3PHP, yielding 3-phosphoserine (3PS) and α-ketoglutarate. Finally, 3PS is hydrolyzed by phosphoserine phosphatase (encoded by *PSPH*) in an irreversible reaction producing L-serine (Pan et al., 2021).

L-serine is not only a proteinogenic amino acid, but also the precursor of several biochemical species crucial to cellular and neuronal survival and activity. It is reversibly converted in glycine by serine hydroxymethyltransferase 1 or 2, respectively the cytosolic and mitochondrial forms of the enzyme, encoded by paralog genes *SHMT1* and *SHMT2*. This reaction frees a methyl, or 1C, group which feeds the folate and methionine cycles, known together as *one-carbon metabolism*, a complex system of interlinked biochemical pathways used to produce cosubstrates for methylation, transsulfuration, and aminopropylation reactions. The antioxidant molecule NADPH is a relevant secondary product of this pathway. In detail, tetrahydrofolate (THF) accepts this 1C unit, to form 5,10-methylenetetrahydrofolate (me-THF). Subsequently, methylenetetrahydrofolate reductase (encoded by *MTHFR*) reduces me-THF to 5-methyltetrahydrofolate (mTHF). To close the cycle, mTHF is demethylated to THF, liberating the methyl group which is used to remethylate homocysteine to methionine. This reaction brings the 1C group into the

methionine cycle. Methionine is used to produce S-Adenosyl methionine (SAM), often considered the main methyl donor in the eukaryotic cell. Losing a methyl group, SAM becomes S-Adenosyl homocysteine (SAH), which is hydrolyzed to adenosine and homocysteine. To conclude the cycle, another 1C group is necessary to remethylate homocysteine to methionine. This can either be obtained from the folate cycle, as described before, or from betaine (Lan et al., 2018; Newman & Maddocks, 2017).

This large overview of serine-glycine-one carbon metabolism conveys the idea that L-serine is not only used as a building block for protein synthesis, but also as precursor of key biochemical species such as phosphoglycerides, sphingolypids, and various substrates for methylation and transsulfuration reactions. Through the folate cycle, it participates to nucleoside and nucleotide synthesis; serine and glycine backbones constitute the basis for the synthesis of the most important antioxidant, glutathione (Murtas et al., 2020; M. Yang & Vousden, 2016). In the nervous system, L-serine is also converted by the enzyme serine racemase (encoded by the *SRR* gene) into its enantiomer D-serine, which acts, in the same way as glycine, as co-agonist on NMDA receptors (Wolosker et al., 1999).

Although serine can be easily acquired through intestinal absorption of dietary protein, impaired L-serine production due to pathogenic variants in the genes encoding for its biosynthetic enzymes causes severe pediatric syndromes characterized by multi-organ deficits, almost invariably including severe neurological symptoms (PHGDH deficiency, MIM#601815, Neu-Laxova syndrome, MIM#256520, PSPH deficiency, MIM#614023). This is generally thought to be due to the low permeability of the blood-brain barrier to L-serine and glycine, but since the effect is also observed *in vitro*, at the cellular level, some authors attempted to give a biochemical, rather than anatomical, explanation (Murtas et al., 2020; Possemato et al., 2011; J. H. Yang et al., 2010).

Although controversial, the topic of serine metabolism in Alzheimer's Disease, which together with PD constitutes the large majority of neurodegenerative disorders, is very hot. Researchers showed that L-serine levels are reduced in Alzheimer's pathology and that supplementation may be beneficial, even though the molecular mechanisms underlying these changes remain elusive (Bonvento et al., 2022; Chen, Calandrelli, et al.,

2022; Le Douce et al., 2020). Moreover, alterations in serine biosynthesis have been recently linked to the other two causative genes of autosomal recessive EOPD, PRKN and PARK7, within and without the context of PD (Liu et al., 2020; Nickels et al., 2019). The proteins encoded by these genes, respectively Parkin and DJ-1, are in a close biochemical and molecular relationship with PINK1. These notions, taken together, constitute a solid scientific ground to investigate the relationship between PINK1 and serine-glycine-one carbon metabolism.

Considering the broad neuroprotective activity of PINK1 and the fact that *in vitro* models of PINK1 depletion are characterized by many of the molecular pathways implicated in aging and frailty, such as mitochondrial dysfunction, increased oxidative stress, and bioenergetic failure (Gautier et al., 2008; Wood-Kaczmar et al., 2008), novel information could prove useful not only in the field of PD, but also for neurodegeneration at large and other aging-related pathologies.

7.2. Results and Discussion

7.2.1. Fibroblasts Carrying Pathogenic *PINK1* Variants Show Lower Expression of Serine Biosynthetic Enzymes

In order to analyze the expression of genes involved in serine biosynthesis and metabolism, I extracted RNA from fibroblasts (passage 5 to 10) obtained from patients with a diagnosis of PD carrying different pathogenic variants in the gene *PINK1* in homozygous or compound heterozygous form. The list of patients and their respective mutations is in section 4.3. (table 2). As reference, I used fibroblasts (passage 6 to 10) obtained from healthy subjects of similar age and sex. Fibroblasts were cultured in standard conditions, i.e., in *complete DMEM* medium at 37°C, 5% CO_2.

When at 70-90% confluence, fibroblasts were harvested one day after media change for RNA extraction, retrotranscription, and RT-qPCR analysis of the genes *PHGDH*, *PSAT1*, *PSPH*, *PINK1*.

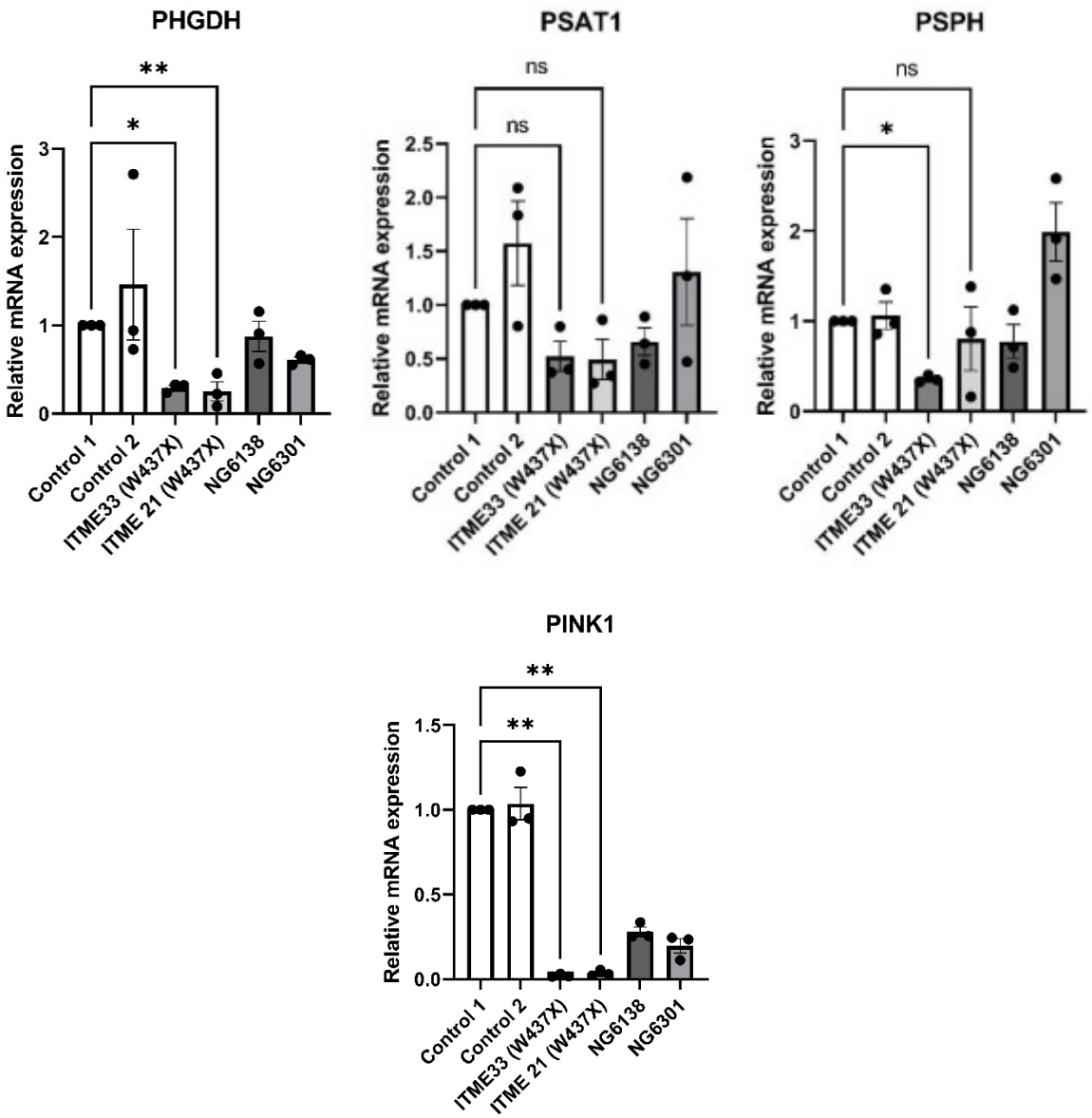

Figure 13. RT-qPCR showing relative mRNA levels of the genes PHGDH, PSAT1, PSPH, PINK1 in two control fibroblast lines (control 1: HDF108; control 2: HDF109) and in fibroblasts derived from patients carrying PINK1 pathogenic mutations in homozygous state (ITME33 and ITME21) or compound heterozygous state (NG6138, NG6301); mean ± SEM.

The result of the statistical analysis highlighted significantly lower levels of relative mRNA expression of *PHGDH* in fibroblasts carrying the W437X homozygous variant (lines ITME33 and ITME22). The two lines carrying compound heterozygous *PINK1* variants (NG6138 and NG6301) showed levels of *PHGDH* mRNA intermediate between control and

W437X fibroblasts, but values reached statistical significance only for NG6301. The expression of other genes of the phosphorylated pathway *PSAT1* and *PSPH* was similarly reduced in fibroblasts carrying *PINK1* pathogenic variants, but the effect was less dramatic than for *PHGDH*, with differences that often resulted statistically nonsignificant. An interesting finding was that ITME33 and ITME22 fibroblasts, homozygous carriers of the W437X mutation, expressed virtually null levels of *PINK1* mRNA, hinting to nonsense-mediated RNA decay. Previous studies using recombinantly expressed proteins demonstrated that PINK1 W437X maintains a discrete kinase activity and is able to interact with its substrates (Pridgeon et al., 2007); however, the present result raises the issue whether the endogenous protein is expressed at all.

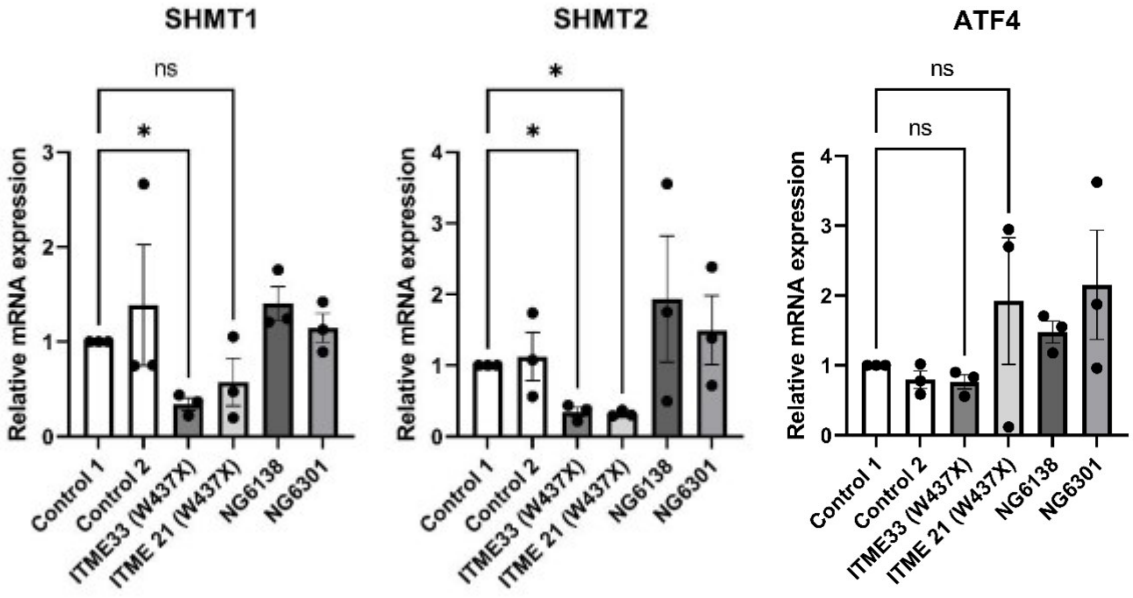

Figure 14. RT-qPCR showing relative mRNA levels of the genes SHMT1, SHMT2, ATF4 in two control fibroblast lines (control 1: HDF108; control 2: HDF109) and in fibroblasts derived from patients carrying PINK1 pathogenic mutations in homozygous state (ITME33 and ITME21) or compound heterozygous state (NG6138, NG6301); mean ± SEM.

The analysis was extended to genes upstream and downstream of the serine synthesis pathway. SHMT1 and SHMT2 are the two enzymes, respectively located in the cytosol and in the mitochondria, responsible for conversion of L-serine into glycine, the reaction

that liberates a methyl group and connects serine biosynthesis to one-carbon metabolism. mRNA levels of *SHMT1* and *SHMT2* were only reduced in the lines ITME33 and ITME21, but not in the two cell lines carrying compound heterozygous mutations.
I also assayed mRNA levels of *ATF4*, a key transcription factor involved in the regulation of serine biosynthesis subject itself to transcriptional regulation (DeNicola et al., 2015; Reich et al., 2020). Increased expression of the *ATF4* gene is mediated by mTORC1 (Selvarajah et al., 2019; Ye et al., 2012), and PINK1 is believed to be a modulator of the mTOR pathway. However, mRNA levels of *ATF4* did not show any reduction in patients' fibroblasts compared to control fibroblasts, suggesting that in this experiment the effect observed on *PHGDH* is not mediated by this axis.

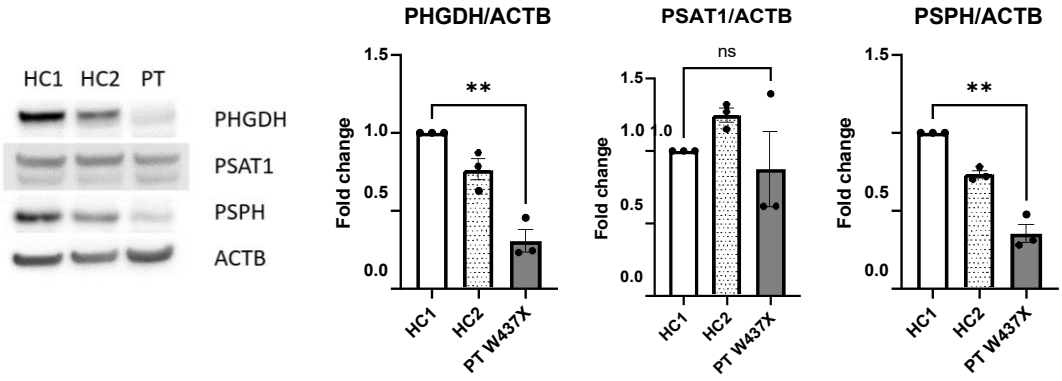

Figure 15. Representative Western Blot showing PHGDH, PSAT1, PSPH, and ACTB from whole cell lysates of fibroblasts from two healthy controls (HC1: HDF108; HC2: HDF109) and from the PD patient ITME66, homozygous carrier of the PINK1 W437X variant; densitometric analysis of protein levels of PHGDH, PSAT1, PSPH normalized to ACTB; mean ± SEM.

Cell pellets for Western Blot were collected in parallel with those for RT-qPCR for fibroblasts carrying the homozygous *PINK1* W437X variant and healthy controls. The results, shown in figure 15, demonstrated a significant reduction in PHGDH and PSPH protein concentration in the cells carrying the pathogenic *PINK1* variant compared to the controls.
These data suggest that fibroblasts from PD patients carrying pathogenic variants in the gene *PINK1*, especially the W437X homozygous mutation, may have reduced levels of serine biosynthetic enzymes. The observed effect could, at least in part, be mediated by

a transcriptional downregulation of the genes involved in serine synthesis and metabolism; however, since the levels of the transcription factor *ATF4* were found to be unchanged, the mechanisms of such downregulation remain elusive. Further studies, for example analyzing protein degradation of PHGDH in PINK1-depleted cells, will be needed to understand whether this could play a role in reducing protein levels. Of note, a recent study demonstrated that, in cancer models, Parkin regulates ubiquitination and degradation of PHGDH through the UPS (Liu et al., 2020), and PINK1 could potentially participate in this mechanism.

7.2.2. PINK1 Silencing Induces a Downregulation of Serine Biosynthetic Enzymes in SH-SY5Y Cells

SH-SY5Y cells were infected with lentiviruses expressing two shRNAs (shRNA #101, shRNA #193) targeting PINK1, inducing its post-transcriptional downregulation via RNA interference. Lentiviruses expressing a nonspecific scramble shRNA were used as control. Cells were harvested 7 days after viral transduction for RNA extraction and analysis by RT-qPCR. As shown in figure 16, both shRNAs induced a statistically significant reduction in relative mRNA levels of the genes PHGDH, PSAT1, PSPH, and SLC1A4. Stark downregulation of *PINK1* mRNA levels provided a proof of silencing efficiency.

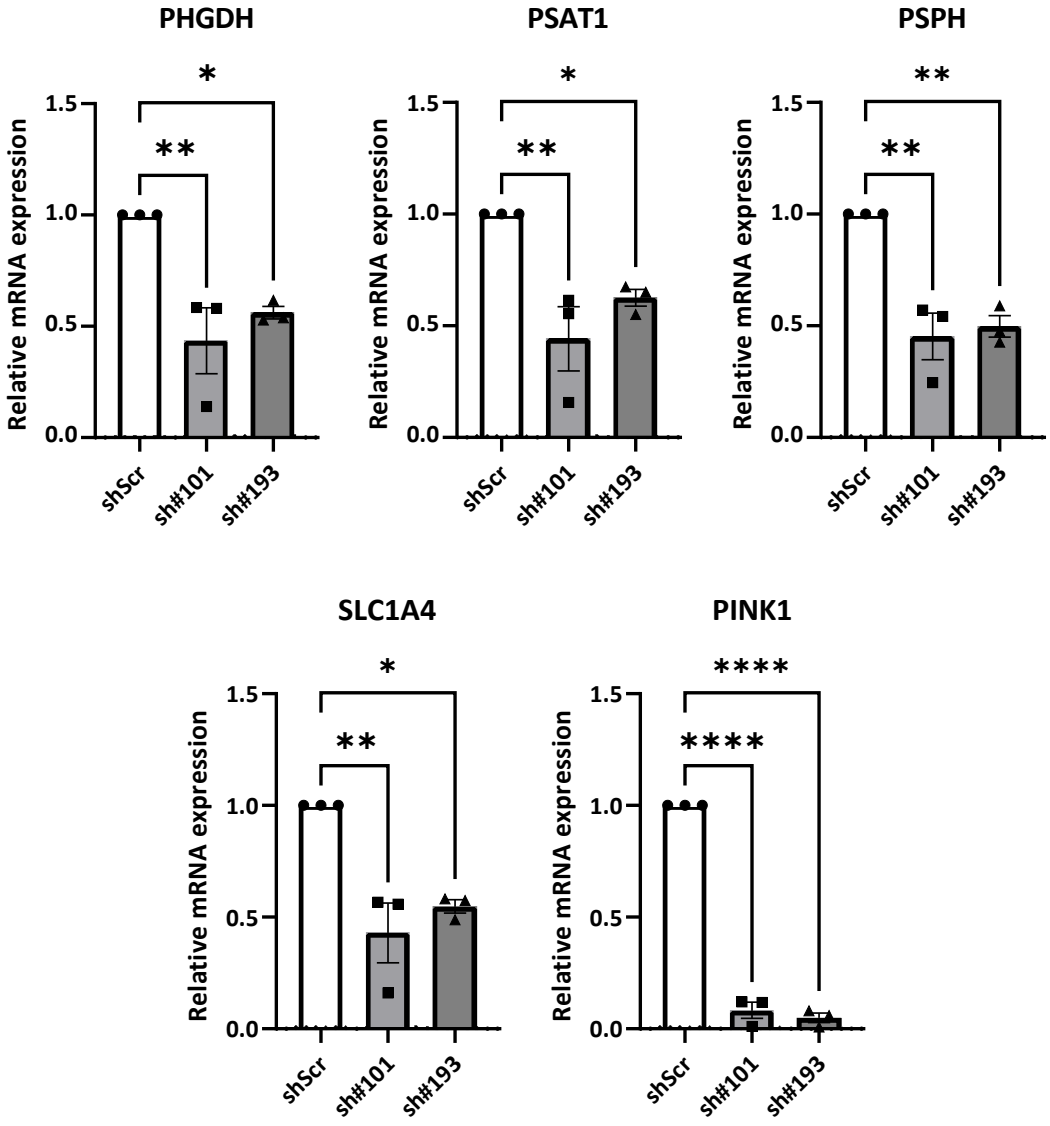

Figure 16. RT-qPCR showing relative mRNA levels of the genes PHGDH, PSAT1, PSPH, SLC1A4, PINK1 in SH-SY5Y cells transduced with a control scramble shRNA (shScr) or two PINK1 silencing shRNAs (sh#101, sh#193); normalized to ACTB, mean ± SEM.

Cell pellets obtained in the same experiments were processed for protein extraction and WB, but the resulting images had a poor quality, possibly due to sample degradation or improper handling. However, the statistical analysis of triplicate experiments, represented in figure 17, showed a tendency towards a lower protein concentration of PHGDH, PSAT1, and PSPH, although not statistically significant.

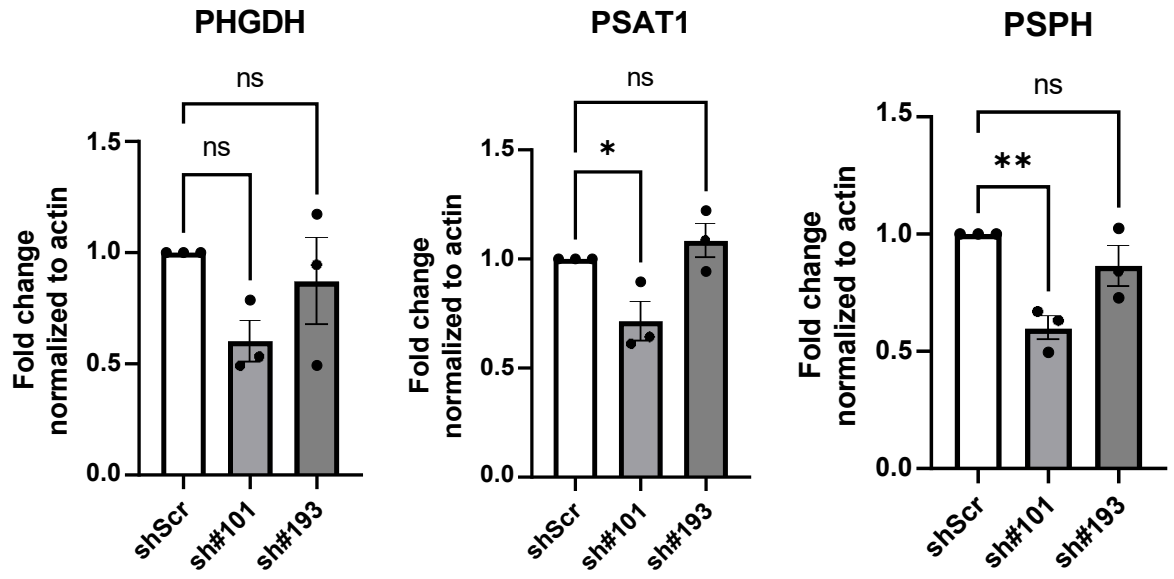

Figure 17. Western Blot densitometric analysis representing the protein concentration of PHGDH, PSAT1, PSPH normalized to ACTB in SH-SY5Y cells transduced with scramble (shScr) or PINK1 silencing (sh#101, sh#193) shRNAs; mean ± SEM.

Lentiviral transduction of shRNAs can result in an unwanted activation of the cellular interferon pathway due to the recognition as foreign nucleic acids of specific and scramble interfering RNAs (Olejniczak et al., 2010). Since PINK1 has been described in different ways as modulator of innate immune pathways linked to interferon production (Sliter et al., 2018; Zhou et al., 2019), and interferon signaling and serine metabolism appear to be interconnected (Shen et al., 2021; Yu et al., 2019), I investigated whether the observed effect could stem from a different activation of the interferon pathway due to *PINK1* silencing. To do so, I assessed the mRNA expression levels of effectors of the interferon pathway that are transcriptionally regulated (OAS1, EIF2a, IFRG15) in SH-SY5Y cells transduced with shScr, sh#101, sh#193 relative to non-transduced cells.

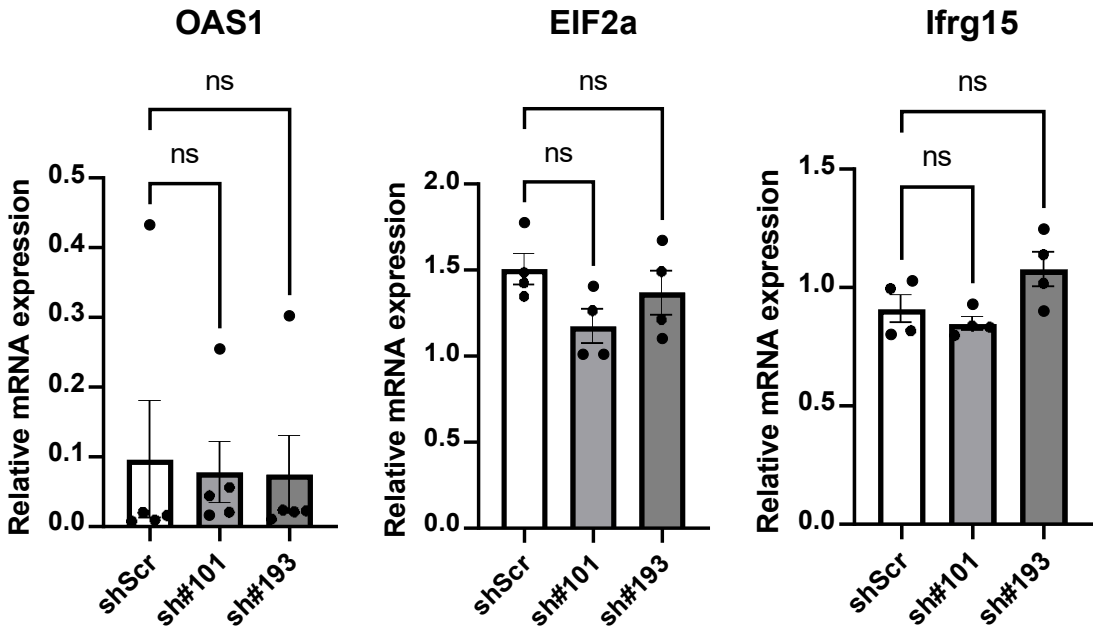

Figure 18. RT-qPCR showing mRNA levels of the genes OAS1, eIF2a, Ifrg15 in SH-SY5Y cells transduced with a control scramble shRNA (shScr) or two PINK1 silencing shRNAs (sh#101, sh#193) relative to untransduced SH-SY5Y cells; normalized to ACTB, mean ± SEM.

As shown in figure 18, in these experimental conditions there was no undesirable induction of interferon signaling. Contrary to expectations, relative mRNA levels of the gene OAS1 were lower in transduced than in non-transduced cells. Anyways, since there was no significant differential activation of the pathway between nonspecific and *PINK1*-silencing shRNAs, the effect observed on genes of serine biosynthesis did not seem to be mediated by interferon signaling.

7.2.3. *PINK1* Silencing Induces a Downregulation of Serine Biosynthetic Enzymes in iPSC-Derived Dopaminergic Neurons

Mesencephalic dopaminergic neurons (DANs) were differentiated for 30 days from wild-type iPSC-derived smNPCs following Reinhardt's protocol (Reinhardt et al., 2013). At differentiation day 23, cultured cells were infected with lentiviruses expressing the shRNAs #101 and #193, specific for *PINK1* mRNA, or a control scramble shRNA. At

differentiation day 30, cells were harvested for RT-qPCR to assess the relative mRNA expression of the genes of the phosphorylated pathway *PHGDH*, *PSAT1*, *PSPH*, the serine transporter *SLC1A4*, as well as *PINK1* to confirm silencing efficiency.

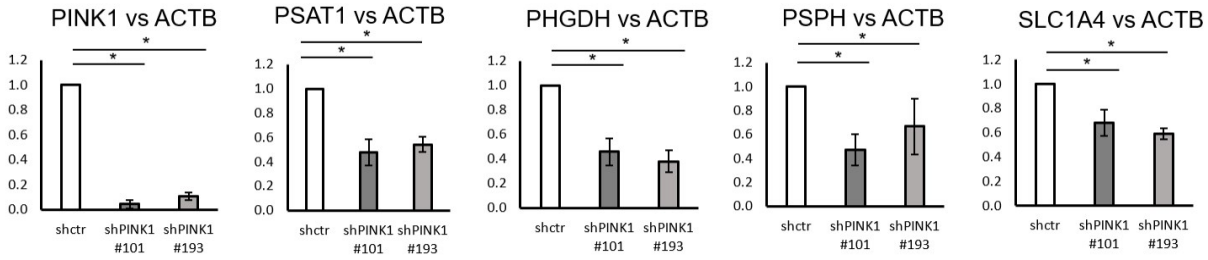

Figure 19. RT-qPCR showing mRNA levels of the genes PINK1, PHGDH, PSAT1, PSPH, SLC1A4 in day 30 mesencephalic dopaminergic neurons transduced with a control scramble shRNA (shScr) or two PINK1 silencing shRNAs (sh#101, sh#193); normalized to ACTB, mean ± SEM.

Results are shown in figure 19. *PINK1* mRNA levels confirmed a satisfactory silencing effectiveness with both shRNAs (≥95% reduction of gene expression). This corresponded to a significant reduction of relative mRNA levels of *PHGDH*, *PSAT1*, and *PSPH* (~50% reduction of gene expression) and a smaller reduction of *SLC1A4* mRNA levels (25-30%). Protein levels were assessed through Western Blots from samples collected during the same experiments.

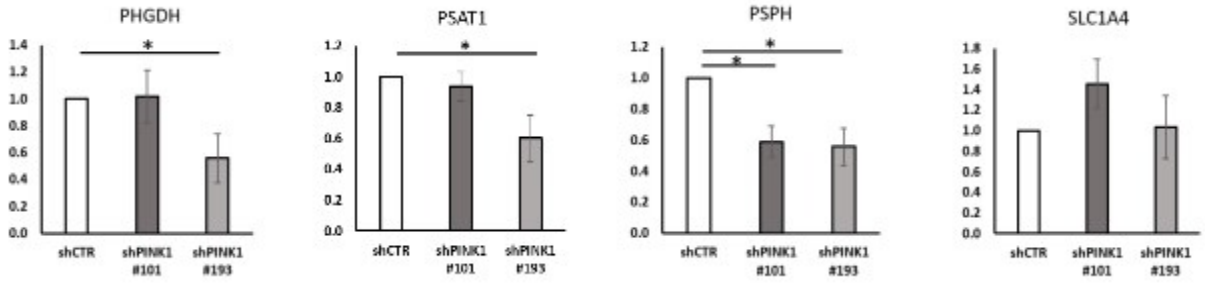

Figure 20. Densitometric analysis of Western Blots showing protein levels of PHGDH, PSAT1, PSPH, SLC1A4 in day 30 mesencephalic dopaminergic neurons transduced with a control scramble shRNA (shCtr) or two PINK1 silencing shRNAs (sh#101, sh#193); expressed as foldchange to shCtr, normalized to ACTB, mean ± SEM.

As shown in figure 20, the reduction in protein levels was moderate compared to the one observed at the mRNA level. However, the reduction was statistically significant for cells transduced with shRNA #193 for PHGDH, PSAT1, PSPH. No reduction in protein levels of the transporter SLC1A4 was observed in these experiments.
Interestingly, attempts to modify the experimental settings seemed to suggest that the removal of antioxidants during the last 2 days of neuronal maturation could emphasize the differences between control and PINK1-depleted cells. This effect, which is shown in the Western Blot in figure 21 and was particularly evident for PHGDH and PSPH, was achieved by removing ascorbic acid, N2 supplement, and B27 supplement from the components of the Maturation Medium.

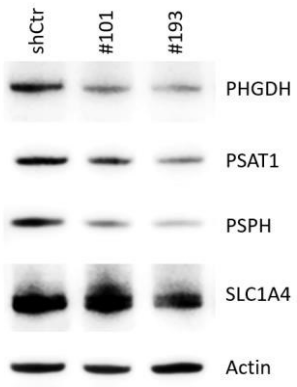

Figure 21. Western Blot showing protein levels of PHGDH, PSAT1, PSPH, SLC1A4, and ACTB as loading control in day 30 midbrain dopaminergic neurons transduced with a control scramble shRNA (shCtr) or two PINK1 silencing shRNAs (sh#101, sh#193); 48 hours before harvesting cell pellets, antioxidants and antiapoptotic factors (ascorbic acid, N2 supplement, B27 supplement) were removed from the cell medium.

7.2.4. PINK1 KO SH-SY5Y Cells Fail to Induce the Serine Synthesis Pathway in Response to Prolonged Serine Deprivation

The expression of the enzymes of the phosphorylated pathway PHGDH, PSAT1, and PSPH was analyzed in wild-type and PINK1 KO SH-SY5Y cells grown in standard growth

medium (i.e., Complete DMEM 10%) or in Starvation MEM. The FBS-deprivation in Starvation MEM induces a so-called *differentiation* of SH-SY5Y neuroblastoma cells, in a way comparable to previously reported protocols to obtain neuronal cultures from this cell line (Shipley et al., 2016). The neuroblastoma cells in Starvation MEM, during my experiments, gradually lost their original epithelial appearance, stopped replicating, and assumed a morphology resembling neurons, with long cellular processes projecting from one cell to another. They did, however, form dense cellular cultures due to intense proliferation during the first days. After 7 days, cells were expressing typical neuronal markers, such as TUJ1/TUBB3 and synaptophysin (figure 22).

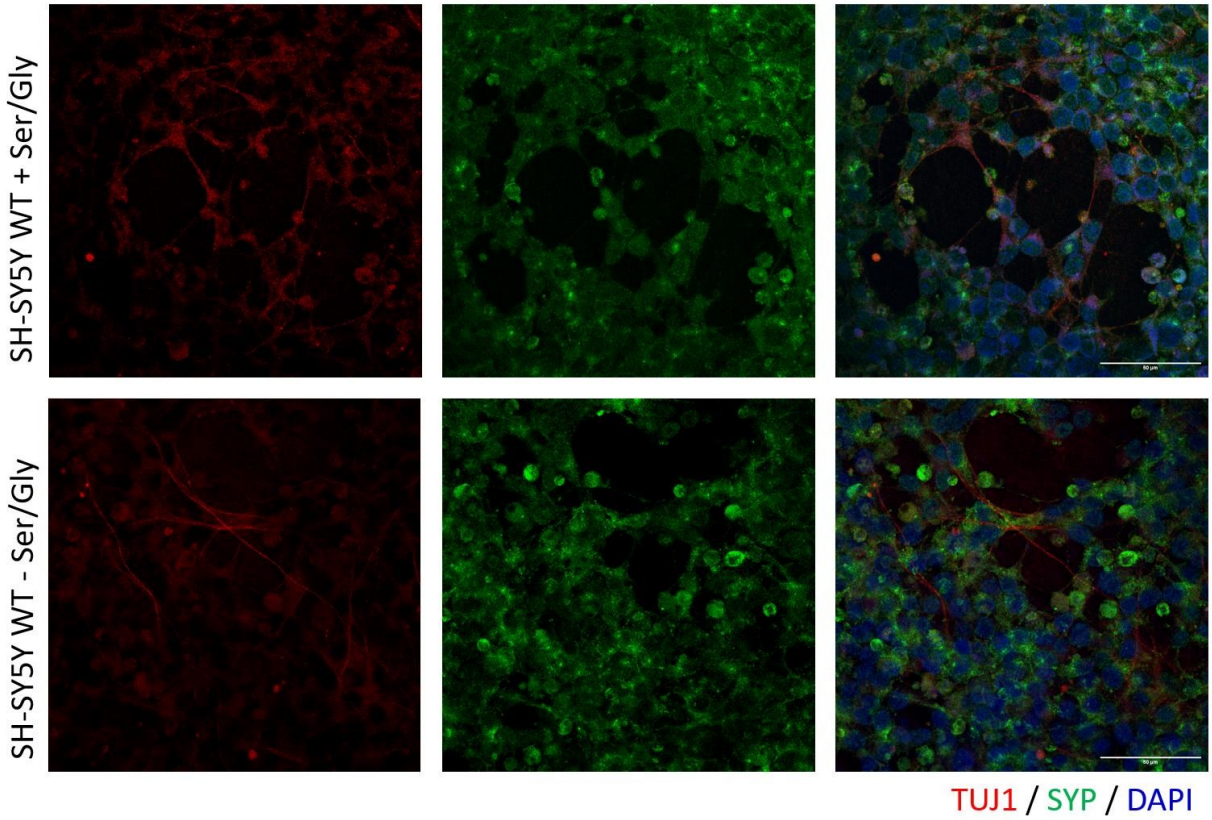

Figure 22. Wild-type SH-SY5Y neuroblastoma cells maintained in Starvation MEM (-Ser/Gly) or Starvation MEM supplemented with 0.4 mM L-serine and glycine (+Ser/Gly). Immunofluorescence showing the expression of neuronal markers TUJ1/TUBB3 (red) and synaptophysin (SYP, green), nuclei stained with DAPI (blue); scalebar 50 µm.

The morphological appearance of living PINK1 KO SH-SY5Y cells was similar to that of wild-type cells when observed under a contrast microscope, except for a slightly higher tendency to grow vertically on top of other layers of cells. However, in most cases the cell lines were indistinguishable in both conditions (Ser/Gly-containing and Ser/Gly-free media). I used immunocytochemistry to analyze qualitatively the expression of the markers TUJ1/TUBB3 and synaptophysin (SYP) in the two experimental conditions. Overall, the expression of these markers did not show major variations.

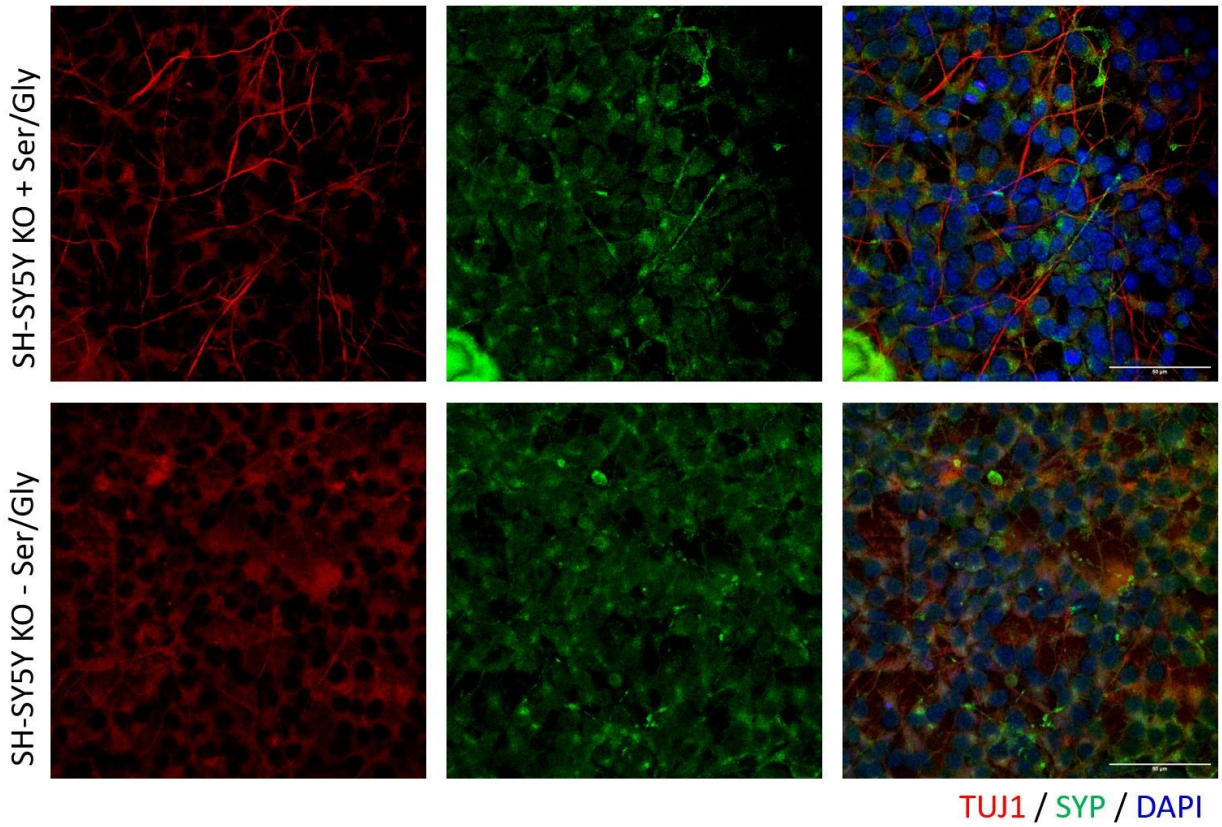

Figure 23. PINK1 KO SH-SY5Y cells maintained in Starvation MEM (-Ser/Gly) or Starvation MEM supplemented with 0.4 mM L-serine and glycine (+Ser/Gly). Immunofluorescence showing the expression of neuronal markers TUJ1/TUBB3 (red) and synaptophysin (SYP, green), nuclei stained with DAPI (blue); scalebar 50 µm.

In basal conditions, PINK 1 KO cells did not show any reduction in serine biosynthetic enzymes compared to wild-type cells, as shown in figure 23.

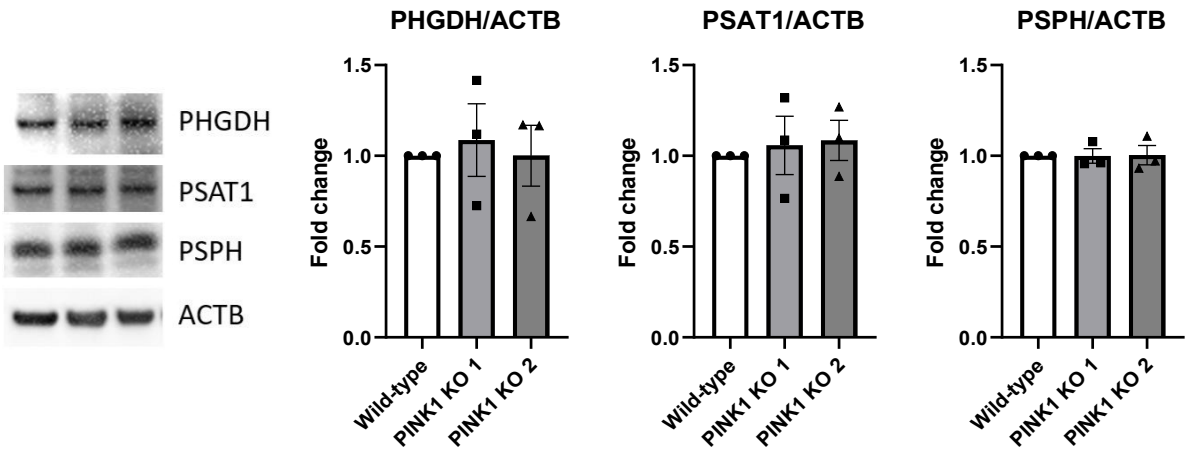

Figure 24. Western Blot showing PHGDH, PSAT1, PSPH, and ACTB as loading control in wild-type SH-SY5Y cells and two PINK1 KO SH-SY5Y clones. Densitometric analysis of PHGDH, PSAT1, PSPH; values are expressed as fold change relative to wild-type control; bars represent mean ± SEM.

No change was observed in protein levels of PHGDH, PSAT1, and PSPH in wild-type SH-SY5Y cells versus two PINK1 KO clones (figure 24). The same result was obtained after keeping the cells in Starvation MEM for 1 or 2 days (data not shown).

However, after 7 days of L-serine and glycine deprivation in Starvation MEM, PHGDH protein levels increased significantly in WT cells, while in KO cells they remained unaltered.

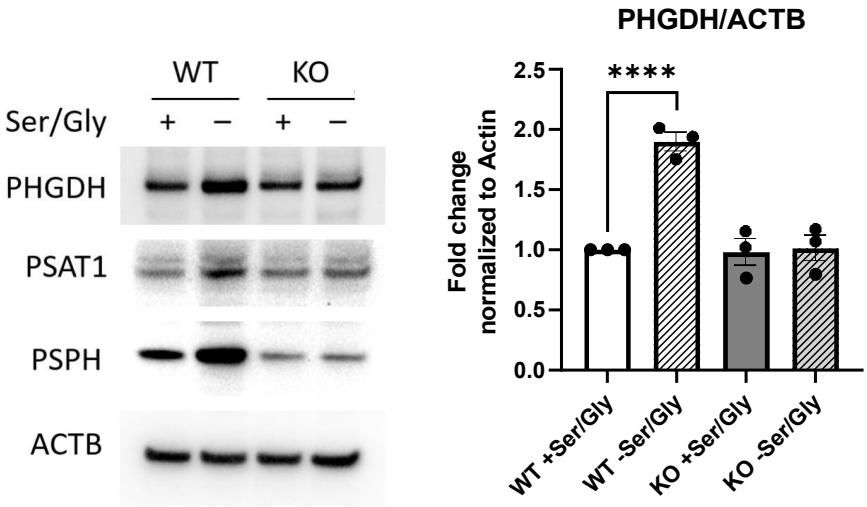

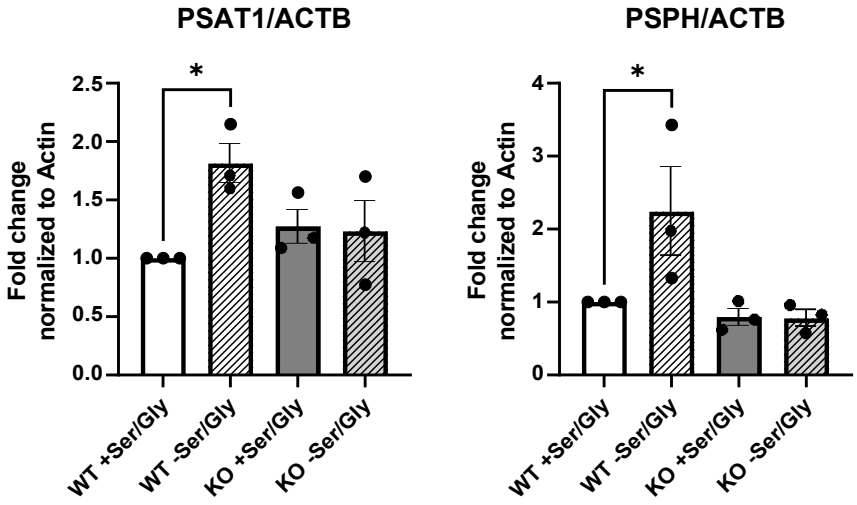

Figure 25. Western Blot showing PHGDH, PSAT1, PSPH, and ACTB as loading control in wild-type and PINK1 KO SH-SY5Y cells after 7 days in Starvation MEM (-) or Starvation MEM supplemented with 0.4 mM L-serine and 0.4 mM glycine. Densitometric analysis of PHGDH, PSAT1, PSPH; values are expressed as fold change relative to wild-type control in Ser/Gly-containing medium; bars represent mean ± SEM.

These results suggest that, although in basal conditions (e.g., in Complete DMEM 10%) or after a short time of serine and glycine deprivation PINK1 KO SH-SY5Y cells do not show any significant difference in protein levels of PHGDH, PSAT1, and PSPH compared to wild-type cells, they may be unable to significantly induce the serine synthesis pathway in conditions of prolonged serine deprivation. It is important to note that, while after 1 or 2 days in Starvation MEM SH-SY5Y cells keep their “undifferentiated”, epithelial-like morphology, at the 7-day timepoint they assume a fully neural-like, “differentiated” phenotype. The effect, therefore, could potentially not only be linked to the duration of serine starvation *per se*, but also to the intrinsic cellular changes that happen during the intercurrent time.

7.2.5. PINK1 KO SH-SY5Y Cells Fail to Proliferate in Conditions of Serine Deprivation

There is abundant evidence that serine-glycine-one-carbon metabolism supports cell proliferation and growth in cancer (Amelio et al., 2014; Labuschagne et al., 2014; M. Yang

& Vousden, 2016), but information concerning neuronal cell models is scarce and, to the present date, no study investigated the interplay among PINK1, serine metabolism, and cellular growth rate. For this reason, I performed an assay to measure cell proliferation in wild-type and PINK1 KO SH-SY5Y neuroblastoma cells.

Starting from the same number of seeded cells, the two lines were grown in either Starvation MEM without Ser/Gly or Starvation MEM supplemented with 0.4 mM Ser/Gly. After 4 days, cells were counted by blinded operators.

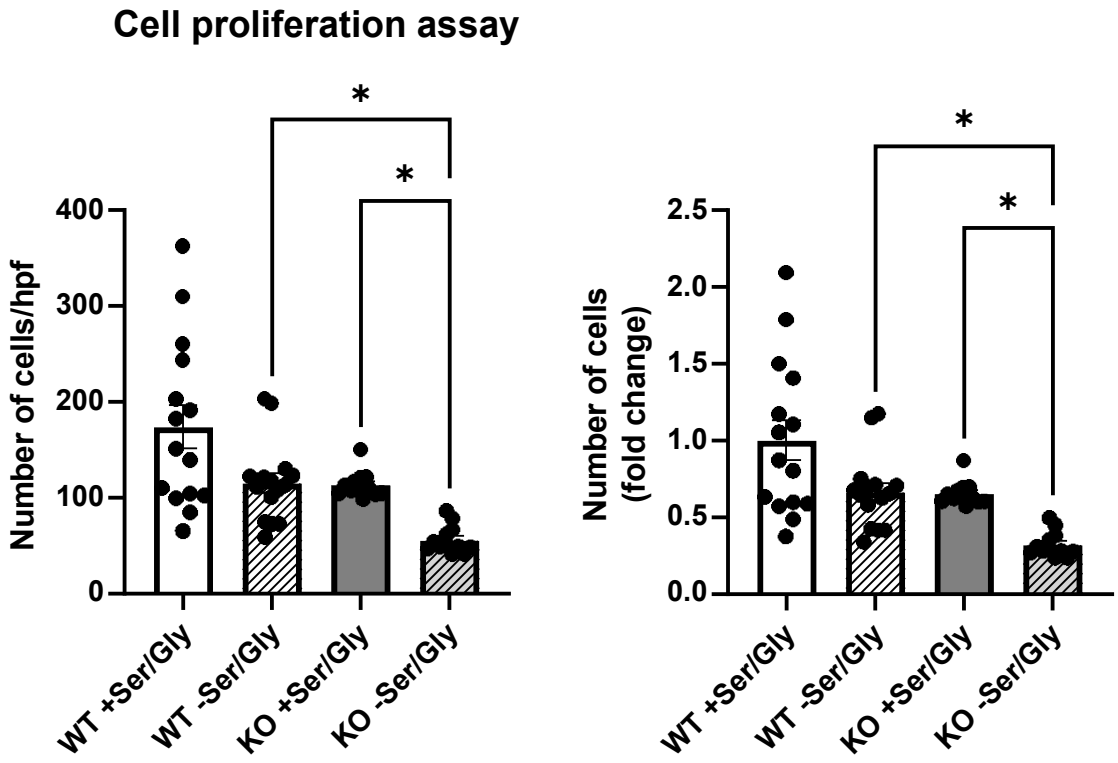

Figure 26. Cell proliferation assay. Wild-type and PINK1 KO SH-SY5Y neuroblastoma cells were grown for 4 days in Starvation MEM either without L-serine and glycine (-Ser/Gly) or supplemented with 0.4 mM L-serine and glycine (+Ser/Gly). Then, blinded operators acquired random pictures and counted cells. Results are shown as cell count per high-power field (hpf) and fold change; bars represent mean ± SEM.

As represented in figure 26, PINK1 KO cells showed a significant deficit of proliferation in Ser/Gly-free medium, reaching a number of cells/hpf equal to approximately half that

of wild-type cells in the same medium. Strikingly, the simple addition of L-serine and glycine could rescue the phenotype, bringing the proliferation rate back to values similar of those of wild-type cells. However, wild-type cells in Ser/Gly-containing media grew even more, suggesting that the absence of PINK1 alone could not explain the deficit of proliferation observed in Ser/Gly-free media. In other words, based on the presented data it is impossible to exclude whether the observed phenomenon could be due to the combined effect of two independent growth hampering conditions (i.e., serine deprivation and PINK1 deficiency), rather than an interplay between PINK1 and serine metabolism.
An effect of serine and its metabolism on proliferation and growth in different cellular models has been reported before (Diehl et al., 2019)

7.2.6. PINK1 KO SH-SY5Y Cells Have Higher Levels of ROS, but Serine Supplementation Does Not Reduce Their Oxidative Burden

PINK1 (or Parkin) loss of function results in increased cellular oxidative stress due to mitochondrial dysfunction (Barodia et al., 2017). Since serine and glycine are metabolic precursors of glutathione, a critical antioxidant, I wanted to test the combined effect of PINK1 deficiency and serine deprivation on the oxidative status of SH-SY5Y neuroblastoma cells. To do so, I performed an assay to measure cellular levels of ROS *in vivo*, by means of H2-DCFDA, a sensitive, cell permeating dye that emits fluorescence proportionally to the concentration of oxidative species.
Wild-type and PINK1 KO SH-SY5Y cells were grown in presence or absence of L-serine and glycine, H_2O_2 was used to induce oxidative stress, as positive control. Fluorescence was measured with a well-scanning plate reader.

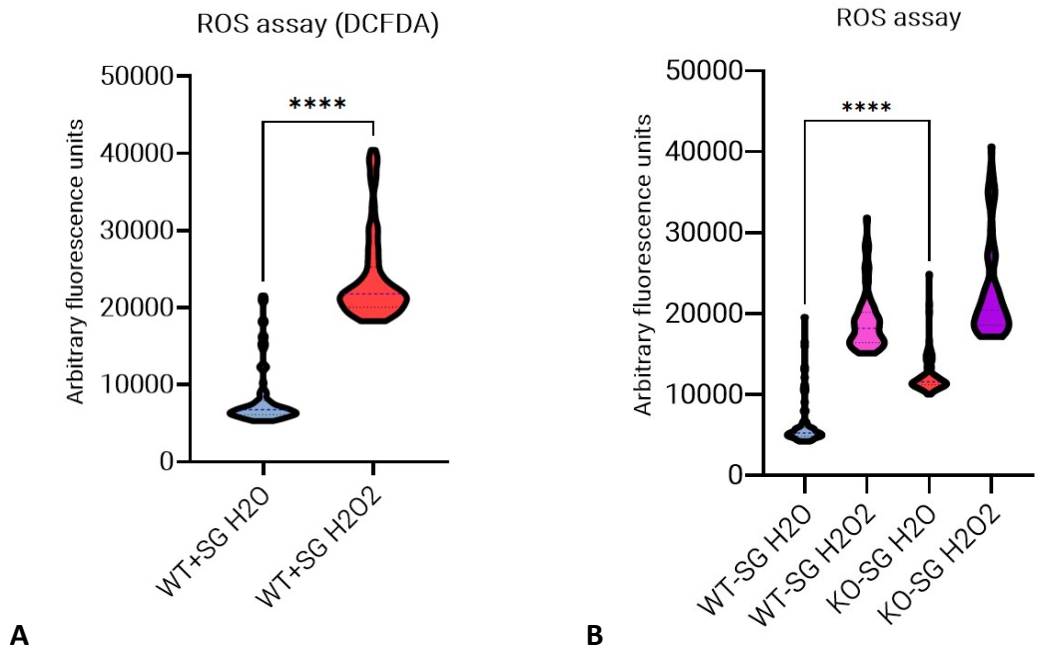

Figure 27. A. Wild-type SH-SY5Y cells (WT) maintained in medium containing 0.4 mM L-serine and 0.4 mM glycine (+SG), treated with either H_2O as negative control or H_2O_2 to test the effectiveness of the assay. B. Wild-type (WT) or PINK1 KO (KO) SH-SY5Y cells in Ser/Gly-free medium (-SG) treated with either H_2O or H_2O_2.

As shown in figure 27A, H_2O_2 in wild-type cells grown in standard conditions induced an important increase in ROS detected as significantly higher measured fluorescence levels, providing proof of concept for the assay. In figure 27B, as expected, PINK1 KO cells presented significantly higher levels of oxidative species than wild-type cells, and treatment with H_2O_2 increased fluorescence even further in both cell lines.

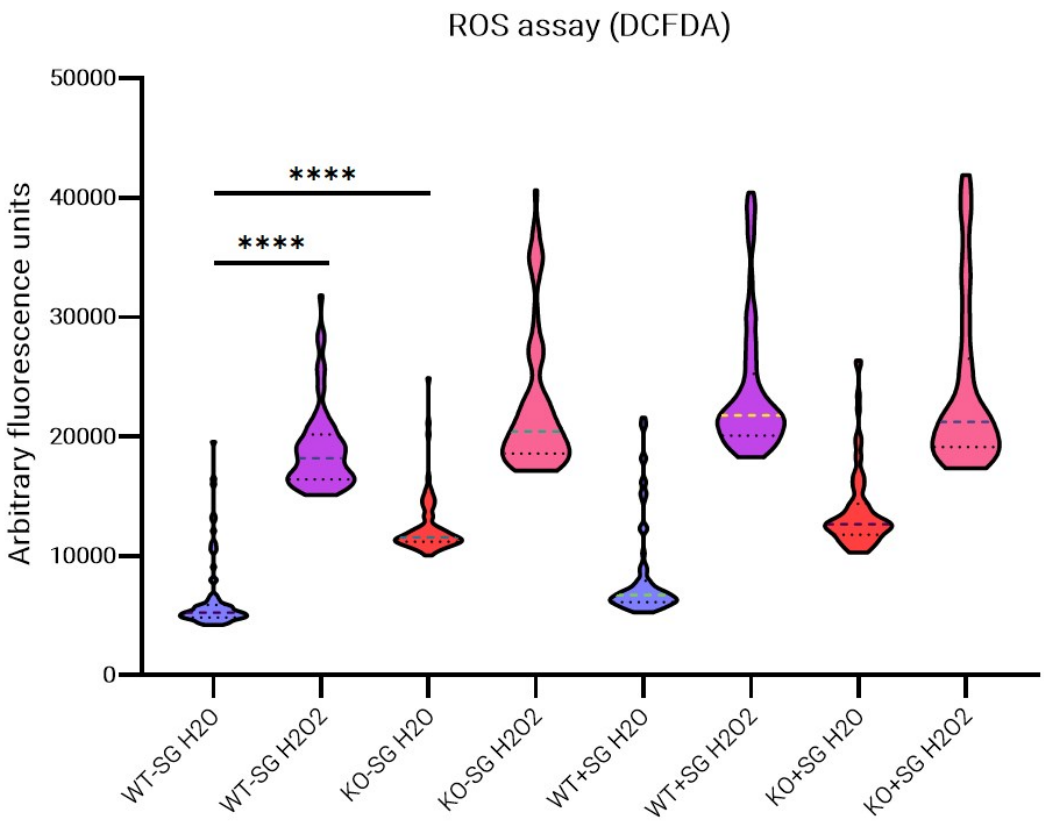

Figure 28. Wild-type (WT) or PINK1 KO (KO) SH-SY5Y cells in Ser/Gly-free medium (left hand side of the graph, labeled -SG) or medium containing 0.4 mM L-serine and 0.4 mM glycine (right hand side of the graph, labeled +SG) treated with either H_2O or H_2O_2.

However, as shown in figure 28, addition of 0.4 mM L-serine and 0.4 mM glycine did not reduce oxidative stress in these cellular models; actually, it caused a slight increase in measured fluorescence in all lines and conditions tested.

7.2.7. Intracellular and Extracellular Serine Quantification by LC-MS

In order to quantify the amount of intracellular and extracellular serine in our cellular model, I collected pellets and media samples from wild-type SH-SY5Y cells and two PINK1 KO clones grown for 4 days in Ser/Gly-free MEM.

These samples were analyzed in the Unit of Clinical and Experimental Pharmacology of our university with a LC-MS approach based on a published protocol (Sugimoto et al., 2015).

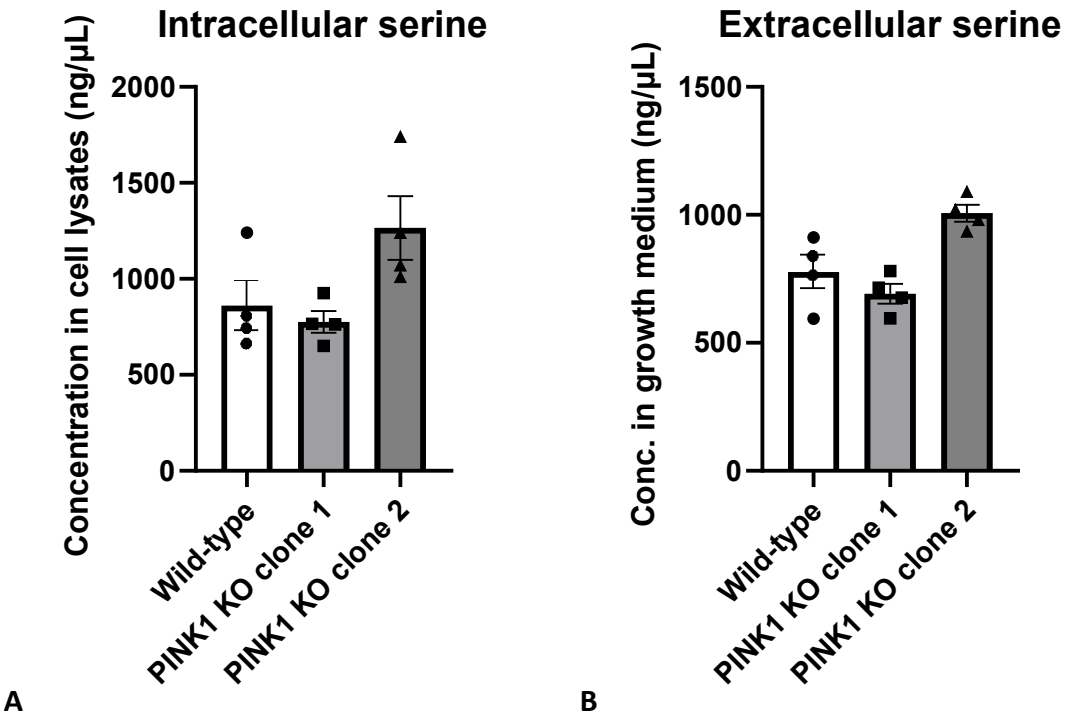

Figure 29. A. Serine concentration in SH-SY5Y cell lysates (wild-type and two PINK1 KO clones) measured by LC-MS; mean ± SEM. B. Serine concentration in cell culture medium in which SH-SY5Y cells (wild-type and two PINK1 KO clones) were maintained measured by LC-MS; mean ± SEM.

The analysis, however, did not identify any relevant difference in intracellular or extracellular serine concentration between wild-type and PINK1 KO clones.

7.2.8. Seahorse XF Cell Mito Stress Test

Wild-type and PINK1 KO SH-SY5Y neuroblastoma cells were tested with the Seahorse XF Cell Mito Stress Test using the standard (L-serine- and glycine-containing) media provided with the commercial kit. In this assay, cultured cells are exposed to different chemicals in sequence: 1) oligomycin, an ATP-synthase inhibitor, 2) carbonyl cyanide-4

trifluoromethoxy phenylhydrazone (FCCP), an uncoupling agent that depolarizes the mitochondrial membrane, and 3) a mixture of rotenone and antimycin A, respectively a complex I and complex III inhibitor. Oxygen consumption rate (OCR) and extracellular acidification rate (ECAR) are measured at baseline and at regular timepoints after each injection (Divakaruni et al., 2014).

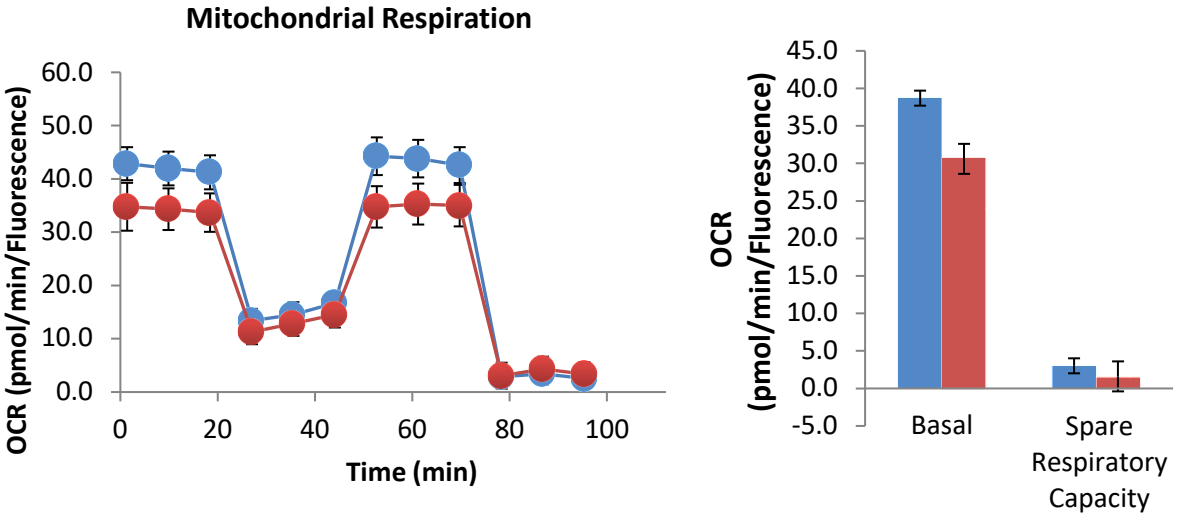

Figure 30. Seahorse XF Cell Mito Stress Test on wild-type (blue) and PINK1 KO (red) SH-SY5Y cells. Cells were afterwards fixed and stained with DAPI to measure fluorescence as a proxy of cell density to normalize raw data.

The analysis highlighted a slightly lower oxygen consumption rate (OCR) in PINK1 KO cells at basal, minimal, and maximal levels of respiration. However, both wild-type and PINK1 KO cells showed very small spare respiratory capacity. This finding, in line with data from previous studies (Jeong et al., 2018; Xun et al., 2012), means that SH-SY5Y cells almost use their entire respiratory capacity in the initial, pre-treatment, conditions. This is suboptimal, as in most cellular models the most significative differences (e.g., between wild-type and KO) are revealed at maximal respiration.

7.2.9. iPSC-Derived Midbrain Dopaminergic Neurons Carrying Pathogenic *PINK1* Variants Do Not Show a Downregulation of the Phosphorylated Pathway

Midbrain dopaminergic neurons were differentiated from iPSC-derived smNPCs following Reinhardt's protocol, as described in the Material and Methods. On differentiation day 30, cells were harvested for RT-qPCR and Western Blot.

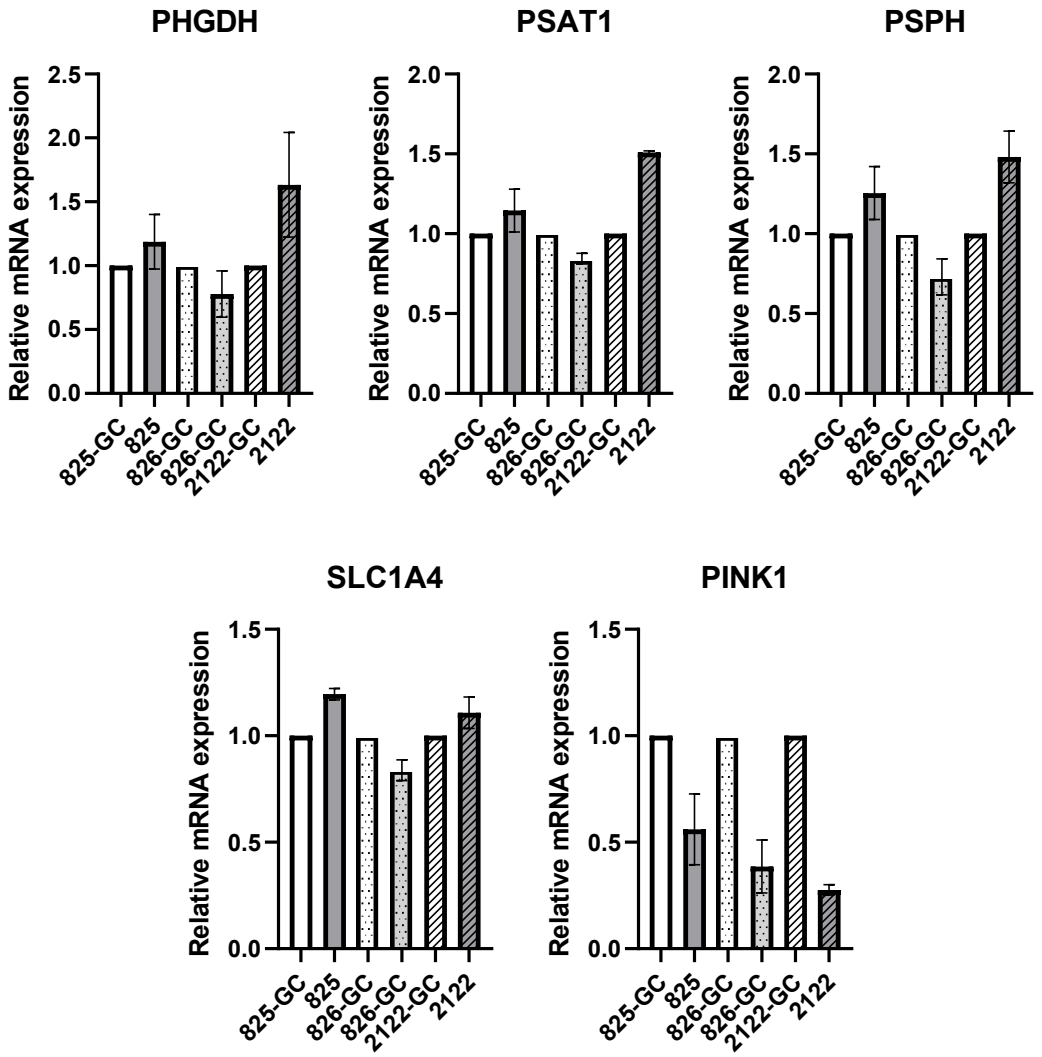

Figure 31. RT-qPCR data showing the relative mRNA expression levels of PHGDH, PSAT1, PSPH, SLC1A4, and PINK1 in day 30 midbrain dopaminergic neurons derived from PD patients carrying the PINK1 Q456X homozygous variant (825, 826, 2122) relative to their isogenic gene-corrected controls (825-GC, 826-GC, 2122-GC); ACTB was used as housekeeping gene for normalization.

No significant variation was observed in the relative mRNA expression levels of *PHGDH*, *PSAT1*, *PSPH*, *SLC1A4* in day 30 midbrain dopaminergic neurons derived from PD patients carrying the *PINK1* Q456X homozygous variant compared to isogenic gene-corrected controls. The relative mRNA levels of *PINK1* showed a 50-80% reduction, suggesting a degree of nonsense-mediated RNA decay.

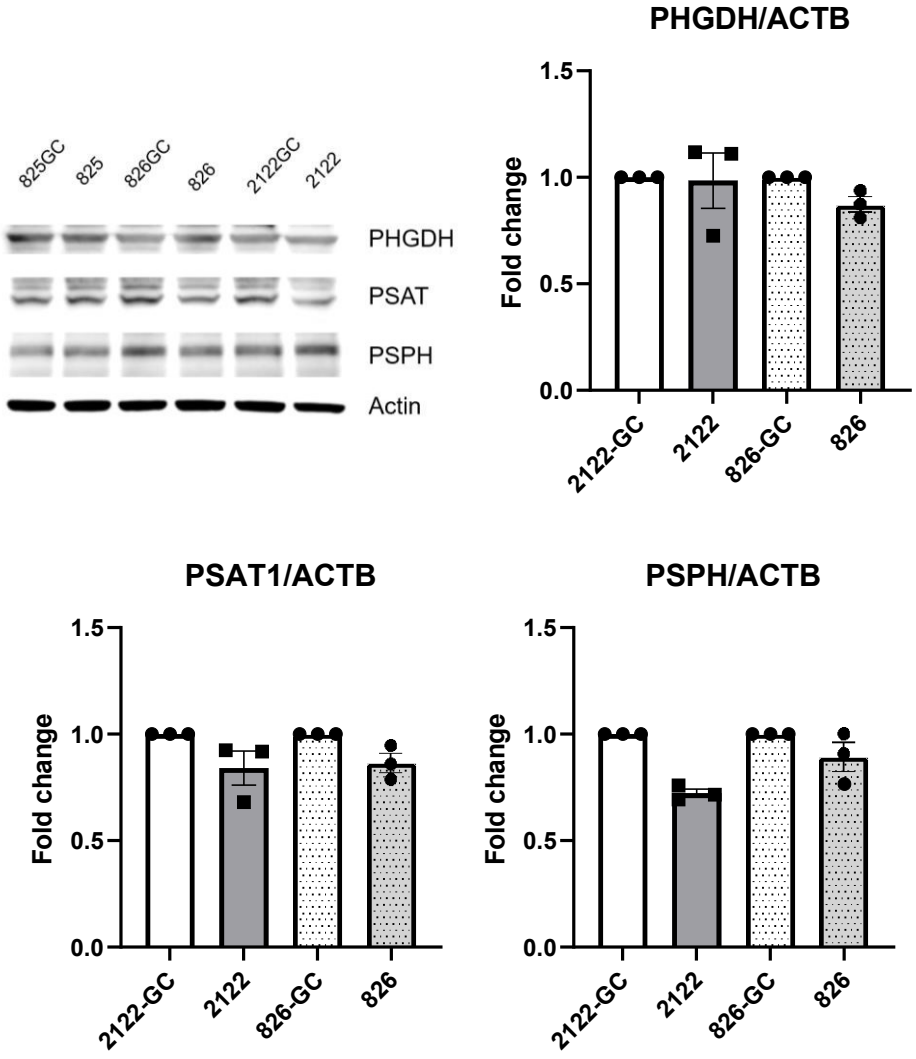

Figure 32. Representative Western Blot showing PHGDH, PSAT1, PSPH, and ACTB as loading control from whole cell lysates of day 30 midbrain dopaminergic neurons from three PD patients carrying the PINK1 Q456X homozygous variant (825, 826, 2122) and isogenic gene-corrected lines (825-GC, 826-GC, 2122-GC); densitometric analysis of protein levels of PHGDH, PSAT1, PSPH normalized to ACTB in day 30 midbrain dopaminergic neurons from PD patients carrying the PINK1

Q456X homozygous variant (826, 2122) and isogenic gene-corrected lines (826-GC, 2122-GC); mean ± SEM.

In Western Blots, no significant difference was observed in protein levels of serine biosynthetic enzymes in dopaminergic neurons carrying the *PINK1* Q456X variant compared to isogenic gene-corrected lines (figure 33).

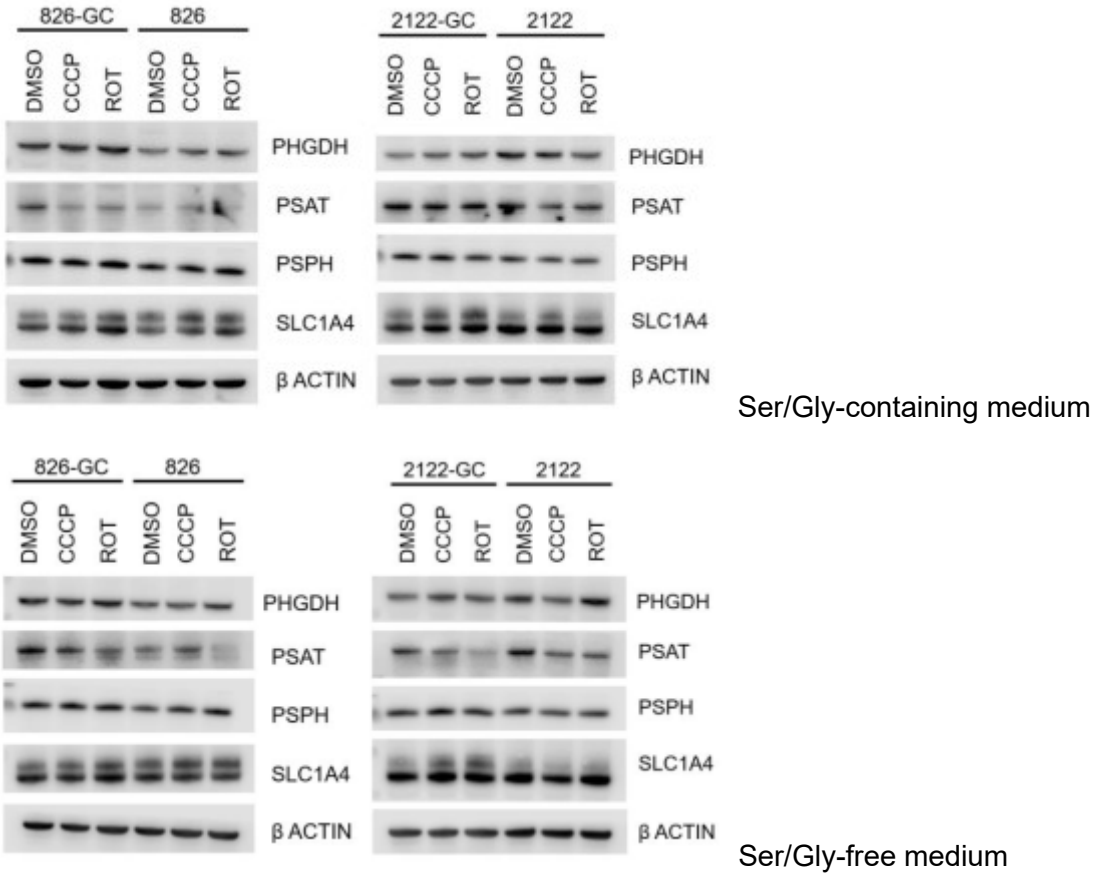

Figure 33. Western Blots showing PHGDH, PSAT1, PSPH, SLC1A4, and ACTB as loading control from whole cell lysates of day 30 midbrain dopaminergic neurons from PD patients carrying the PINK1 Q456X homozygous variant (826, 2122) and isogenic gene-corrected lines (826-GC, 2122-GC) maintained in Ser/Gly-containing or Ser/Gly-free media and treated overnight either with DMSO, 20 µM CCCP, or rotenone.

7.2.10. Dopaminergic Neurons Carrying Pathogenic *PINK1* Variants Develop a Stunted Neurite Arborization in Conditions of Serine Deprivation

To quantitatively evaluate the extension of neurite arborization during dopaminergic neuron differentiation, I adapted Reinhardt's protocol to differentiate smNPCs into mesencephalic dopaminergic neurons in suspension, as neurospheres, for 4 days in serine and glycine-free or serine and glycine-containing media. The neurospheres obtained from patients' or gene-corrected smNPCs in different media were uniform in size and morphology (figure 34A), averaging ~150 µm in diameter (figure 34B).

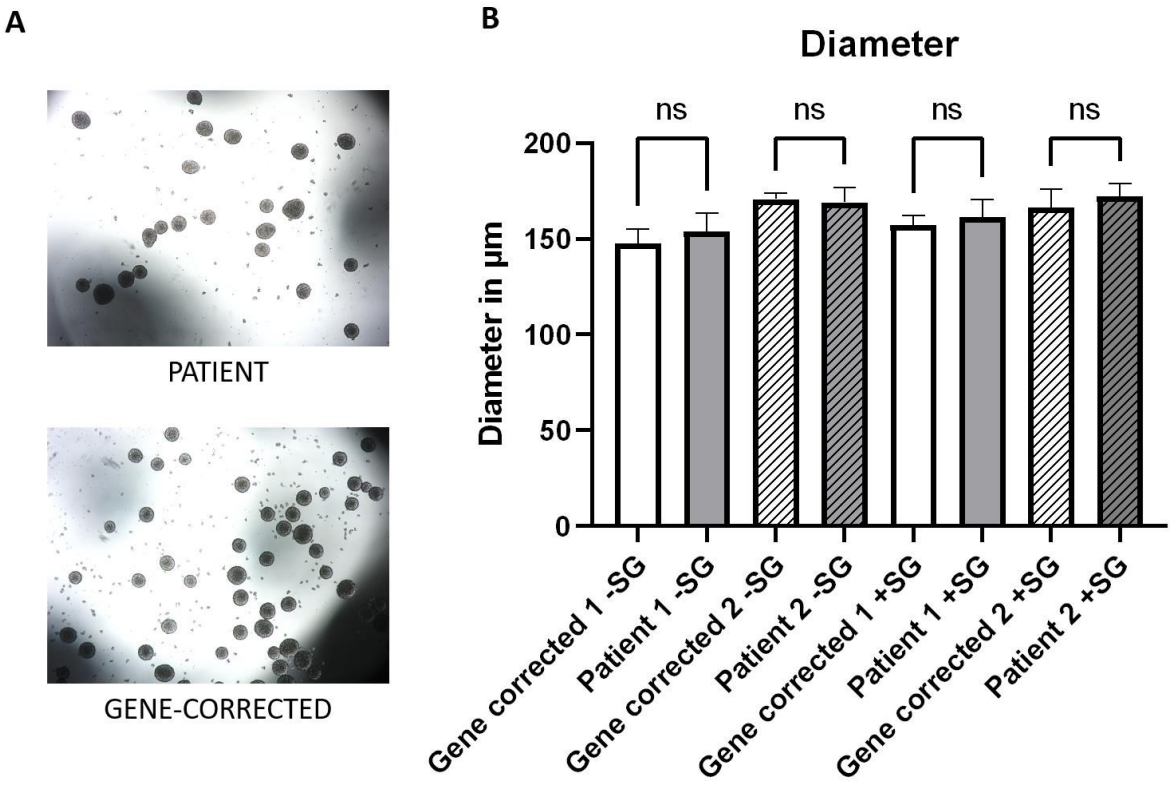

Figure 34. A. Contrast microscopy images of neurospheres derived from patient and isogenic gene-corrected smNPCs in suspension after 6 days of differentiation. B. Analysis of the measured diameter of neurospheres derived from patient and isogenic gene-corrected smNPCs in suspension after 6 days of differentiation in Ser/Gly-free media (-SG) or the same medium supplemented with 0.4 mM L-serine and 0.4 mM glycine (+SG); average ± SEM.

After 4 days of growth and differentiation in suspension in serine and glycine-free or serine and glycine-containing media, neurospheres were plated on Geltrex in the same media. For the following 2 days, neurites spurred from each neurosphere, forming a defined tree that could be imaged and analyzed by software.

Neurospheres carrying the *PINK1* Q456X variant grown and plated in serine and glycine-free media showed a significantly smaller neurite arborization than gene-corrected ones, with reduced number and length of neurites. A supplementation of serine and glycine at standard concentration (0.4 mM), however, was sufficient to rescue the phenotype.

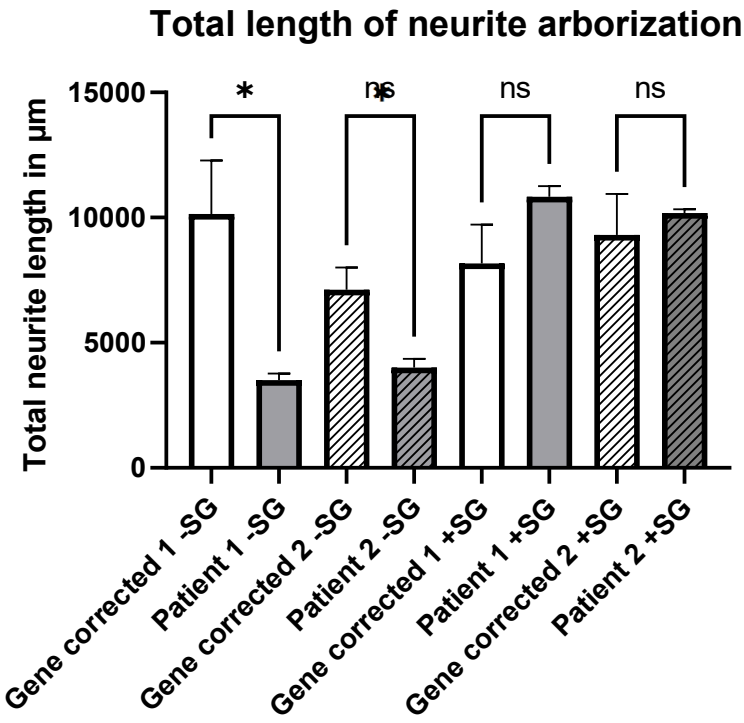

Figure 35. Total length of neurite arborization (sum of all neurite branches growing from a sphere) of dopaminergic neuron neurospheres differentiated from the smNPCs of two patients carrying the PINK1 Q456X pathogenic variant and isogenic gene-corrected smNPCs either in Ser/Gly-free medium (-SG) or in the same medium supplemented with 0.4 mM L-serine and glycine (+SG); mean ± SEM.

As represented in figure 35, neurospheres differentiated from both smNPCs lines carrying the PINK1 Q456X variant in Ser/Gly-free media showed a significantly smaller total length of neurite arborization than isogenic gene-corrected counterparts. However, addition of

0.4 mM L-serine and 0.4 mM glycine to the cell culture medium rescued entirely the observed phenotype, bringing the total length of the neurite tree to values similar to those of gene-corrected cells.

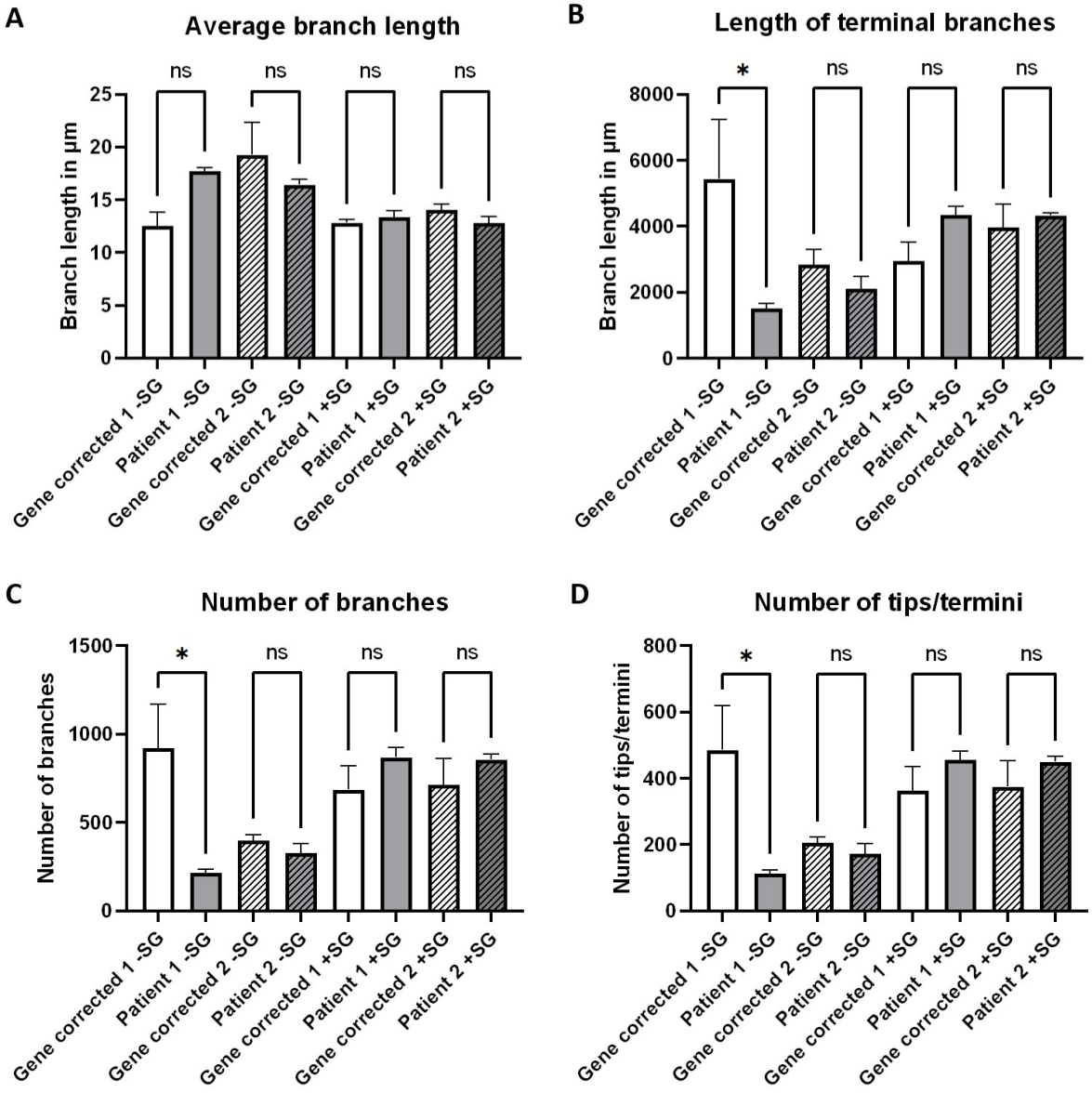

Figure 36. A. Average branch length of dopaminergic neuron neurospheres differentiated from the smNPCs of two patients carrying the PINK1 Q456X pathogenic variant and isogenic gene-corrected smNPCs either in Ser/Gly-free medium (-SG) or in the same medium supplemented with 0.4 mM L-serine and glycine (+SG); mean ± SEM. B. Length of terminal branches of dopaminergic neuron neurospheres differentiated from the smNPCs of two patients carrying the PINK1 Q456X

pathogenic variant and isogenic gene-corrected smNPCs either in Ser/Gly-free medium (-SG) or in the same medium supplemented with 0.4 mM L-serine and glycine (+SG); mean ± SEM. C. Number of branches (including primary, secondary, tertiary, …to terminal branches) of dopaminergic neuron neurospheres differentiated from the smNPCs of two patients carrying the PINK1 Q456X pathogenic variant and isogenic gene-corrected smNPCs either in Ser/Gly-free medium (-SG) or in the same medium supplemented with 0.4 mM L-serine and glycine (+SG); mean ± SEM. D. Number of tips/number of termini of dopaminergic neuron neurospheres differentiated from the smNPCs of two patients carrying the PINK1 Q456X pathogenic variant and isogenic gene-corrected smNPCs either in Ser/Gly-free medium (-SG) or in the same medium supplemented with 0.4 mM L-serine and glycine (+SG); mean ± SEM.

Several other parameters were measured from the images, including average branch length, length of terminal branches, number of branches, and number of tips/termini. Except for the average branch length, which did not change significantly across different lines and different conditions, neurons lacking a functional PINK1 consistently reached lower lengths or lower numbers in conditions of serine deprivation. This difference was statistically significant only for one patient-isogenic gene-corrected pair.

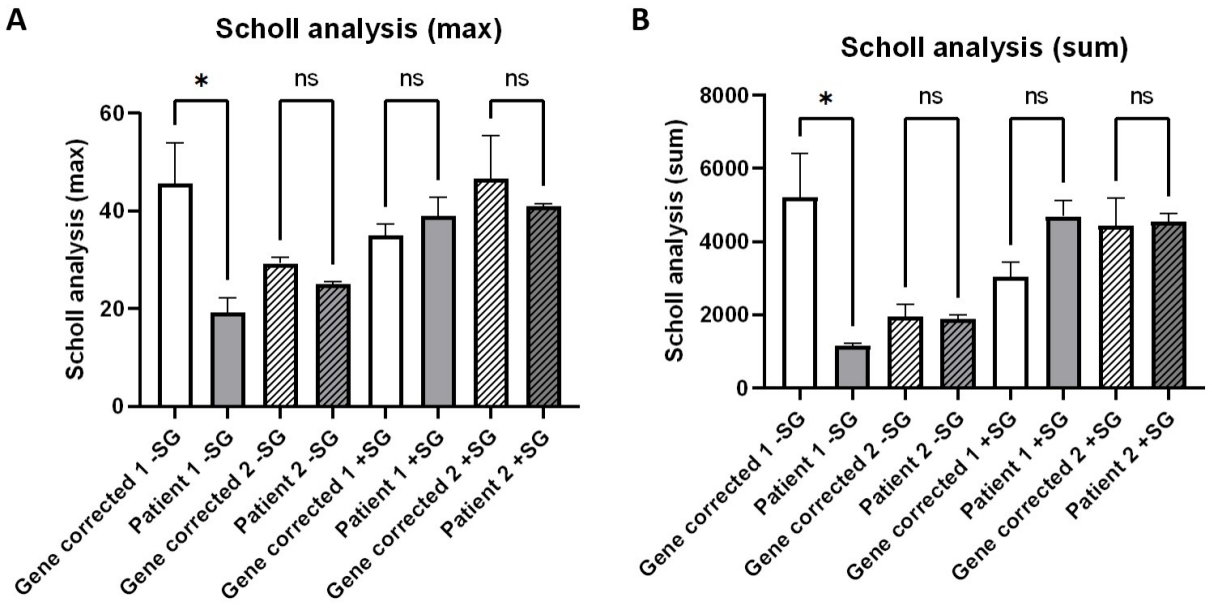

Figure 37. A. Maximum Scholl number of dopaminergic neuron neurospheres differentiated from the smNPCs of two patients carrying the PINK1 Q456X pathogenic variant and isogenic gene-

corrected smNPCs either in Ser/Gly-free medium (-SG) or in the same medium supplemented with 0.4 mM L-serine and glycine (+SG); mean ± SEM. B. Sum of Scholl numbers of dopaminergic neuron neurospheres differentiated from the smNPCs of two patients carrying the PINK1 Q456X pathogenic variant and isogenic gene-corrected smNPCs either in Ser/Gly-free medium (-SG) or in the same medium supplemented with 0.4 mM L-serine and glycine (+SG); mean ± SEM.

Scholl analysis is a simple method to characterize quantitatively the morphology of neurons. It consists in drawing concentric circles (in this case, centered on the neurosphere) and counting the number of intersections of each circle with cellular processes radiating from the center. This analysis too demonstrated that, in Ser/Gly-free medium, neurons carrying *PINK1* variants grow fewer neurites that reach shorter distances than gene-corrected counterparts. This difference, however, disappeared in Ser/Gly-containing medium.

7.2.11. Astrocytes

Most recent studies point to astrocytes as the main serine-producing cells in the human CNS (Murtas et al., 2020). Based on this evidence, I differentiated astrocytes from iPSCs to assess whether they show levels of serine biosynthetic enzymes higher than iPSC-derived neurons and/or show a significant induction of the phosphorylated pathway during serine starvation. Conventional NSCs were derived from wild-type iPSC HDF108 and then further differentiated to astrocytes for 60 days.

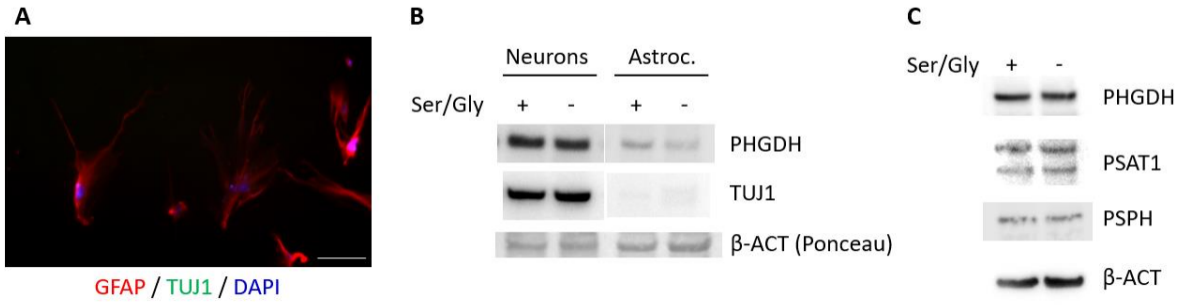

Figure 38. A. Immunofluorescence showing iPSC-derived astrocytes at maturation day 60 stained with anti-GFAP Ab (red), anti-TUJ1/TUBB3 Ab (green), and DAPI (blue); scalebar 50 µm. B. Western

Blot of lysates of astrocytes and iPSC-derived neurons grown in Ser/Gly-containing or Ser/Gly-free media for 7 days. C. Western Blot of astrocyte lysates grown in Ser/Gly-containing or Ser/Gly-free media for 7 days.

After 60 days of maturation, the culture was formed predominantly of star-shaped cells expressing GFAP but not TUJ1/TUBB3 (figure 38A). However, contrary to previous reports, astrocytes showed lower levels of PHGDH than iPSC-derived neurons in the tested conditions, i.e., 7 days of culture in Ser/Gly-containing or Ser/Gly-free media, as detected by Western Blot in figure 38B. Moreover, prolonged serine starvation failed to induce an upregulation of the enzymes of the phosphorylated pathway in astrocytes, as shown in figure 38C.

8. Conclusion

In this chapter I will provide a final overview of the research outcomes of the projects included in this dissertation, putting them in relation to the aims and research questions formulated at the beginning of this doctoral degree. I will also mention some limitations of the used experimental approaches, contextualize the findings, and delineate possible future developments.

Part I describes the generation and characterization of two iPSC lines derived from PD patients carrying pathogenic *PINK1* variants in compound heterozygous form. The obtained cell lines showed optimal and stable morphology, high expression of pluripotency markers, and absence of deleterious chromosomal abnormalities, supporting their staminal nature. They became then available for future studies. Both patients (and iPSC lines) were monoallelic carriers of the *PINK1* Q456X variant, the effects of which have been described in several studies, including in iPSC-based models. The mutations on the second allele, however, were in both cases rare and, so far, never mentioned in functional studies, especially in iPSC-based models. The general utility of iPSCs in PD research is unmistakable and related to the possibility of generating terminally differentiating cells – such as neurons – with the exact same genetic background of patients. The usefulness of producing iPSCs carrying a variety of mutations, instead, resides on one hand on the opportunity of establishing genotype-phenotype correlations, on the other hand on the necessity of identifying a common molecular mechanism that could be responsible for the development of the disease. The choice of pathogenic variants was limited by the availability of fibroblasts collected recently, as a first attempt at reprogramming older cells yielded iPSCs of poor quality.

Specific studies concerning novel and uncommon functions of PINK1 are described in *Part II* and *Part III*. The identified molecular mechanism by which this protein protects cells from staurosporine-induced apoptosis could not only be relevant in the context of neuroprotection, but it may also constitute a potential therapeutic target in the field of proliferative diseases. In fact, our findings, together with previous results from our group

and from others, provide strong support for a two-faceted nature of PINK1, which, on one side, protects dopaminergic cells from degeneration, but on the other could be hijacked from neoplastic cells to support proliferation and inhibit the apoptotic machinery.

These results were obtained in SH-SY5Y neuroblastoma cells, which, although partially sharing biochemical markers and physiological activities with neurons, are a cancer cell line. Unfortunately, I was unable to replicate the results in iPSC-derived neurons, which constitutes an evident limitation of the study. It is not clear whether the difficulty in causing staurosporine-induced apoptosis in neurons was due to intrinsic properties of these cells or to the culturing conditions. Future efforts may either lead to the identification of the experimental conditions necessary to recapitulate the described effects in neurons or confirm that this function of PINK1 is restricted to some cell populations, better defining the context in which this pathway may be addressed as a therapeutic target.

Finally, the described changes of serine biosynthesis are an entirely novel characteristic of PINK1-deficient cells. Considering the central position of serine in metabolism, its alterations can possibly result in deleterious effects in various cellular functions, such as regulation of oxidative status, mitochondrial activity, proliferation. The results elucidated in *Part III* constitute a preliminary report of this so far undescribed feature and of the first attempts to investigate its effects at the functional level. Future studies are required to identify the molecular mechanism which links PINK1 with serine metabolism. The most intriguing aspect of this research is that the described biochemical pathways are amenable to treatment and tentative clinical trials on serine supplementation in patients affected by neurodegenerative diseases have started already.

Altogether, the data included in this dissertation provide fresh insights on new or unusual functions of the protein PINK1. Moreover, they support the value of iPSC-based models in clarifying the mechanisms of neurodegeneration posing a basis for future research towards innovative therapeutic approaches.

9. Bibliography

Amelio, I., Cutruzzolá, F., Antonov, A., Agostini, M., & Melino, G. (2014). Serine and glycine metabolism in cancer. *Trends in Biochemical Sciences*, *39*(4), 191–198. https://doi.org/10.1016/J.TIBS.2014.02.004

Arena, G., Gelmetti, V., Torosantucci, L., Vignone, D., Lamorte, G., De Rosa, P., Cilia, E., Jonas, E. A., & Valente, E. M. (2013). PINK1 protects against cell death induced by mitochondrial depolarization, by phosphorylating Bcl-xL and impairing its pro-apoptotic cleavage. *Cell Death and Differentiation*, *20*(7), 920–930. https://doi.org/10.1038/cdd.2013.19

Arena, G., & Valente, E. M. (2017). PINK1 in the limelight: multiple functions of an eclectic protein in human health and disease. In *Journal of Pathology* (Vol. 241, Issue 2, pp. 251–263). https://doi.org/10.1002/path.4815

Armstrong, M. J., & Okun, M. S. (2020). Diagnosis and Treatment of Parkinson Disease: A Review. *JAMA*, *323*(6), 548–560. https://doi.org/10.1001/JAMA.2019.22360

Arshadi, C., Günther, U., Eddison, M., Harrington, K. I. S., & Ferreira, T. A. (2021). SNT: a unifying toolbox for quantification of neuronal anatomy. *Nature Methods 2021 18:4*, *18*(4), 374–377. https://doi.org/10.1038/s41592-021-01105-7

Ascherio, A., & Schwarzschild, M. A. (2016). The epidemiology of Parkinson's disease: risk factors and prevention. *The Lancet Neurology*, *15*(12), 1257–1272. https://doi.org/10.1016/S1474-4422(16)30230-7

Assou, S., Bouckenheimer, J., & De Vos, J. (2018). Concise Review: Assessing the Genome Integrity of Human Induced Pluripotent Stem Cells: What Quality Control Metrics? *Stem Cells (Dayton, Ohio)*, *36*(6), 814–821. https://doi.org/10.1002/STEM.2797

Bandres-Ciga, S., Diez-Fairen, M., Kim, J. J., & Singleton, A. B. (2020). Genetics of Parkinson's disease: An introspection of its journey towards precision medicine. *Neurobiology of Disease*, *137*, 104782. https://doi.org/10.1016/J.NBD.2020.104782

Barodia, S. K., Creed, R. B., & Goldberg, M. S. (2017). *Parkin and PINK1 functions in*

oxidative stress and neurodegeneration. *133*, 51–59. https://pubmed.ncbi.nlm.nih.gov/28017782/

Bernheimer, H., Birkmayer, W., Hornykiewicz, O., Jellinger, K., & Seitelberger, F. (1973). Brain dopamine and the syndromes of Parkinson and Huntington Clinical, morphological and neurochemical correlations. *Journal of the Neurological Sciences*. https://doi.org/10.1016/0022-510X(73)90175-5

Bloem, B. R., Okun, M. S., & Klein, C. (2021). Parkinson's disease. *Lancet (London, England)*, *397*(10291), 2284–2303. https://doi.org/10.1016/S0140-6736(21)00218-X

Bonvento, G., Oliet, S. H. R., & Panatier, A. (2022). Glycolysis-derived L-serine levels versus PHGDH expression in Alzheimer's disease. *Cell Metabolism*, *34*(5), 654–655. https://doi.org/10.1016/J.CMET.2022.04.002

Book, A., Guella, I., Candido, T., Brice, A., Hattori, N., Jeon, B., & Farrer, M. J. (2018). A meta-analysis of α-synuclein multiplication in familial parkinsonism. *Frontiers in Neurology*, *9*, 1021. https://doi.org/10.3389/FNEUR.2018.01021/BIBTEX

Brunelli, F., Torosantucci, L., Gelmetti, V., Franzone, D., Grünewald, A., Krüger, R., Arena, G., & Valente, E. M. (2022). PINK1 Protects against Staurosporine-Induced Apoptosis by Interacting with Beclin1 and Impairing Its Pro-Apoptotic Cleavage. *Cells*, *11*(4). https://doi.org/10.3390/CELLS11040678

Brunelli, F., Valente, E. M., & Arena, G. (2020). Mechanisms of neurodegeneration in Parkinson's disease: keep neurons in the PINK1. *Mechanisms of Ageing and Development*, *189*. https://doi.org/10.1016/j.mad.2020.111277

Burciu, R. G., Ofori, E., Archer, D. B., Wu, S. S., Pasternak, O., McFarland, N. R., Okun, M. S., & Vaillancourt, D. E. (2017). Progression marker of Parkinson's disease: a 4-year multi-site imaging study. *Brain : A Journal of Neurology*, *140*(8), 2183–2192. https://doi.org/10.1093/BRAIN/AWX146

Camacho-Soto, A., Warden, M. N., Searles Nielsen, S., Salter, A., Brody, D. L., Prather, H., & Racette, B. A. (2017). Traumatic brain injury in the prodromal period of Parkinson's disease: A large epidemiological study using medicare data. *Annals of Neurology*, *82*(5), 744–754. https://doi.org/10.1002/ANA.25074

Chahine, L. M., Beach, T. G., Brumm, M. C., Adler, C. H., Coffey, C. S., Mosovsky, S., Caspell-Garcia, C., Serrano, G. E., Munoz, D. G., White, C. L., Crary, J. F., Jennings, D., Taylor, P., Foroud, T., Arnedo, V., Kopil, C. M., Riley, L., Dave, K. D., & Mollenhauer, B. (2020). In vivo distribution of α-synuclein in multiple tissues and biofluids in Parkinson disease. *Neurology*, *95*(9), E1267–E1284. https://doi.org/10.1212/WNL.0000000000010404

Chartier-Harlin, M.-C., Dachsel, J. C., Vilariño-Güell, C., Lincoln, S. J., Leprêtre, F., Hulihan, M. M., Kachergus, J., Milnerwood, A. J., Tapia, L., Song, M.-S., Le Rhun, E., Mutez, E., Larvor, L., Duflot, A., Vanbesien-Mailliot, C., Kreisler, A., Ross, O. A., Nishioka, K., Soto-Ortolaza, A. I., … Farrer, M. J. (2011). Translation Initiator EIF4G1 Mutations in Familial Parkinson Disease. *The American Journal of Human Genetics*, *89*(3), 398–406. https://doi.org/10.1016/j.ajhg.2011.08.009

Chen, X., Calandrelli, R., Girardini, J., Yan, Z., Tan, Z., Xu, X., Hiniker, A., & Zhong, S. (2022). PHGDH expression increases with progression of Alzheimer's disease pathology and symptoms. *Cell Metabolism*, *34*(5), 651–653. https://doi.org/10.1016/j.cmet.2022.02.008

Chen, X., Wang, Q., Li, S., Li, X. J., & Yang, W. (2022). Mitochondrial-Dependent and Independent Functions of PINK1. *Frontiers in Cell and Developmental Biology*, *10*, 1409. https://doi.org/10.3389/FCELL.2022.954536/BIBTEX

Cherian, A., & Divya, K. P. (2020). Genetics of Parkinson's disease. *Acta Neurologica Belgica*, *120*(6), 1297–1305. https://doi.org/10.1007/S13760-020-01473-5/METRICS

Choy, R. W. Y., Park, M., Temkin, P., Herring, B. E., Marley, A., Nicoll, R. A., & Von Zastrow, M. (2014). Retromer Mediates a Discrete Route of Local Membrane Delivery to Dendrites. *Neuron*, *82*(1), 55–62. https://doi.org/10.1016/J.NEURON.2014.02.018

Cookson, M. R. (2012). Cellular effects of LRRK2 mutations. *Biochemical Society Transactions*, *40*(5), 1070–1073. https://doi.org/10.1042/BST20120165

da Silva Siqueira, L., Majolo, F., da Silva, A. P. B., da Costa, J. C., & Marinowic, D. R. (2021). Neurospheres: a potential in vitro model for the study of central nervous system disorders. *Molecular Biology Reports*, *48*(4), 3649–3663.

https://doi.org/10.1007/S11033-021-06301-4

Damodaran, M., & Ramaswamy, R. (1937). Isolation of l-3:4-dihydroxyphenylalanine from the seeds of Mucuna pruriens. *The Biochemical Journal*, *31*(12), 2149–2152. http://www.ncbi.nlm.nih.gov/pubmed/16746556

Day, J. O., & Mullin, S. (2021). The Genetics of Parkinson's Disease and Implications for Clinical Practice. *Genes 2021, Vol. 12, Page 1006*, *12*(7), 1006. https://doi.org/10.3390/GENES12071006

Deas, E., Plun-Favreau, H., Gandhi, S., Desmond, H., Kjaer, S., Loh, S. H. Y., Renton, A. E. M., Harvey, R. J., Whitworth, A. J., Martins, L. M., Abramov, A. Y., & Wood, N. W. (2011). PINK1 cleavage at position A103 by the mitochondrial protease PARL. *Human Molecular Genetics*, *20*(5), 867–879. https://doi.org/10.1093/hmg/ddq526

DeNicola, G. M., Chen, P. H., Mullarky, E., Sudderth, J. A., Hu, Z., Wu, D., Tang, H., Xie, Y., Asara, J. M., Huffman, K. E., Wistuba, I. I., Minna, J. D., DeBerardinis, R. J., & Cantley, L. C. (2015). NRF2 regulates serine biosynthesis in non-small cell lung cancer. *Nature Genetics*, *47*(12), 1475–1481. https://doi.org/10.1038/NG.3421

Deuschl, G., Beghi, E., Fazekas, F., Varga, T., Christoforidi, K. A., Sipido, E., Bassetti, C. L., Vos, T., & Feigin, V. L. (2020). The burden of neurological diseases in Europe: an analysis for the Global Burden of Disease Study 2017. *The Lancet. Public Health*, *5*(10), e551–e567. https://doi.org/10.1016/S2468-2667(20)30190-0

Diao, J., Burré, J., Vivona, S., Cipriano, D. J., Sharma, M., Kyoung, M., Südhof, T. C., & Brunger, A. T. (2013). Native α-synuclein induces clustering of synaptic-vesicle mimics via binding to phospholipids and synaptobrevin-2/VAMP2. *ELife*, *2*, e00592. https://doi.org/10.7554/eLife.00592

Diehl, F. F., Lewis, C. A., Fiske, B. P., & Vander Heiden, M. G. (2019). Cellular redox state constrains serine synthesis and nucleotide production to impact cell proliferation. *Nature Metabolism 2019 1:9*, *1*(9), 861–867. https://doi.org/10.1038/s42255-019-0108-x

Divakaruni, A. S., Paradyse, A., Ferrick, D. A., Murphy, A. N., & Jastroch, M. (2014). Analysis and Interpretation of Microplate-Based Oxygen Consumption and pH Data. *Methods in Enzymology*, *547*(C), 309–354. https://doi.org/10.1016/B978-0-12-801415-

8.00016-3

Dorsey, E. R., Sherer, T., Okun, M. S., & Bloemd, B. R. (2018). The Emerging Evidence of the Parkinson Pandemic. *Journal of Parkinson's Disease*, *8*(s1), S3–S8. https://doi.org/10.3233/JPD-181474

Dorsey, R., Sherer, T., Okun, M. S., & Bloem, B. R. (2020). *Ending Parkinson's disease : a prescription for action*. https://books.google.com/books/about/Ending_Parkinson_s_Disease.html?hl=de&id=TVShDwAAQBAJ

Eldeeb, M. A., & Ragheb, M. A. (2020). N-degron-mediated degradation and regulation of mitochondrial PINK1 kinase. *Current Genetics*, *66*(4), 693–701. https://doi.org/10.1007/S00294-020-01062-2

Espay, A. J., & Okun, M. S. (2023). Abandoning the Proteinopathy Paradigm in Parkinson Disease. *JAMA Neurology*, *80*(2), 123–124. https://doi.org/10.1001/JAMANEUROL.2022.4193

Exner, N., Lutz, A. K., Haass, C., & Winklhofer, K. F. (2012). Mitochondrial dysfunction in Parkinson's disease: molecular mechanisms and pathophysiological consequences. *The EMBO Journal*, *31*(14), 3038–3062. https://doi.org/10.1038/emboj.2012.170

Fakhree, M. A. A., Nolten, I. S., Blum, C., & Claessens, M. M. A. E. (2018). Different Conformational Subensembles of the Intrinsically Disordered Protein α-Synuclein in Cells. *Journal of Physical Chemistry Letters*, *9*(6), 1249–1253. https://doi.org/10.1021/ACS.JPCLETT.8B00092/SUPPL_FILE/JZ8B00092_SI_001.PDF

Fang, X., Han, D., Cheng, Q., Zhang, P., Zhao, C., Min, J., & Wang, F. (2018). Association of Levels of Physical Activity With Risk of Parkinson Disease: A Systematic Review and Meta-analysis. *JAMA Network Open*, *1*(5), e182421. https://doi.org/10.1001/JAMANETWORKOPEN.2018.2421

Feigin, V. L., Nichols, E., Alam, T., Bannick, M. S., Beghi, E., Blake, N., Culpepper, W. J., Dorsey, E. R., Elbaz, A., Ellenbogen, R. G., Fisher, J. L., Fitzmaurice, C., Giussani, G., Glennie, L., James, S. L., Johnson, C. O., Kassebaum, N. J., Logroscino, G., Marin, B., …Vos, T. (2019). Global, regional, and national burden of neurological disorders,

1990-2016: a systematic analysis for the Global Burden of Disease Study 2016. *The Lancet. Neurology*, *18*(5), 459–480. https://doi.org/10.1016/S1474-4422(18)30499-X

Funayama, M., Ohe, K., Amo, T., Furuya, N., Yamaguchi, J., Saiki, S., Li, Y., Ogaki, K., Ando, M., Yoshino, H., Tomiyama, H., Nishioka, K., Hasegawa, K., Saiki, H., Satake, W., Mogushi, K., Sasaki, R., Kokubo, Y., Kuzuhara, S., … Hattori, N. (2015). CHCHD2 mutations in autosomal dominant late-onset Parkinson's disease: a genome-wide linkage and sequencing study. *The Lancet Neurology*, *14*(3), 274–282. https://doi.org/10.1016/S1474-4422(14)70266-2

Gan, Z. Y., Callegari, S., Cobbold, S. A., Cotton, T. R., Mlodzianoski, M. J., Schubert, A. F., Geoghegan, N. D., Rogers, K. L., Leis, A., Dewson, G., Glukhova, A., & Komander, D. (2021). Activation mechanism of PINK1. *Nature 2021 602:7896*, *602*(7896), 328–335. https://doi.org/10.1038/s41586-021-04340-2

Gandhi, S., Wood-Kaczmar, A., Yao, Z., Plun-Favreau, H., Deas, E., Klupsch, K., Downward, J., Latchman, D. S., Tabrizi, S. J., Wood, N. W., Duchen, M. R., & Abramov, A. Y. (2009). PINK1-Associated Parkinson's Disease Is Caused by Neuronal Vulnerability to Calcium-Induced Cell Death. *Molecular Cell*, *33*(5–3), 627. https://doi.org/10.1016/J.MOLCEL.2009.02.013

Gautier, C. A., Kitada, T., & Shen, J. (2008). Loss of PINK1 causes mitochondrial functional defects and increased sensitivity to oxidative stress. *Proceedings of the National Academy of Sciences of the United States of America*, *105*(32), 11364–11369. https://doi.org/10.1073/pnas.0802076105

Gelmetti, V., De Rosa, P., Torosantucci, L., Marini, E. S., Romagnoli, A., Di Rienzo, M., Arena, G., Vignone, D., Fimia, G. M., & Valente, E. M. (2017). PINK1 and BECN1 relocalize at mitochondria-associated membranes during mitophagy and promote ER-mitochondria tethering and autophagosome formation. *Autophagy*, *13*(4), 654–669. https://doi.org/10.1080/15548627.2016.1277309

Goetz, C. G. (2011). The History of Parkinson's Disease: Early Clinical Descriptions and Neurological Therapies. *Cold Spring Harbor Perspectives in Medicine*, *1*(1), a008862–a008862. https://doi.org/10.1101/cshperspect.a008862

Gravitz, L. (2021). The promise and potential of stem cells in Parkinson's disease. *Nature*, *597*(7878), S8–S10. https://doi.org/10.1038/D41586-021-02622-3

Greene, A. W., Grenier, K., Aguileta, M. A., Muise, S., Farazifard, R., Haque, M. E., McBride, H. M., Park, D. S., & Fon, E. A. (2012). Mitochondrial processing peptidase regulates PINK1 processing, import and Parkin recruitment. *EMBO Reports*, *13*(4), 378–385. https://doi.org/10.1038/embor.2012.14

Guardia-Laguarta, C., Liu, Y., Lauritzen, K. H., Erdjument-Bromage, H., Martin, B., Swayne, T. C., Jiang, X., & Przedborski, S. (2019). PINK1 Content in Mitochondria is Regulated by ER-Associated Degradation. *Journal of Neuroscience*, *39*(36), 7074–7085. https://doi.org/10.1523/JNEUROSCI.1691-18.2019

Ha, J. Y., Kim, J. S., Kim, S. E., & Son, J. H. (2014). Simultaneous activation of mitophagy and autophagy by staurosporine protects against dopaminergic neuronal cell death. *Neuroscience Letters*, *561*, 101–106. https://doi.org/10.1016/J.NEULET.2013.12.064

Haehner, A., Boesveldt, S., Berendse, H. W., Mackay-Sim, A., Fleischmann, J., Silburn, P. A., Johnston, A. N., Mellick, G. D., Herting, B., Reichmann, H., & Hummel, T. (2009). Prevalence of smell loss in Parkinson's disease--a multicenter study. *Parkinsonism & Related Disorders*, *15*(7), 490–494. https://doi.org/10.1016/J.PARKRELDIS.2008.12.005

Hall, S., Surova, Y., Öhrfelt, A., Blennow, K., Zetterberg, H., & Hansson, O. (2016). Longitudinal Measurements of Cerebrospinal Fluid Biomarkers in Parkinson's Disease. *Movement Disorders : Official Journal of the Movement Disorder Society*, *31*(6), 898–905. https://doi.org/10.1002/MDS.26578

Hamasaki, M., Furuta, N., Matsuda, A., Nezu, A., Yamamoto, A., Fujita, N., Oomori, H., Noda, T., Haraguchi, T., Hiraoka, Y., Amano, A., & Yoshimori, T. (2013). Autophagosomes form at ER-mitochondria contact sites. *Nature*. https://doi.org/10.1038/nature11910

Hanagasi, H. A., Tufekcioglu, Z., & Emre, M. (2017). Dementia in Parkinson's disease. *Journal of the Neurological Sciences*, *374*, 26–31. https://doi.org/10.1016/j.jns.2017.01.012

Hanss, Z., Larsen, S. B., Antony, P., Mencke, P., Massart, F., Jarazo, J., Schwamborn, J. C., Barbuti, P. A., Mellick, G. D., & Krüger, R. (2021). Mitochondrial and Clearance Impairment in p.D620N VPS35 Patient-Derived Neurons. *Movement Disorders*, *36*(3), 704–715. https://doi.org/10.1002/MDS.28365

Hayes, M. T. (2019). Parkinson's Disease and Parkinsonism. *The American Journal of Medicine*, *132*(7), 802–807. https://doi.org/10.1016/J.AMJMED.2019.03.001

Heo, J.-M., Ordureau, A., Paulo, J. A., Rinehart, J., & Harper, J. W. (2015). The PINK1-PARKIN Mitochondrial Ubiquitylation Pathway Drives a Program of OPTN/NDP52 Recruitment and TBK1 Activation to Promote Mitophagy. *Molecular Cell*, *60*(1), 7–20. https://doi.org/10.1016/j.molcel.2015.08.016

Hess, C. W., & Hallett, M. (2017). The Phenomenology of Parkinson's Disease. *Seminars in Neurology*, *37*(2), 109–117. https://doi.org/10.1055/S-0037-1601869

Hiller, B. M., Marmion, D. J., Thompson, C. A., Elliott, N. A., Federoff, H., Brundin, P., Mattis, V. B., McMahon, C. W., & Kordower, J. H. (2022). Optimizing maturity and dose of iPSC-derived dopamine progenitor cell therapy for Parkinson's disease. *NPJ Regenerative Medicine*, *7*(1). https://doi.org/10.1038/S41536-022-00221-Y

Imaizumi, Y., Okada, Y., Akamatsu, W., Koike, M., Kuzumaki, N., Hayakawa, H., Nihira, T., Kobayashi, T., Ohyama, M., Sato, S., Takanashi, M., Funayama, M., Hirayama, A., Soga, T., Hishiki, T., Suematsu, M., Yagi, T., Ito, D., Kosakai, A., … Okano, H. (2012). Mitochondrial dysfunction associated with increased oxidative stress and α-synuclein accumulation in PARK2 iPSC-derived neurons and postmortem brain tissue. *Molecular Brain*, *5*(1), 35. https://doi.org/10.1186/1756-6606-5-35

Jantas, D., Szymanska, M., Budziszewska, B., & Lason, W. (2009). An involvement of BDNF and PI3-K/Akt in the anti-apoptotic effect of memantine on staurosporine-evoked cell death in primary cortical neurons. *Apoptosis : An International Journal on Programmed Cell Death*, *14*(7), 900–912. https://doi.org/10.1007/S10495-009-0370-6

Jeong, J. S., Piao, Y., Kang, S., Son, M., Kang, Y. C., Du, X. F., Ryu, J., Cho, Y. W., Jiang, H. H., Oh, M. S., Hong, S. P., Oh, Y. J., & Pak, Y. K. (2018). Triple herbal extract DA-9805 exerts a neuroprotective effect via amelioration of mitochondrial damage in

experimental models of Parkinson's disease. *Scientific Reports*, *8*(1). https://doi.org/10.1038/S41598-018-34240-X

Jin, S. M., Lazarou, M., Wang, C., Kane, L. A., Narendra, D. P., & Youle, R. J. (2010). Mitochondrial membrane potential regulates PINK1 import and proteolytic destabilization by PARL. *The Journal of Cell Biology*, *191*(5), 933–942. https://doi.org/10.1083/jcb.201008084

Jin, S. M., & Youle, R. J. (2013). The accumulation of misfolded proteins in the mitochondrial matrix is sensed by PINK1 to induce PARK2/Parkin-mediated mitophagy of polarized mitochondria. *Autophagy*, *9*(11), 1750–1757. http://www.ncbi.nlm.nih.gov/pubmed/24149988

Kalia, L. V., & Lang, A. E. (2015). Parkinson's disease. *The Lancet*, *386*(9996), 896–912. https://doi.org/10.1016/S0140-6736(14)61393-3

Kanchan, K., Iyer, K., Yanek, L. R., Carcamo-Orive, I., Taub, M. A., Malley, C., Baldwin, K., Becker, L. C., Broeckel, U., Cheng, L., Cowan, C., D'Antonio, M., Frazer, K. A., Quertermous, T., Mostoslavsky, G., Murphy, G., Rabinovitch, M., Rader, D. J., Steinberg, M. H., … Mathias, R. A. (2020). Genomic integrity of human induced pluripotent stem cells across nine studies in the NHLBI NextGen program. *Stem Cell Research*, *46*. https://doi.org/10.1016/J.SCR.2020.101803

Kane, L. A., Lazarou, M., Fogel, A. I., Li, Y., Yamano, K., Sarraf, S. A., Banerjee, S., & Youle, R. J. (2014). PINK1 phosphorylates ubiquitin to activate Parkin E3 ubiquitin ligase activity. *The Journal of Cell Biology*, *205*(2), 143–153. https://doi.org/10.1083/jcb.201402104

Kawaji, H., Kasukawa, T., Forrest, A., Carninci, P., & Hayashizaki, Y. (2017). The FANTOM5 collection, a data series underpinning mammalian transcriptome atlases in diverse cell types. *Scientific Data 2017 4:1*, *4*(1), 1–3. https://doi.org/10.1038/sdata.2017.113

Kazlauskaite, A., Kondapalli, C., Gourlay, R., Campbell, D. G., Ritorto, M. S., Hofmann, K., Alessi, D. R., Knebel, A., Trost, M., & Muqit, M. M. K. (2014). Parkin is activated by PINK1-dependent phosphorylation of ubiquitin at Ser ^{65}. *Biochemical Journal*, *460*(1), 127–141. https://doi.org/10.1042/BJ20140334

Kim, S.-J., Khan, M., Quan, J., Till, A., Subramani, S., & Siddiqui, A. (2013). Hepatitis B Virus Disrupts Mitochondrial Dynamics: Induces Fission and Mitophagy to Attenuate Apoptosis. *PLoS Pathogens*, *9*(12), e1003722. https://doi.org/10.1371/journal.ppat.1003722

Kim, S.-J., Syed, G. H., & Siddiqui, A. (2013). Hepatitis C Virus Induces the Mitochondrial Translocation of Parkin and Subsequent Mitophagy. *PLoS Pathogens*, *9*(3), e1003285. https://doi.org/10.1371/journal.ppat.1003285

Klein, C., & Westenberger, A. (2012). Genetics of Parkinson's Disease. *Cold Spring Harbor Perspectives in Medicine*, *2*(1), a008888. https://doi.org/10.1101/CSHPERSPECT.A008888

Koh, J. Y., Wie, M. B., Gwag, B. J., Sensi, S. L., Canzoniero, L. M. T., Demaro, J., Csernansky, C., & Choi, D. W. (1995). Staurosporine-induced neuronal apoptosis. *Experimental Neurology*, *135*(2), 153–159. https://doi.org/10.1006/exnr.1995.1074

Kostic, M., Ludtmann, M. H. R., Bading, H., Hershfinkel, M., Steer, E., Chu, C. T., Abramov, A. Y., & Sekler, I. (2015). PKA Phosphorylation of NCLX Reverses Mitochondrial Calcium Overload and Depolarization, Promoting Survival of PINK1-Deficient Dopaminergic Neurons. *Cell Reports*, *13*(2), 376–386. https://doi.org/10.1016/J.CELREP.2015.08.079

Koyano, F., Okatsu, K., Kosako, H., Tamura, Y., Go, E., Kimura, M., Kimura, Y., Tsuchiya, H., Yoshihara, H., Hirokawa, T., Endo, T., Fon, E. A., Trempe, J.-F., Saeki, Y., Tanaka, K., & Matsuda, N. (2014). Ubiquitin is phosphorylated by PINK1 to activate parkin. *Nature*, *510*(7503), 162–166. https://doi.org/10.1038/nature13392

Kumar, A., Tamjar, J., Waddell, A. D., Woodroof, H. I., Raimi, O. G., Shaw, A. M., Peggie, M., Muqit, M. M., & van Aalten, D. M. (2017). Structure of PINK1 and mechanisms of Parkinson's disease-associated mutations. *ELife*, *6*. https://doi.org/10.7554/eLife.29985

Labuschagne, C. F., van den Broek, N. J. F., Mackay, G. M., Vousden, K. H., & Maddocks, O. D. K. (2014). Serine, but not glycine, supports one-carbon metabolism and proliferation of cancer cells. *Cell Reports*, *7*(4), 1248–1258. https://doi.org/10.1016/J.CELREP.2014.04.045

Lamotte, G., & Benarroch, E. E. (2021). What Is the Clinical Correlation of Cardiac Noradrenergic Denervation in Parkinson Disease? *Neurology*, *96*(16), 748–753. https://doi.org/10.1212/WNL.0000000000011805

Lan, X., Field, M. S., & Stover, P. J. (2018). Cell cycle regulation of folate-mediated one-carbon metabolism. *Wiley Interdisciplinary Reviews. Systems Biology and Medicine*, *10*(6). https://doi.org/10.1002/WSBM.1426

Lazarou, M., Jin, S. M., Kane, L. A., & Youle, R. J. (2012). Role of PINK1 Binding to the TOM Complex and Alternate Intracellular Membranes in Recruitment and Activation of the E3 Ligase Parkin. *Developmental Cell*, *22*(2), 320–333. https://doi.org/10.1016/j.devcel.2011.12.014

Lazarou, M., Sliter, D. A., Kane, L. A., Sarraf, S. A., Wang, C., Burman, J. L., Sideris, D. P., Fogel, A. I., & Youle, R. J. (2015). The ubiquitin kinase PINK1 recruits autophagy receptors to induce mitophagy. *Nature*, *524*(7565), 309–314. https://doi.org/10.1038/nature14893

Le Douce, J., Maugard, M., Veran, J., Matos, M., Jégo, P., Vigneron, P. A., Faivre, E., Toussay, X., Vandenberghe, M., Balbastre, Y., Piquet, J., Guiot, E., Tran, N. T., Taverna, M., Marinesco, S., Koyanagi, A., Furuya, S., Gaudin-Guérif, M., Goutal, S., …Bonvento, G. (2020). Impairment of Glycolysis-Derived l-Serine Production in Astrocytes Contributes to Cognitive Deficits in Alzheimer's Disease. *Cell Metabolism*, *31*(3), 503-517.e8. https://doi.org/10.1016/J.CMET.2020.02.004

Lee, K. S., Huh, S., Lee, S., Wu, Z., Kim, A. K., Kang, H. Y., & Lu, B. (2018). Altered ER-mitochondria contact impacts mitochondria calcium homeostasis and contributes to neurodegeneration in vivo in disease models. *Proceedings of the National Academy of Sciences of the United States of America*, *115*(38), E8844–E8853. https://doi.org/10.1073/PNAS.1721136115/SUPPL_FILE/PNAS.1721136115.SAPP.PDF

Lee, S., Imai, Y., Gehrke, S., Liu, S., & Lu, B. (2012). The synaptic function of LRRK2. *Biochemical Society Transactions*, *40*(5), 1047–1051. https://doi.org/10.1042/BST20120113

Lin, C. H., Li, C. H., Yang, K. C., Lin, F. J., Wu, C. C., Chieh, J. J., & Chiu, M. J. (2019). Blood

NfL: A biomarker for disease severity and progression in Parkinson disease. *Neurology*, *93*(11), e1104–e1111. https://doi.org/10.1212/WNL.0000000000008088

Liu, J., Zhang, C., Wu, H., Sun, X. X., Li, Y., Huang, S., Yue, X., Lu, S. E., Shen, Z., Su, X., White, E., Haffty, B. G., Hu, W., & Feng, Z. (2020). Parkin ubiquitinates phosphoglycerate dehydrogenase to suppress serine synthesis and tumor progression. *The Journal of Clinical Investigation*, *130*(6), 3253–3269. https://doi.org/10.1172/JCI132876

Mackay, D. F., Russell, E. R., Stewart, K., MacLean, J. A., Pell, J. P., & Stewart, W. (2019). Neurodegenerative disease mortality in former professional soccer players. *The New England Journal of Medicine*, *381*(19), 1801. https://doi.org/10.1056/NEJMOA1908483

Marongiu, R., Spencer, B., Crews, L., Adame, A., Patrick, C., Trejo, M., Dallapiccola, B., Valente, E. M., & Masliah, E. (2009). Mutant Pink1 induces mitochondrial dysfunction in a neuronal cell model of Parkinson's disease by disturbing calcium flux. *Journal of Neurochemistry*, *108*(6), 1561–1574. https://doi.org/10.1111/j.1471-4159.2009.05932.x

Marques, T. M., Van Rumund, A., Oeckl, P., Kuiperij, H. B., Esselink, R. A. J., Bloem, B. R., Otto, M., & Verbeek, M. M. (2019). Serum NFL discriminates Parkinson disease from atypical parkinsonisms. *Neurology*, *92*(13), E1479–E1486. https://doi.org/10.1212/WNL.0000000000007179

Marsili, L., Rizzo, G., & Colosimo, C. (2018). Diagnostic Criteria for Parkinson's Disease: From James Parkinson to the Concept of Prodromal Disease. *Frontiers in Neurology*, *9*(MAR). https://doi.org/10.3389/FNEUR.2018.00156

Martin, I., Kim, J. W., Lee, B. D., Kang, H. C., Xu, J.-C., Jia, H., Stankowski, J., Kim, M.-S., Zhong, J., Kumar, M., Andrabi, S. A., Xiong, Y., Dickson, D. W., Wszolek, Z. K., Pandey, A., Dawson, T. M., & Dawson, V. L. (2014). Ribosomal Protein s15 Phosphorylation Mediates LRRK2 Neurodegeneration in Parkinson's Disease. *Cell*, *157*(2), 472–485. https://doi.org/10.1016/j.cell.2014.01.064

Matheoud, D., Cannon, T., Voisin, A., Penttinen, A. M., Ramet, L., Fahmy, A. M., Ducrot, C., Laplante, A., Bourque, M. J., Zhu, L., Cayrol, R., Le Campion, A., McBride, H. M.,

Gruenheid, S., Trudeau, L. E., & Desjardins, M. (2019). Intestinal infection triggers Parkinson's disease-like symptoms in Pink1 −/− mice. In *Nature* (Vol. 571, Issue 7766, pp. 565–569). Nature Publishing Group. https://doi.org/10.1038/s41586-019-1405-y

Matheoud, D., Sugiura, A., Bellemare-Pelletier, A., Laplante, A., Rondeau, C., Chemali, M., Fazel, A., Bergeron, J. J., Trudeau, L. E., Burelle, Y., Gagnon, E., McBride, H. M., & Desjardins, M. (2016). Parkinson's Disease-Related Proteins PINK1 and Parkin Repress Mitochondrial Antigen Presentation. *Cell*, *166*(2), 314–327. https://doi.org/10.1016/j.cell.2016.05.039

Meissner, C., Lorenz, H., Weihofen, A., Selkoe, D. J., & Lemberg, M. K. (2011). The mitochondrial intramembrane protease PARL cleaves human Pink1 to regulate Pink1 trafficking. *Journal of Neurochemistry*, *117*(5), 856–867. https://doi.org/10.1111/j.1471-4159.2011.07253.x

Michely, J., Volz, L. J., Barbe, M. T., Hoffstaedter, F., Viswanathan, S., Timmermann, L., Eickhoff, S. B., Fink, G. R., & Grefkes, C. (2015). Dopaminergic modulation of motor network dynamics in Parkinson's disease. *Brain : A Journal of Neurology*, *138*(Pt 3), 664–678. https://doi.org/10.1093/BRAIN/AWU381

Michiorri, S., Gelmetti, V., Giarda, E., Lombardi, F., Romano, F., Marongiu, R., Nerini-Molteni, S., Sale, P., Vago, R., Arena, G., Torosantucci, L., Cassina, L., Russo, M. A., Dallapiccola, B., Valente, E. M., & Casari, G. (2010). The Parkinson-associated protein PINK1 interacts with Beclin1 and promotes autophagy. *Cell Death and Differentiation*, *17*(6), 962–974. https://doi.org/10.1038/cdd.2009.200

Moisoi, N., Klupsch, K., Fedele, V., East, P., Sharma, S., Renton, A., Plun-Favreau, H., Edwards, R. E., Teismann, P., Esposti, M. D., Morrison, A. D., Wood, N. W., Downward, J., & Martins, L. M. (2009). Mitochondrial dysfunction triggered by loss of HtrA2 results in the activation of a brain-specific transcriptional stress response. *Cell Death & Differentiation*, *16*(3), 449–464. https://doi.org/10.1038/cdd.2008.166

Murtas, G., Marcone, G. L., Sacchi, S., & Pollegioni, L. (2020). L-serine synthesis via the phosphorylated pathway in humans. *Cellular and Molecular Life Sciences 2020 77:24*, *77*(24), 5131–5148. https://doi.org/10.1007/S00018-020-03574-Z

Narendra, D. P., Jin, S. M., Tanaka, A., Suen, D. F., Gautier, C. A., Shen, J., Cookson, M. R., & Youle, R. J. (2010). PINK1 is selectively stabilized on impaired mitochondria to activate Parkin. *PLoS Biology*, *8*(1). https://doi.org/10.1371/journal.pbio.1000298

Newman, A. C., & Maddocks, O. D. K. (2017). One-carbon metabolism in cancer. *British Journal of Cancer*, *116*(12), 1499–1504. https://doi.org/10.1038/BJC.2017.118

Nickels, S. L., Walter, J., Bolognin, S., Gérard, D., Jaeger, C., Qing, X., Tisserand, J., Jarazo, J., Hemmer, K., Harms, A., Halder, R., Lucarelli, P., Berger, E., Antony, P. M. A., Glaab, E., Hankemeier, T., Klein, C., Sauter, T., Sinkkonen, L., & Schwamborn, J. C. (2019). Impaired serine metabolism complements LRRK2-G2019S pathogenicity in PD patients. *Parkinsonism and Related Disorders*, *67*, 48–55. http://www.prd-journal.com/article/S1353802019303955/fulltext

Noguchi, S., Arakawa, T., Fukuda, S., Furuno, M., Hasegawa, A., Hori, F., Ishikawa-Kato, S., Kaida, K., Kaiho, A., Kanamori-Katayama, M., Kawashima, T., Kojima, M., Kubosaki, A., Manabe, R. I., Murata, M., Nagao-Sato, S., Nakazato, K., Ninomiya, N., Nishiyori-Sueki, H., … Hayashizaki, Y. (2017). FANTOM5 CAGE profiles of human and mouse samples. *Scientific Data 2017 4:1*, *4*(1), 1–10. https://doi.org/10.1038/sdata.2017.112

Noyce, A. J., Bestwick, J. P., Silveira-Moriyama, L., Hawkes, C. H., Giovannoni, G., Lees, A. J., & Schrag, A. (2012). Meta-analysis of early nonmotor features and risk factors for Parkinson disease. *Annals of Neurology*, *72*(6), 893–901. https://doi.org/10.1002/ana.23687

Okatsu, K., Uno, M., Koyano, F., Go, E., Kimura, M., Oka, T., Tanaka, K., & Matsuda, N. (2013). A dimeric PINK1-containing complex on depolarized mitochondria stimulates Parkin recruitment. *The Journal of Biological Chemistry*, *288*(51), 36372–36384. https://doi.org/10.1074/JBC.M113.509653

Olejniczak, M., Galka, P., & Krzyzosiak, W. J. (2010). Sequence-non-specific effects of RNA interference triggers and microRNA regulators. *Nucleic Acids Research*, *38*(1), 1–16. https://doi.org/10.1093/NAR/GKP829

Omura, S., Iwai, Y., Hirano, A., Nakagawa, A., Awaya, J., Tsuchiya, H., Takahashi, Y., & Masuma, R. (1977). A new alkaloid AM-2282 OF Streptomyces origin. Taxonomy, fermentation, isolation and preliminary characterization. *The Journal of Antibiotics*,

30(4), 275–282. https://doi.org/10.7164/ANTIBIOTICS.30.275

Oosterveld, L. P., Verberk, I. M. W., Majbour, N. K., El-Agnaf, O. M., Weinstein, H. C., Berendse, H. W., Teunissen, C. E., & van de Berg, W. D. J. (2020). CSF or serum neurofilament light added to α-Synuclein panel discriminates Parkinson's from controls. *Movement Disorders : Official Journal of the Movement Disorder Society*, *35*(2), 288–295. https://doi.org/10.1002/MDS.27897

Ovallath, S., & Deepa, P. (2013). The history of parkinsonism: Descriptions in ancient Indian medical literature. *Movement Disorders*, *28*(5), 566–568. https://doi.org/10.1002/mds.25420

Palm, T., Bolognin, S., Meiser, J., Nickels, S., Träger, C., Meilenbrock, R. L., Brockhaus, J., Schreitmüller, M., Missler, M., & Schwamborn, J. C. (2015). Rapid and robust generation of long-term self-renewing human neural stem cells with the ability to generate mature astroglia. *Scientific Reports 2015 5:1*, *5*(1), 1–16. https://doi.org/10.1038/srep16321

Pan, S., Fan, M., Liu, Z., Li, X., & Wang, H. (2021). Serine, glycine and one-carbon metabolism in cancer (Review). *International Journal of Oncology*, *58*(2), 158–170. https://doi.org/10.3892/IJO.2020.5158/HTML

Patergnani, S., Suski, J. M., Agnoletto, C., Bononi, A., Bonora, M., De Marchi, E., Giorgi, C., Marchi, S., Missiroli, S., Poletti, F., Rimessi, A., Duszynski, J., Wieckowski, M. R., & Pinton, P. (2011). Calcium signaling around Mitochondria Associated Membranes (MAMs). *Cell Communication and Signaling : CCS*, *9*. https://doi.org/10.1186/1478-811X-9-19

Petrelli, A., Kaesberg, S., Barbe, M. T., Timmermann, L., Rosen, J. B., Fink, G. R., Kessler, J., & Kalbe, E. (2015). Cognitive training in Parkinson's disease reduces cognitive decline in the long term. *European Journal of Neurology*, *22*(4), 640–647. https://doi.org/10.1111/ENE.12621

Plun-Favreau, H., Klupsch, K., Moisoi, N., Gandhi, S., Kjaer, S., Frith, D., Harvey, K., Deas, E., Harvey, R. J., McDonald, N., Wood, N. W., Martins, L. M., & Downward, J. (2007). The mitochondrial protease HtrA2 is regulated by Parkinson's disease-associated kinase PINK1. *Nature Cell Biology*, *9*(11), 1243–1252. https://doi.org/10.1038/ncb1644

Possemato, R., Marks, K. M., Shaul, Y. D., Pacold, M. E., Kim, D., Birsoy, K., Sethumadhavan, S., Woo, H. K., Jang, H. G., Jha, A. K., Chen, W. W., Barrett, F. G., Stransky, N., Tsun, Z. Y., Cowley, G. S., Barretina, J., Kalaany, N. Y., Hsu, P. P., Ottina, K., …Sabatini, D. M. (2011). Functional genomics reveal that the serine synthesis pathway is essential in breast cancer. *Nature 2011 476:7360*, *476*(7360), 346–350. https://doi.org/10.1038/nature10350

Post, K. K., Singer, C., & Papapetropoulos, S. (2008). Cardiac denervation and dysautonomia in Parkinson's disease: a review of screening techniques. *Parkinsonism & Related Disorders*, *14*(7), 524–531. https://doi.org/10.1016/J.PARKRELDIS.2008.03.008

Poston, K. L., Thaler, A., & Alcalay, R. N. (2022). Diagnosis and Medical Management of Parkinson Disease. *Continuum (Minneapolis, Minn.)*, *28*(5), 1281–1300. https://doi.org/10.1212/CON.0000000000001152

Postuma, R. B., Berg, D., Stern, M., Poewe, W., Olanow, C. W., Oertel, W., Obeso, J., Marek, K., Litvan, I., Lang, A. E., Halliday, G., Goetz, C. G., Gasser, T., Dubois, B., Chan, P., Bloem, B. R., Adler, C. H., & Deuschl, G. (2015). MDS clinical diagnostic criteria for Parkinson's disease. *Movement Disorders : Official Journal of the Movement Disorder Society*, *30*(12), 1591–1601. https://doi.org/10.1002/MDS.26424

Pridgeon, J. W., Olzmann, J. A., Chin, L.-S., & Li, L. (2007). PINK1 Protects against Oxidative Stress by Phosphorylating Mitochondrial Chaperone TRAP1. *PLoS Biology*, *5*(7), e172. https://doi.org/10.1371/journal.pbio.0050172

Puschmann, A., Fiesel, F. C., Caulfield, T. R., Hudec, R., Ando, M., Truban, D., Hou, X., Ogaki, K., Heckman, M. G., James, E. D., Swanberg, M., Jimenez-Ferrer, I., Hansson, O., Opala, G., Siuda, J., Boczarska-Jedynak, M., Friedman, A., Koziorowski, D., Aasly, J. O., …Springer, W. (2017). Heterozygous PINK1 p.G411S increases risk of Parkinson's disease via a dominant-negative mechanism. *Brain*, *140*(1), 98–117. https://doi.org/10.1093/brain/aww261

Rafanelli, M., Walsh, K., Hamdan, M. H., & Buyan-Dent, L. (2019). Autonomic dysfunction: Diagnosis and management. *Handbook of Clinical Neurology*, *167*, 123–137. https://doi.org/10.1016/B978-0-12-804766-8.00008-X

Rakovic, A., Shurkewitsch, K., Seibler, P., Grünewald, A., Zanon, A., Hagenah, J., Krainc, D., & Klein, C. (2013). Phosphatase and tensin homolog (PTEN)-induced Putative Kinase 1 (PINK1)-dependent ubiquitination of endogenous parkin attenuates mitophagy: Study in human primary fibroblasts and induced pluripotent stem cell-derived neurons. *Journal of Biological Chemistry*, *288*(4), 2223–2237. https://doi.org/10.1074/jbc.M112.391680

Rasool, S., Veyron, S., Soya, N., Eldeeb, M. A., Lukacs, G. L., Fon, E. A., & Trempe, J. F. (2022). Mechanism of PINK1 activation by autophosphorylation and insights into assembly on the TOM complex. *Molecular Cell*, *82*(1), 44-59.e6. https://doi.org/10.1016/j.molcel.2021.11.012

Reed, X., Bandrés-Ciga, S., Blauwendraat, C., & Cookson, M. R. (2019). The role of monogenic genes in idiopathic Parkinson's disease. *Neurobiology of Disease*, *124*, 230. https://doi.org/10.1016/J.NBD.2018.11.012

Reich, S., Nguyen, C. D. L., Has, C., Steltgens, S., Soni, H., Coman, C., Freyberg, M., Bichler, A., Seifert, N., Conrad, D., Knobbe-Thomsen, C. B., Tews, B., Toedt, G., Ahrends, R., & Medenbach, J. (2020). *A multi-omics analysis reveals the unfolded protein response regulon and stress-induced resistance to folate-based antimetabolites*. *11*(1), 1–15. https://pubmed.ncbi.nlm.nih.gov/32522993/

Reinhardt, P., Glatza, M., Hemmer, K., Tsytsyura, Y., Thiel, C. S., Höing, S., Moritz, S., Parga, J. A., Wagner, L., Bruder, J. M., Wu, G., Schmid, B., Röpke, A., Klingauf, J., Schwamborn, J. C., Gasser, T., Schöler, H. R., & Sterneckert, J. (2013). Derivation and Expansion Using Only Small Molecules of Human Neural Progenitors for Neurodegenerative Disease Modeling. *PLoS ONE*, *8*(3). https://doi.org/10.1371/journal.pone.0059252

Richter, B., Sliter, D. A., Herhaus, L., Stolz, A., Wang, C., Beli, P., Zaffagnini, G., Wild, P., Martens, S., Wagner, S. A., Youle, R. J., & Dikic, I. (2016). Phosphorylation of OPTN by TBK1 enhances its binding to Ub chains and promotes selective autophagy of damaged mitochondria. *Proceedings of the National Academy of Sciences*, *113*(15), 4039–4044. https://doi.org/10.1073/pnas.1523926113

Rossi, A., Berger, K., Chen, H., Leslie, D., Mailman, R. B., & Huang, X. (2018). Projection of

the prevalence of Parkinson's disease in the coming decades: Revisited. *Movement Disorders : Official Journal of the Movement Disorder Society*, *33*(1), 156–159. https://doi.org/10.1002/MDS.27063

Rothfuss, O., Fischer, H., Hasegawa, T., Maisel, M., Leitner, P., Miesel, F., Sharma, M., Bornemann, A., Berg, D., Gasser, T., & Patenge, N. (2009). Parkin protects mitochondrial genome integrity and supports mitochondrial DNA repair. *Human Molecular Genetics*, *18*(20), 3832–3850. https://doi.org/10.1093/HMG/DDP327

Sanna, G., Del Giudice, M. G., Crosio, C., & Iaccarino, C. (2012). LRRK2 and vesicle trafficking. *Biochemical Society Transactions*, *40*(5), 1117–1122. https://doi.org/10.1042/BST20120117

Schindelin, J., Arganda-Carreras, I., Frise, E., Kaynig, V., Longair, M., Pietzsch, T., Preibisch, S., Rueden, C., Saalfeld, S., Schmid, B., Tinevez, J. Y., White, D. J., Hartenstein, V., Eliceiri, K., Tomancak, P., & Cardona, A. (2012). Fiji: an open-source platform for biological-image analysis. *Nature Methods 2012 9:7*, *9*(7), 676–682. https://doi.org/10.1038/nmeth.2019

Schubert, A. F., Gladkova, C., Pardon, E., Wagstaff, J. L., Freund, S. M. V., Steyaert, J., Maslen, S. L., & Komander, D. (2017). Structure of PINK1 in complex with its substrate ubiquitin. *Nature*, *552*(7683), 1–28. https://doi.org/10.1038/nature24645

Selvarajah, B., Azuelos, I., Platé, M., Guillotin, D., Forty, E. J., Contento, G., Woodcock, H. V., Redding, M., Taylor, A., Brunori, G., Durrenberger, P. F., Ronzoni, R., Blanchard, A. D., Mercer, P. F., Anastasiou, D., & Chambers, R. C. (2019). MTORC1 amplifies the ATF4-dependent de novo serine-glycine pathway to supply glycine during TGF-1-induced collagen biosynthesis. *Science Signaling*, *12*(582). https://doi.org/10.1126/SCISIGNAL.AAV3048/SUPPL_FILE/AAV3048_SM.PDF

Sezgin, M., Bilgic, B., Tinaz, S., & Emre, M. (2019). Parkinson's Disease Dementia and Lewy Body Disease. *Seminars in Neurology*, *39*(2), 274–282. https://doi.org/10.1055/S-0039-1678579/ID/JR180061-31

Shahmoradian, S. H., Lewis, A. J., Genoud, C., Hench, J., Moors, T. E., Navarro, P. P., Castaño-Díez, D., Schweighauser, G., Graff-Meyer, A., Goldie, K. N., Sütterlin, R., Huisman, E., Ingrassia, A., Gier, Y. de, Rozemuller, A. J. M., Wang, J., Paepe, A. De,

Erny, J., Staempfli, A., …Lauer, M. E. (2019). Lewy pathology in Parkinson's disease consists of crowded organelles and lipid membranes. *Nature Neuroscience 2019 22:7*, *22*(7), 1099–1109. https://doi.org/10.1038/s41593-019-0423-2

Shen, L., Hu, P., Zhang, Y., Ji, Z., Shan, X., Ni, L., Ning, N., Wang, J., Tian, H., Shui, G., Yuan, Y., Li, G., Zheng, H., Yang, X. P., Huang, D., Feng, X., Li, M. J., Liu, Z., Wang, T., & Yu, Q. (2021). Serine metabolism antagonizes antiviral innate immunity by preventing ATP6V0d2-mediated YAP lysosomal degradation. *Cell Metabolism*, *33*(5), 971-987.e6. https://doi.org/10.1016/J.CMET.2021.03.006

Shipley, M. M., Mangold, C. A., & Szpara, M. L. (2016). Differentiation of the SH-SY5Y human neuroblastoma cell line. *Journal of Visualized Experiments*, *2016*(108). https://doi.org/10.3791/53193

Sidransky, E., & Lopez, G. (2012). The link between the GBA gene and parkinsonism. *The Lancet Neurology*, *11*(11), 986–998. https://doi.org/10.1016/S1474-4422(12)70190-4

Sidransky, E., Nalls, M. A., Aasly, J. O., Aharon-Peretz, J., Annesi, G., Barbosa, E. R., Bar-Shira, A., Berg, D., Bras, J., Brice, A., Chen, C.-M., Clark, L. N., Condroyer, C., De Marco, E. V., Dürr, A., Eblan, M. J., Fahn, S., Farrer, M. J., Fung, H.-C., …Ziegler, S. G. (2009). Multicenter analysis of glucocerebrosidase mutations in Parkinson's disease. *The New England Journal of Medicine*, *361*(17), 1651–1661. https://doi.org/10.1056/NEJMOA0901281

Simon, D. K., Tanner, C. M., & Brundin, P. (2020). Parkinson Disease Epidemiology, Pathology, Genetics, and Pathophysiology. *Clinics in Geriatric Medicine*, *36*(1), 1–12. https://doi.org/10.1016/J.CGER.2019.08.002

Skrahina, V., Gaber, H., Vollstedt, E. J., Förster, T. M., Usnich, T., Curado, F., Brüggemann, N., Paul, J., Bogdanovic, X., Zülbahar, S., Olmedillas, M., Skobalj, S., Ameziane, N., Bauer, P., Csoti, I., Koleva-Alazeh, N., Grittner, U., Westenberger, A., Kasten, M., … Rolfs, A. (2021). The Rostock International Parkinson's Disease (ROPAD) Study: Protocol and Initial Findings. *Movement Disorders : Official Journal of the Movement Disorder Society*, *36*(4), 1005–1010. https://doi.org/10.1002/MDS.28416

Sliter, D. A., Martinez, J., Hao, L., Chen, X., Sun, N., Fischer, T. D., Burman, J. L., Li, Y., Zhang,

Z., Narendra, D. P., Cai, H., Borsche, M., Klein, C., & Youle, R. J. (2018). Parkin and PINK1 mitigate STING-induced inflammation. *Nature*, *561*(7722), 258–262. https://doi.org/10.1038/s41586-018-0448-9

Soman, S., Keatinge, M., Moein, M., Da Costa, M., Mortiboys, H., Skupin, A., Sugunan, S., Bazala, M., Kuznicki, J., & Bandmann, O. (2017). Inhibition of the mitochondrial calcium uniporter rescues dopaminergic neurons in pink1−/− zebrafish. *European Journal of Neuroscience*, *45*(4), 528–535. https://doi.org/10.1111/ejn.13473

Spillantini, M. G., Schmidt, M. L., Lee, V. M.-Y., Trojanowski, J. Q., Jakes, R., & Goedert, M. (1997). α-Synuclein in Lewy bodies. *Nature*, *388*(6645), 839–840. https://doi.org/10.1038/42166

Sugimoto, H., Kakehi, M., & Jinno, F. (2015). Bioanalytical method for the simultaneous determination of D- and L-serine in human plasma by LC/MS/MS. *Analytical Biochemistry*, *487*, 38–44. https://doi.org/10.1016/J.AB.2015.07.004

Takahashi, K., & Yamanaka, S. (2006). Induction of Pluripotent Stem Cells from Mouse Embryonic and Adult Fibroblast Cultures by Defined Factors. *Cell*, *126*(4), 663–676. https://doi.org/10.1016/j.cell.2006.07.024

Tanaka, A., Cleland, M. M., Xu, S., Narendra, D. P., Suen, D.-F., Karbowski, M., & Youle, R. J. (2010). Proteasome and p97 mediate mitophagy and degradation of mitofusins induced by Parkin. *The Journal of Cell Biology*, *191*(7), 1367–1380. https://doi.org/10.1083/jcb.201007013

Thul, P. J., Akesson, L., Wiking, M., Mahdessian, D., Geladaki, A., Ait Blal, H., Alm, T., Asplund, A., Björk, L., Breckels, L. M., Bäckström, A., Danielsson, F., Fagerberg, L., Fall, J., Gatto, L., Gnann, C., Hober, S., Hjelmare, M., Johansson, F., …Lundberg, E. (2017). A subcellular map of the human proteome. *Science*, *356*(6340). https://doi.org/10.1126/SCIENCE.AAL3321/SUPPL_FILE/AAL3321_THUL_SM_TABLE_S9.XLSX

Tolosa, E., Garrido, A., Scholz, S. W., & Poewe, W. (2021). Challenges in the diagnosis of Parkinson's disease. *The Lancet Neurology*, *20*(5), 385–397. https://doi.org/10.1016/S1474-4422(21)00030-2

Epidemiology of Parkinson's disease, 124 Journal of Neural Transmission 901 (2017).

https://doi.org/10.1007/s00702-017-1686-y

Uhlén, M., Fagerberg, L., Hallström, B. M., Lindskog, C., Oksvold, P., Mardinoglu, A., Sivertsson, Å., Kampf, C., Sjöstedt, E., Asplund, A., Olsson, I. M., Edlund, K., Lundberg, E., Navani, S., Szigyarto, C. A. K., Odeberg, J., Djureinovic, D., Takanen, J. O., Hober, S., … Pontén, F. (2015). Tissue-based map of the human proteome. *Science*, *347*(6220). https://doi.org/10.1126/SCIENCE.1260419/SUPPL_FILE/1260419_UHLEN.SM.PDF

Unoki, M., & Nakamura, Y. (2001). Growth-suppressive effects of BPOZ and EGR2, two genes involved in the PTEN signaling pathway. *Oncogene*. https://doi.org/10.1038/sj.onc.1204608

Valente, E. M., Abou-Sleiman, P. M., Caputo, V., Muqit, M. M. K., Harvey, K., Gispert, S., Ali, Z., Del Turco, D., Bentivoglio, A. R., Healy, D. G., Albanese, A., Nussbaum, R., González-Maldonado, R., Deller, T., Salvi, S., Cortelli, P., Gilks, W. P., Latchman, D. S., Harvey, R. J., … Wood, N. W. (2004). Hereditary Early-Onset Parkinson's Disease Caused by Mutations in PINK1. *Science*, *304*(5674), 1158–1160. https://doi.org/10.1126/science.1096284

Vande Walle, L., Lamkanfi, M., & Vandenabeele, P. (2008). The mitochondrial serine protease HtrA2/Omi: an overview. *Cell Death & Differentiation*, *15*(3), 453–460. https://doi.org/10.1038/sj.cdd.4402291

Váradi, C. (2020). Clinical Features of Parkinson's Disease: The Evolution of Critical Symptoms. *Biology 2020, Vol. 9, Page 103*, *9*(5), 103. https://doi.org/10.3390/BIOLOGY9050103

Wade Harper, J., Ordureau, A., & Heo, J. M. (2018). Building and decoding ubiquitin chains for mitophagy. *Nature Reviews Molecular Cell Biology 2018 19:2*, *19*(2), 93–108. https://doi.org/10.1038/nrm.2017.129

Wakita, S., Izumi, Y., Nakai, T., Adachi, K., Takada-Takatori, Y., Kume, T., & Akaike, A. (2014). Staurosporine induces dopaminergic neurite outgrowth through AMP-activated protein kinase/mammalian target of rapamycin signaling pathway. *Neuropharmacology*, *77*, 39–48. https://doi.org/10.1016/J.NEUROPHARM.2013.09.012

Wang, X., Winter, D., Ashrafi, G., Schlehe, J., Wong, Y. L. L., Selkoe, D., Rice, S., Steen, J., Lavoie, M. J. J., & Schwarz, T. L. L. (2011). PINK1 and Parkin Target Miro for Phosphorylation and Degradation to Arrest Mitochondrial Motility. *Cell*, *147*(4), 893–906. https://doi.org/10.1016/j.cell.2011.10.018

Willis, A. W., Roberts, E., Beck, J. C., Fiske, B., Ross, W., Savica, R., Van Den Eeden, S. K., Tanner, C. M., Marras, C., Alcalay, R., Schwarzschild, M., Racette, B., Chen, H., Church, T., Wilson, B., & Doria, J. M. (2022). Incidence of Parkinson disease in North America. *Npj Parkinson's Disease 2022 8:1*, *8*(1), 1–7. https://doi.org/10.1038/s41531-022-00410-y

Wolosker, H., Sheth, K. N., Takahashi, M., Mothet, J. P., Brady, R. O., Ferris, C. D., & Snyder, S. H. (1999). Purification of serine racemase: biosynthesis of the neuromodulator D-serine. *Proceedings of the National Academy of Sciences of the United States of America*, *96*(2), 721–725. https://doi.org/10.1073/PNAS.96.2.721

Wood-Kaczmar, A., Gandhi, S., Yao, Z., Abramov, A. S. Y., Miljan, E. A., Keen, G., Stanyer, L., Hargreaves, I., Klupsch, K., Deas, E., Downward, J., Mansfield, L., Jat, P., Taylor, J., Heales, S., Duchen, M. R., Latchman, D., Tabrizi, S. J., & Wood, N. W. (2008). PINK1 is necessary for long term survival and mitochondrial function in human dopaminergic neurons. *PloS One*, *3*(6). https://doi.org/10.1371/JOURNAL.PONE.0002455

Xun, Z., Lee, D. Y., Lim, J., Canaria, C. A., Barnebey, A., Yanonne, S. M., & McMurray, C. T. (2012). Retinoic acid-induced differentiation increases the rate of oxygen consumption and enhances the spare respiratory capacity of mitochondria in SH-SY5Y cells. *Mechanisms of Ageing and Development*, *133*(4), 176–185. https://doi.org/10.1016/J.MAD.2012.01.008

Yamano, K., & Youle, R. J. (2013). PINK1 is degraded through the N-end rule pathway. *Autophagy*, *9*(11), 1758–1769. https://doi.org/10.4161/auto.24633

Yang, J. H., Wada, A., Yoshida, K., Miyoshi, Y., Sayano, T., Esaki, K., Kinoshita, M. O., Tomonaga, S., Azuma, N., Watanabe, M., Hamase, K., Zaitsu, K., MacHida, T., Messing, A., Itohara, S., Hirabayashi, Y., & Furuya, S. (2010). Brain-specific Phgdh deletion reveals a pivotal role for L-serine biosynthesis in controlling the level of D-serine, an N-methyl-D-aspartate receptor co-agonist, in adult brain. *The Journal of*

Biological Chemistry, *285*(53), 41380–41390. https://doi.org/10.1074/JBC.M110.187443

Yang, M., & Vousden, K. H. (2016). *Serine and one-carbon metabolism in cancer*. *16*(10), 650–662. https://pubmed.ncbi.nlm.nih.gov/27634448/

Ye, J., Mancuso, A., Tong, X., Ward, P. S., Fan, J., Rabinowitz, J. D., & Thompson, C. B. (2012). Pyruvate kinase M2 promotes de novo serine synthesis to sustain mTORC1 activity and cell proliferation. *Proceedings of the National Academy of Sciences of the United States of America*, *109*(18), 6904–6909. https://doi.org/10.1073/PNAS.1204176109

Yoboue, E. D., & Valente, E. M. (2020). PINK1 and Parkin: The odd couple. *Neuroscience Research*, *159*, 25–33. https://doi.org/10.1016/J.NEURES.2020.04.007

Yoo, L., & Chung, K. C. (2018). The ubiquitin E3 ligase CHIP promotes proteasomal degradation of the serine/threonine protein kinase PINK1 during staurosporine-induced cell death. *Journal of Biological Chemistry*, *293*(4), 1286–1297. https://doi.org/10.1074/JBC.M117.803890

Yu, W., Wang, Z., Zhang, K., Chi, Z., Xu, T., Jiang, D., Chen, S., Li, W., Yang, X., Zhang, X., Wu, Y., & Wang, D. (2019). One-Carbon Metabolism Supports S-Adenosylmethionine and Histone Methylation to Drive Inflammatory Macrophages. *Molecular Cell*, *75*(6), 1147-1160.e5. https://doi.org/10.1016/J.MOLCEL.2019.06.039

Zhang, Y., Gao, J., Chung, K. K. K., Huang, H., Dawson, V. L., & Dawson, T. M. (2000). Parkin functions as an E2-dependent ubiquitin- protein ligase and promotes the degradation of the synaptic vesicle-associated protein, CDCrel-1. *Proceedings of the National Academy of Sciences of the United States of America*, *97*(24), 13354–13359. https://doi.org/10.1073/PNAS.240347797

Zhou, J., Yang, R., Zhang, Z., Liu, Q., Zhang, Y., Wang, Q., & Yuan, H. (2019). Mitochondrial Protein PINK1 Positively Regulates RLR Signaling. *Frontiers in Immunology*, *10*(MAY), 1069. https://doi.org/10.3389/FIMMU.2019.01069

Appendix

Composition of Growth Media for Cell Culture

Complete DMEM 10%

DMEM high glucose with sodium pyruvate (EuroClone #ECB7501L) with 10% heat-inactivated FBS (EuroClone #ECS5000DH), 1% L-glutamine (EuroClone #ECB3000D), and 1% penicillin/streptomycin (EuroClone #ECB3001D).

"CytoTune" Fibroblast Medium

DMEM high glucose w/o Sodium Pyruvate w/o L-Glutamine (EuroClone #ECM0101L), 10% heat-inactivated FBS (EuroClone #ECS5000DH), 1% L-glutamine (EuroClone #ECB3000D), 1% MEM Non-Essential Amino Acids Solution (Thermo Fisher Scientific #11140050), 0.1% β-mercaptoethanol 55 mM (Thermo Fisher Scientific #21985023).

E8 Flex Medium

Essential 8™ Flex is a commercial medium (Thermo Fisher Scientific #A2858501). The final medium is prepared by adding the content of one Essential 8 Flex Supplement vial (thawed overnight at 4°C) to one bottle Essential 8 Flex Basal Medium. Aliquots of 40 mL were then prepared and stored at -20°C; thawed overnight at 4°C when needed.

E8 Homemade Medium

DMEM/F-12 with HEPES (Thermo Fisher Scientific #31330038) with added 1% Insulin-Transferrin-Selenium solution (Thermo Fisher Scientific #41400045), 1% penicillin/streptomycin (EuroClone #ECB3001D), plus 64 µg/mL ascorbic acid (Merck #A8960), 10 ng/mL FGF2 (Peprotech #100-18B), 2 ng/mL TGF-β1 (Peprotech #100-21), 100 ng/mL Heparin: (Merck #H3149).

Starvation MEM

MEM, no glutamine (Thermo Fisher Scientific #21090022) with 1% dialyzed FBS (Thermo Fisher Scientific #A3382001), 1% L-glutamine (EuroClone #ECB3000D), and 1% penicillin/streptomycin (EuroClone #ECB3001D).

N2B27 Medium

To prepare ~500 mL of medium, mix 250 mL DMEM/F-12, no glutamine (Thermo Fisher Scientific #21331046), 250 mL Neurobasal™ Medium (Thermo Fisher Scientific #21103049), 5 mL GlutaMAX™ Supplement (Thermo Fisher Scientific #35050061), 5 mL penicillin/streptomycin (EuroClone #ECB3001D), 5 mL B-27™ Supplement (50X), minus vitamin A (Thermo Fisher Scientific #12587010), 2.5 mL N-2 Supplement (Thermo Fisher Scientific #17502048); in a biosafety cabinet, filter through a Stericup filter (Merck #S2GPU05RE). The medium can be conserved at 4°C for 3-4 weeks.

smNPC Maintenance Medium

N2B27 Medium with added 3 µM CHIR-99021 (MedChemExpress #HY-10182), 150 µM ascorbic acid (Merck #A8960), 0.5 µM Purmorphamine (Merck #SML0868).

Neuron Maturation Medium

N2B27 Medium supplemented with 1 ng/mL TGFβ3 (Peprotech #100-36E), 500 µM dbcAMP (Santa Cruz #sc-201567C), 20 ng/ml BDNF (Peprotech #450-02), 10 ng/ml GDNF (Peprotech #450-10) and and 200 µM ascorbic acid (Merck #A8960).

Ser/Gly-free N2B27 Medium

To prepare ~500 mL of medium, mix 500 mL MEM, no glutamine (Thermo Fisher Scientific #21090022), 5 mL GlutaMAX™ Supplement (Thermo Fisher Scientific #35050061), 5 mL penicillin/streptomycin (EuroClone #ECB3001D), 5 mL B-27™ Supplement (50X), minus vitamin A (Thermo Fisher Scientific #12587010), 2.5 mL N-2 Supplement (Thermo Fisher Scientific #17502048); in a biosafety cabinet, filter through

a Stericup filter (Merck #S2GPU05RE). The medium can be conserved at 4°C for 3-4 weeks.

Astrocyte Medium

DMEM/F-12 (Thermo Fisher Scientific #21331046) supplemented with 1% L-glutamine (EuroClone #ECB3000D), 1% penicillin/streptomycin (EuroClone #ECB3001D), and 1% heat-inactivated FBS (EuroClone #ECS5000DH).

List of Publications Related to This Doctoral Dissertation

1. Brunelli F*, Torosantucci L*, Gelmetti V, Franzone D, Grünewald A, Krüger R, Arena G*, Valente EM*. PINK1 Protects against Staurosporine-Induced Apoptosis by Interacting with Beclin1 and Impairing Its Pro-Apoptotic Cleavage. Cells. 2022 Feb 15;11(4):678. doi: 10.3390/cells11040678. PMID: 35203326; PMCID: PMC8870463.
2. Jarazo J, Barmpa K, Modamio J, Saraiva C, Sabaté-Soler S, Rosety I, Griesbeck A, Skwirblies F, Zaffaroni G, Smits LM, Su J, Arias-Fuenzalida J, Walter J, Gomez-Giro G, Monzel AS, Qing X, Vitali A, Cruciani G, Boussaad I, Brunelli F, Jäger C, Rakovic A, Li W, Yuan L, Berger E, Arena G, Bolognin S, Schmidt R, Schröder C, Antony PMA, Klein C, Krüger R, Seibler P, Schwamborn JC. Parkinson's Disease Phenotypes in Patient Neuronal Cultures and Brain Organoids Improved by 2-Hydroxypropyl-β-Cyclodextrin Treatment. Mov Disord. 2022 Jan;37(1):80-94. doi: 10.1002/mds.28810. Epub 2021 Oct 12. PMID: 34637165; PMCID: PMC9291890.
3. Brunelli F, Valente EM, Arena G. Mechanisms of neurodegeneration in Parkinson's disease: keep neurons in the PINK1. Mech Ageing Dev. 2020 Jul;189:111277. doi: 10.1016/j.mad.2020.111277. Epub 2020 Jun 3. PMID: 32504621.
4. *In preparation*. Generation and characterization of two iPSC lines from Parkinson's Disease patients with compound heterozygous mutations in PINK1.
5. *In preparation*. Serine-glycine dysmetabolism in PINK1-deficient neuronal models of Parkinson's Disease.

* joint first or last authorship.

List of Abbreviations

3PG, 3-Phosphoglyceric acid

3PHP, 3-phosphohydroxypyruvate

3PS, 3-phosphoserine

AD, autosomal dominant

AR, autosomal recessive

BSA, bovine serum albumin

CCCP, carbonyl cyanide m-chlorphenyl hydrazine

cDNA, complementary deoxyribonucleic acid

CNS, central nervous system

CSF, cerebrospinal fluid

CTE, C-terminal extension

DAPI, 4',6-diamidino-2-phenylindole

DMEM, Dulbecco-modified Eagle Medium

DMSO, dimethyl sulfoxide

DNA, deoxyribonucleic acid

DPBS, Dulbecco's phosphate-based saline

ECAR, extracellular acidification rate

ECL, enhanced chemiluminescence

EDTA, ethylenediaminetetraacetic acid

EOPD, early-onset Parkinson's Disease

ER, endoplasmic reticulum

FACS, fluorescence-activated cell sorting

FBS, fetal bovine serum

FCCP, carbonyl cyanide-4 trifluoromethoxy phenylhydrazone

Gly, glycine

GWAS, genome-wide association studies

HEPES, 4-(2-hydroxyethyl)-1-piperazineethanesulfonic acid

HRP, horseradish peroxidase

iPSC, induced pluripotent stem cell

KO, knock-out

LC-MS, liquid chromatography-mass spectrometry

L-Ser, L-serine

mAb, monoclonal antibody

MAM, mitochondria-associated ER membrane

MDS, Movement Disorder Society

MDV, mitochondria-derived vesicle

MEM, minimum essential medium

me-THF, 5,10-methylenetetrahydrofolate

MOM, mitochondrial outer membrane

mRNA, messenger ribonucleic acid

mTHF, 5-methyltetrahydrofolate

MTS, mitochondrial targeting sequence

NTC, no template control

OCR, Oxygen consumption rate

pAb, polyclonal antibody

PAGE, polyacrylamide gel electrophoresis

PCR, polymerase chain reaction

PD, Parkinson's Disease

qPCR, quantitative polymerase chain reaction

RBD, REM sleep behavior disorder

REM (sleep), rapid eye movement (sleep)

RNA, ribonucleic acid

ROS, reactive oxygen species

RT, reverse transcriptase

SAH, S-Adenosyl homocysteine

SAM, S-Adenosyl methionine

SDS, sodium dodecyl sulfate

SEM, standard error of the mean

shRNA, small hairpin ribonucleic acid

smNPC, small molecule neural precursor cell

SNpc, *substantia nigra pars compacta*

STR, short tandem repeat

STS, staurosporine

TH, thyrosine hydroxylase

THF, tetrahydrofolate

TIM (complex), transporter of inner membrane (complex)

TM, transmembrane

TOM (complex), transporter of outer membrane (complex)

UKPDSBB, United Kingdom Parkinson’s Disease Society Brain Bank